

Aus der Klinik für Innere Medizin mit Schwerpunkt Nephrologie
der Medizinischen Fakultät der Charité – Universitätsmedizin Berlin

DISSERTATION

**Nitric oxide-cGMP signal transduction in the
injury, matrix expansion and progression of
anti-thy1-induced renal disease of the rat**

Zur Erlangung des akademischen Grades
Doctor medicinae (Dr. med.)

vorgelegt der Medizinischen Fakultät der Charité -
Universitätsmedizin Berlin

von
Yingrui Wang
aus Guangdong, V.R. China

Dekan: Prof. Dr. med. Martin Paul

Gutachter: 1. Prof. Dr. med. Frank Strutz
 2. PD. Dr. med. Ulrich Wenzel
 3. PD. Dr. med. Harm Peters

Datum der Promotion: 14 März 2005

1	Introduction	1
1.1	Pathogenesis and therapy of chronic progressive renal disease	2
1.1.1	Histological and molecular characteristics	2
1.1.2	The central role of TGF-beta in renal fibrosis	2
1.1.3	The sequence of phases leading to progressive renal fibrosis	3
1.1.4	Therapeutic approaches to chronic progressive renal disease	4
1.2	The L-arginine-NO pathway in renal disease	5
1.2.1	Two faces of the L-arginine-NO pathway	5
1.2.2	NO synthases	6
1.2.3	Effects of L-arginine supplementation on renal disease	7
1.3	NO-cGMP signaling in renal disease	7
1.3.1	Distribution of NO-cGMP signaling in the glomeruli and the tubulointerstitium	8
1.3.2	The physiology of NO-cGMP signaling	10
1.3.3	The pathophysiology of NO-cGMP signaling	11
1.3.4	Pharmacological stimulators of sGC activity	11
1.4	Aim of the study	13
2	Materials and methods	14
2.1	Materials	14
2.1.1	Chemicals, tools and instruments	14
2.1.2	Computer and software	16
2.2	Animal experiments	16
2.2.1	Animals	16
2.2.2	Production of monoclonal antibody OX-7 and mAb 1-22-3	17
2.2.3	Models of anti-thy1-induced renal disease	18

2.2.4	Food and drinking water intakes	18
2.2.5	Drug administration	19
2.3	Experimental design	19
2.3.1	Protocol 1: NO-cGMP signal transduction in the injury phase of acute anti-thy1 glomerulonephritis (day 1 after antibody injection)	20
2.3.2	Protocol 2: NO-cGMP signal transduction in the matrix expansion phase of acute anti-thy1 glomerulonephritis (day 7 after antibody injection)	20
2.3.3	Protocol 3: NO-cGMP signal transduction in anti-thy1-induced chronic glomerulosclerosis (progression phase)	21
2.4	Harvesting of materials	22
2.4.1	Urine collection	22
2.4.2	Removal of kidney and blood and further processing	22
2.4.3	Cell culture	23
2.5	Measurements	25
2.5.1	Systolic blood pressure	25
2.5.2	Renal function	25
2.5.3	Rat tail bleeding time	26
2.5.4	Urinary protein	26
2.5.5	Basal and LPS-stimulated nitrite production	26
2.5.6	Histology	27
2.5.7	Enzyme-linked immunosorbent assay (ELISA)	30
2.5.8	mRNA analysis	34
2.6	Statistical analysis	39
3	Results	40
3.1	Blood pressure, bleeding time and plasma cGMP levels in acute anti-thy1 glomerulonephritis (injury phase and matrix expansion phase)	40

3.1.1	Systolic blood pressure	40
3.1.2	Bleeding time	40
3.1.3	Plasma cGMP levels	41
3.2	Protocol 1: NO-cGMP signaling in the injury phase 1 day after induction of acute anti-thy1 glomerulonephritis	42
3.2.1	Body weight	42
3.2.2	Proteinuria	42
3.2.3	Mesangial cell lysis	42
3.2.4	Glomerular iNOS-NO pathway	43
3.2.5	Glomerular eNOS-NO-cGMP signaling cascade	45
3.3	Protocol 2: NO-cGMP signaling in the matrix expansion phase 7 days after induction of acute anti-thy1 glomerulonephritis	48
3.3.1	Body weight	48
3.3.2	Proteinuria	48
3.3.3	Markers of glomerular matrix expansion	49
3.3.4	Glomerular eNOS-NO-cGMP signaling cascade	50
3.3.5	Mechanisms of Bay 41-2272's renoprotective effects	52
3.4	Protocol 3: NO-cGMP signaling 16 weeks after induction of anti-thy1-induced chronic glomerulosclerosis (progression phase)	55
3.4.1	Body weight	55
3.4.2	Systolic blood pressure	55
3.4.3	Proteinuria	56
3.4.4	Markers of tubulointerstitial matrix accumulation	57
3.4.5	Markers of glomerular matrix accumulation	61
3.4.6	Markers of renal function	63
3.4.7	Tubulointerstitial eNOS-NO-cGMP signaling cascade	64

3.4.8	Glomerular sGC activity	67
3.4.9	Renal macrophage infiltration	68
4	Discussion	71
4.1	Critical evaluation of the methodology used	71
4.1.1	Animal model of anti-thy1-induced acute and chronic renal disease	71
4.1.2	Analysis of markers of renal fibrosis	72
4.1.3	TGF-beta1 as a key marker of matrix expansion	73
4.1.4	Stimulation of sGC by Bay 41-2272	74
4.2	The NO-cGMP pathway in the injury phase of acute anti-thy1 glomerulonephritis	74
4.2.1	Regulation of NO-cGMP signal transduction	75
4.2.2	Effects of Bay 41-2272 on mesangial cell lysis	75
4.3	The NO-cGMP pathway in the matrix expansion phase of acute anti-thy1 glomerulonephritis	76
4.3.1	Regulation of NO-cGMP signal transduction	76
4.3.2	Antifibrotic effects of Bay 41-2272	77
4.4	The NO-cGMP pathway in anti-thy1-induced chronic glomerulosclerosis	78
4.4.1	Regulation of NO-cGMP signal transduction	78
4.4.2	Antifibrotic effects of Bay 41-2272	79
4.5	Transcriptional regulation of NO-cGMP signal transduction from acute to chronic renal disease	80
4.6	Mechanisms of Bay 41-2272's antifibrotic effects	82
4.6.1	Reduction in blood pressure	83
4.6.2	Blood pressure-independent effects of Bay 41-2272	83
4.7	To differentiate the beneficial and detrimental actions of the L-arginine-NO pathway	86

Contents

5	Summary	88
6	Zusammenfassung	90
	Reference list	93
	Abbreviations	104
	Acknowledgements	107
	Erklärung an Eides Statt	108

1 Introduction

In recent years, the number of patients with end-stage renal disease has dramatically increased worldwide [1]. The progression of chronic renal disease represents one of the biggest challenges in nephrology. Regardless of whether the underlying disease is glomerulonephritis, tubulointerstitial disease, hypertensive or diabetic nephropathy, the histological picture of chronic renal disease is uniformly characterized by a progressive accumulation of extracellular matrix (ECM) proteins that obliterates renal function and leads to organ failure [2]. Enhanced understanding of the diverse pathogenetic mechanisms (vascular, metabolic, or immunologic disorders) has resulted in therapeutic advances. However, efforts to halt or even slow the progression of chronic renal disease have been largely unsuccessful. For this reason, there is still a great need for a better understanding of the molecular and cellular mechanisms involved in renal fibrosis.

A number of previous studies have shown that the small molecule nitric oxide (NO) is critically involved in pathological matrix production and accumulation of the kidney. NO has been found to act as a protective signal molecule in blood pressure regulation, platelet deposition and cell infiltration and as a detrimental effector molecule and free radical in the immune response [3, 4, 5, 6, 7]. The enzyme soluble guanylate cyclase (sGC) represents the main signaling pathway of NO via generation of cyclic guanosine monophosphate (cGMP). So far, the role of sGC in renal disease has not been paid much attention to, since it has generally been assumed that this pathway is constitutively expressed and passes on the NO signal without any further modification of its own. The present study was designed to characterize the activity and expression of the NO-sGC-cGMP cascade in the injury, matrix expansion and progression phases of anti-thy1 antibody-induced renal disease of the rat. In addition, the novel pharmacological sGC stimulator Bay 41-2272 was used to enhance NO-sGC-cGMP signaling and to address the question of whether the beneficial and detrimental actions of NO in kidney disease can be therapeutically separated by this approach.

1.1 Pathogenesis and therapy of chronic progressive renal disease

1.1.1 Histological and molecular characteristics

The progression of end-stage renal disease is often owing to the progressive scarring and fibrosis of the kidney, with associated glomerulosclerosis, tubulointerstitial fibrosis and vascular sclerosis, resulting in the loss of filtration surface and renal function. As a fact of clinical relevance, the rate of decline of the renal function in patients with chronic renal disease correlates strongly with the extent of tubulointerstitial fibrosis [8]. Interactions among renal intrinsic cells, inflammatory cells and platelets lead to activation and proliferation of the cells to release inflammatory factors and also stimulate the accumulation of ECM, which is a hallmark of both acute and chronic renal disease [9]. With the expanding of our understanding of the pathogenesis of renal fibrosis, three mechanisms have been found to play an important role in the matrix expansion at molecular level [2, 10]: (1) an excessive synthesis of ECM components such as fibronectin, laminin, proteoglycans and collagens type I, type III and type IV; (2) an inhibited ECM degradation via increased inhibitors of proteinases, such as tissue inhibitors of matrix metalloproteinases (TIMPs) and plasminogen activator inhibitor type 1 (PAI-1), and decreased matrix proteinases, such as matrix metalloproteinases (MMPs), collagenase (MMP-1), gelatinases (MMP-2/9), elastase and serin-protease; (3) increasing synthesis and expression on the cell membrane of a group of cell-matrix receptors called integrins, which interact with matrix components and infiltrative cells.

1.1.2 The central role of TGF-beta in renal fibrosis

Data from numerous studies of experimental and human diseases have shown that the persistent overexpression of the cytokine TGF-beta plays an important role in progressive renal disease from initial tissue injury to tissue fibrosis [10]. A number of factors known to be injurious to the kidney at the cellular level have now been shown to directly induce TGF-beta overexpression, including angiotensin II, mesangial cell stretch, fluid shear stress, high glucose levels, hypoxia, immune-complexes, protein trafficking, platelet derived growth factor and TGF-beta itself [11]. This increase of TGF-beta directly leads to increased pathological matrix accumulation, independent of the initial injury, via the three molecular mechanisms introduced above: increased matrix production, decreased matrix degradation and increased integrin synthesis and

expression [2]. Thus the idea to normalize TGF-beta expression is a reasonable therapeutic target for renal fibrosis. Neutralizing the actions of TGF-beta with either an antibody or the proteoglycan decorin has been shown to prevent excessive matrix accumulation after tissue injury [12, 13]. In this study, TGF-beta expression is a very important parameter for evaluating the effectiveness of the new therapeutic method.

1.1.3 The sequence of phases leading to progressive renal fibrosis

Keeping in mind studies in dermal wounding, matrix accumulation in the kidney can be understood as renal wound healing. In this concept, various kinds of pathological stimuli such as hypertension, hyperglycemia or inflammation are uniformly perceived as injurious by the kidney (injury phase). Renal tissue injury, in turn, then leads to a uniform response with early cell proliferation and subsequent TGF-beta overexpression and matrix accumulation (matrix expansion phase). In acute renal disease, a single injurious stimulus leads to a transient TGF-beta overexpression and matrix accumulation that resolves by itself without over time intervention (normal wound healing). In contrast, in progressive chronic renal disease tissue injury is constant or repetitive, and subsequent TGF-beta overexpression becomes constant (pathological wound healing). As a result, the renal matrix expands continuously and impairs renal function progressively (progression phase).

The concept of normal and pathological renal wound healing is exemplarily reflected in the rat model of anti-thy1-induced renal disease. While in animals with two kidneys, anti-thy1 antibody injection leads to acute and reversible ECM accumulation, injection of anti-thy1 antibody into uni-nephrectomized rats results in progressive renal fibrosis and insufficiency. The injury, matrix expansion and progression phases of this tandem model are characterized as follows:

- 1. Injury phase.** Injury in anti-thy1 renal disease is immunologically induced. Injection and binding of the antibody to the thy1 antigen on the mesangial cell surface, which is a glycosyl-phosphatidyl-inositol-anchored membrane protein [14], causes an acute complement-dependent and iNOS-mediated loss of mesangial cells (mesangiolysis) in the glomeruli [15]. This phase starts minutes after antibody injection and lasts approximately 24 hours.

- 2. Matrix expansion phase.** Following mesangial cell injury, the matrix expansion phase is characterized by early mesangial cell proliferation and marked glomerular TGF-beta overexpression and ECM accumulation, which peaks at 7 days after antibody injection [16].
- 3. Progression phase.** Following the initial mesangial injury and matrix expansion, consistent with a decrease in TGF-beta production [2], the accumulation of ECM resolves by 6-8 weeks in animals with two kidneys. However, injection of monoclonal antibody into uni-nephrectomy animals demonstrates persistent proteinuria, marked TGF-beta expression and typical progressive fibrotic changes, first in the glomeruli, then in the tubulointerstitium. Over 16-20 weeks, the whole organ becomes fibrotic and the animals develop progressive renal insufficiency. This course is highly analogous to human chronic renal disease of glomerular origin. A continuous hyperfiltration injury of the remaining kidney may relate to the chronic progression.

1.1.4 Therapeutic approaches to chronic progressive renal disease

Progressive tissue fibrosis results from ongoing tissue “injury” and “matrix expansion”, so treatment of tissue fibrosis can aim at limiting tissue injury or at interfering directly with the molecular mechanisms mediating the matrix expansion, i.e. the overexpression of TGF-beta. Conventionally, therapies have aimed at reducing glomerular capillary pressure and the injuries that result, such as blood pressure and glycemic control in patients with hypertension and diabetes, but many patients still show progressive renal fibrosis with well controlled blood pressure and glycemia. Many studies have shown that angiotensin II blockade or low dietary protein have blood pressure-independent effects on the overexpression of TGF-beta and the ECM accumulation, besides reducing glomerular capillary pressure and thus decreasing tissue injury [10]. Future therapies should be focused on the mediators of renal fibrosis, such as TGF-beta overexpression, since the tissue “matrix expansion” and subsequent renal failure might be independent of the primary injury. Up until now, no therapies have been able to reduce TGF-beta expression to normal. New insights into second messengers and intracellular transduction pathways may suggest new interventions aimed at neutralizing fibrogenic mediators.

1.2 The L-arginine-NO pathway in renal disease

The amino acid L-arginine is semi-essential and provides molecular substrate for the generation of NO, polyamines, L-proline and agmatine, all of which have been reported to be involved in renal pathology [3, 6, 17, 18]. Endogenous L-arginine synthesis occurs primarily in the proximal tubule of the kidney, using the non-protein amino acid L-citrulline as a precursor [19]. Minor endogenous L-arginine synthesis has been observed in endothelial cells and macrophages [6, 18].

1.2.1 Two faces of the L-arginine-NO pathway

L-arginine is the main endogenous source for the generation of NO by a highly regulated family of enzymes called NO synthase (NOS) that utilize O_2 and NADPH as co-substrates and generate citrulline as a co-product [3, 6, 17]. NO is a diatomic and highly reactive radical gas and plays an important role in numerous biological processes ranging from neurotransmission to vasodilatation, and from inflammation to cell phenotype regulation. Once NO is produced, there exist two main pathways for it to interfere with renal physiology and pathophysiology: as an indirectly acting signaling and as a directly acting effector molecule [5]. At low physiological concentrations, NO acts locally as an important signaling molecule, because it diffuses freely across cell membranes with a diffusion coefficient 1.4 times that of oxygen in vivo, without being utilized by or reacting with intracellular molecules. The electronic structure of NO makes it an excellent ligand for heme-containing enzymes, which include cytochrome P450, NOS and sGC, allowing it to bind to the sGC heme at a low, non-toxic concentration [20]. Therefore, the signaling of NO is mainly mediated by the activation of sGC to increase cGMP levels and modify many of the biological effects of NO, including vasodilatation, inhibition of platelet activation and leukocyte migration [21].

At high concentrations, NO becomes a relatively non-specific destructive effector molecule of the immune system with a key role in mediating host defense, autoimmunity and self-destruction. Most of NO's cytostatic and cytotoxic potential is induced via the irreversible reaction with superoxide radical (O_2^-) and formation of strong oxidant peroxynitrite ($ONOO^-$) [22], which results in nitration of a tyrosine residue in proteins and subsequent damage, inhibition of key enzymes of the respiratory chain

and DNA synthesis by nitrolysis of their iron-containing catalytic elements and fragmentation of DNA. A high concentration of NO can result in autooxidation and the production of dinitrogen trioxide, which is injurious to biological tissues and causes chemical DNA alteration [23].

1.2.2 NO synthases

The glomerulus is a unique vascular network with three specialized cell types: endothelial cells, mesangial cells and visceral epithelial cells to express three potential nitric oxide synthase enzymes, endothelial, neuronal and inducible NOS (eNOS, nNOS and iNOS). Therefore, it has probably been more difficult to define roles for NO in glomerulonephritis than in most other immune and inflammatory diseases, despite a wealth of data [24]. It is assumed that different activities of NOS isoforms are essential for understanding the effects of in vivo NO.

iNOS can be induced by inflammatory cytokines, especially LPS, interferon γ , interleukin-1, and TNF-alpha, elevated in macrophages, renal mesangial and tubular cells in the diseased kidney, and it produces high levels of NO in a calcium-independent manner [25]. In the presence of iNOS, NO is produced in high concentration and becomes an effector molecule, which plays a key role in the period of rapid initial response to immune injury in glomerulonephritis [24]. Its NO production depends on the extracellular L-arginine supply.

eNOS and nNOS also called constitutive NOS (cNOS), are principally constitutively expressed and regulated by calcium [26]. Cell types containing cNOS generate low fluxes of NO for short periods of time, and signaling effects of NO are predominant. Its NO generation is not dependent on the extracellular L-arginine supply. eNOS is expressed by the endothelium. eNOS-dependent NO regulates vascular tone by promoting cGMP-dependent vascular smooth muscle cell relaxation, inhibits platelet aggregation and adhesion and prevents leukocyte adhesion [27]. nNOS also forms a class of cNOS and is localized in the macula densa and the efferent arterioles in the healthy human kidney [28]. nNOS is involved in the regulation of glomerular hemodynamics via tubulo-glomerular feedback and the release of renin [5].

1.2.3 Effects of L-arginine supplementation on renal disease

Over the last few years, L-arginine supplementation has been used as a novel therapy to modify the L-arginine-NO pathway and to slow the progression of renal fibrosis. However, the results of L-arginine treatment are controversial. Enhanced endothelial signaling NO production appears to mediate protective effects, while NO metabolized through the high-output iNOS seems to be a critical effector molecule in immune-mediated tissue damage [5]. In the injury phase of anti-thy1 glomerulonephritis, lupus nephritis, transplant rejection and acute tubular necrosis, where iNOS is increased, L-arginine intake results in the production of high concentrations of NO, which can worsen tissue injury and subsequent fibrosis. Yet in the matrix expansion phase of anti-thy1 glomerulonephritis, 5/6 nephrectomy, ureteral obstruction and nephropathy to diabetes and hypertension, L-arginine supplementation overcomes chronic NO deficiency by enhancing signaling molecule NO production via eNOS, which can reduce TGF-beta overexpression and matrix expansion. Additionally, there are several by-products in the pathway of L-arginine-NO, such as ornithine, polyamines and proline, which are essential for cellular proliferation and ECM deposits [5]. Interestingly, it has been found that L-arginine restriction limited TGF-beta and matrix accumulation, due to the limitation of substrate for polyamine and L-proline production [29]. These data suggest that both dietary L-arginine restriction and supplementation significantly limit matrix expansion, in contrast to normal L-arginine intake, which produces a more severe disease. The therapeutic and detrimental data of L-arginine supplementation reflect the two faces of the L-arginine-NO pathway. Investigating the question of how to enhance the signaling molecular effect and prevent the effector molecular effect is an aim of this study.

1.3 NO-cGMP signaling in renal disease

The most physiologically relevant action of NO mainly produced by eNOS is the activation of sGC and the conversion of GTP into the intracellular second messenger cGMP [30], a cyclic nucleotide, which regulates various cGMP effector systems such as protein kinases (PKG), phosphodiesterases (PDEs) and ion channels, to modify many physiological processes.

1.3.1 Distribution of NO-cGMP signaling in the glomeruli and the tubulointerstitium

The NO-sGC-cGMP signaling pathway is spatially distributed in the glomerular and tubulointerstitial cells of the kidney to a great extent and explained in the following:

- In the glomeruli

As shown in Figure 1, eNOS distributes in endothelial cells of the glomerular vasculature, and nNOS is found primarily in the macula densa, both of which contribute to the production of NO signaling molecules in the glomeruli. Then NO diffuses freely to sGC, which expresses significantly in glomerular arteriolar walls and mesangial cells of the intra- and extraglomerular mesangium [31]. The activated sGC increases cGMP levels, which mediates its main downstream effects via PKG. PKG is a serine/threonine kinase including the soluble PKGI and the membrane-bound PKGII. PKGI is expressed in most tissues. In the glomeruli, PKGI is localized in arteriolar smooth muscle cells, including afferent and efferent arterioles and mesangial cells [32].

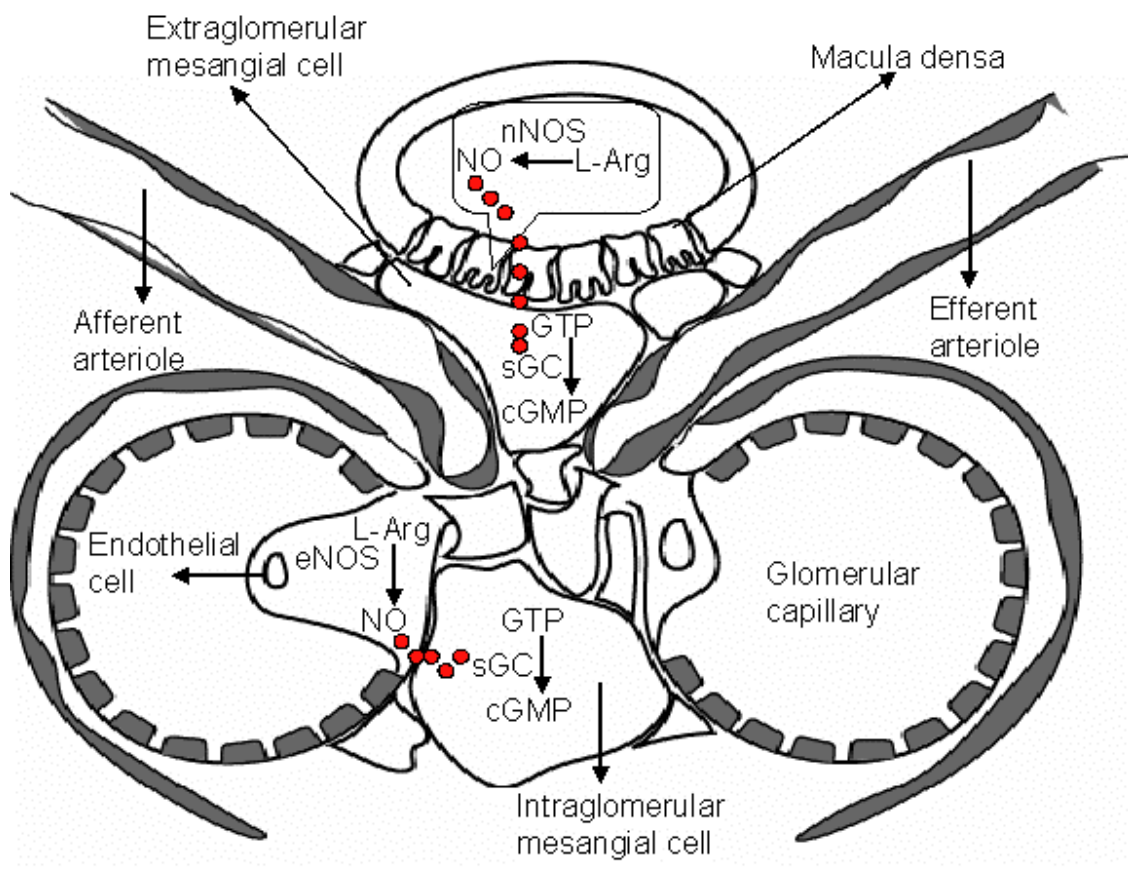


Figure 1: Distribution of NO-cGMP signaling in the glomeruli. L-Arginine (L-Arg), NO (Nitric oxide), Endothelial NO synthase (eNOS), Neuronal NOS (nNOS), cGMP (Cyclic guanosine monophosphate), GTP (Guanosine 5'-triphosphate), sGC (Soluble guanylate cyclase).

- In the tubulointerstitium

As shown in Figure 2, eNOS expresses in endothelial cells of the tubulointerstitial vasculature. Signaling molecule NO generated from eNOS activates sGC in cortical and medullary interstitial fibroblasts and along the renal vasculature outside the glomeruli to increase cGMP levels [31]. The cGMP stimulates PKGI, which has been found in microvascular pericytes and myofibroblasts [32].

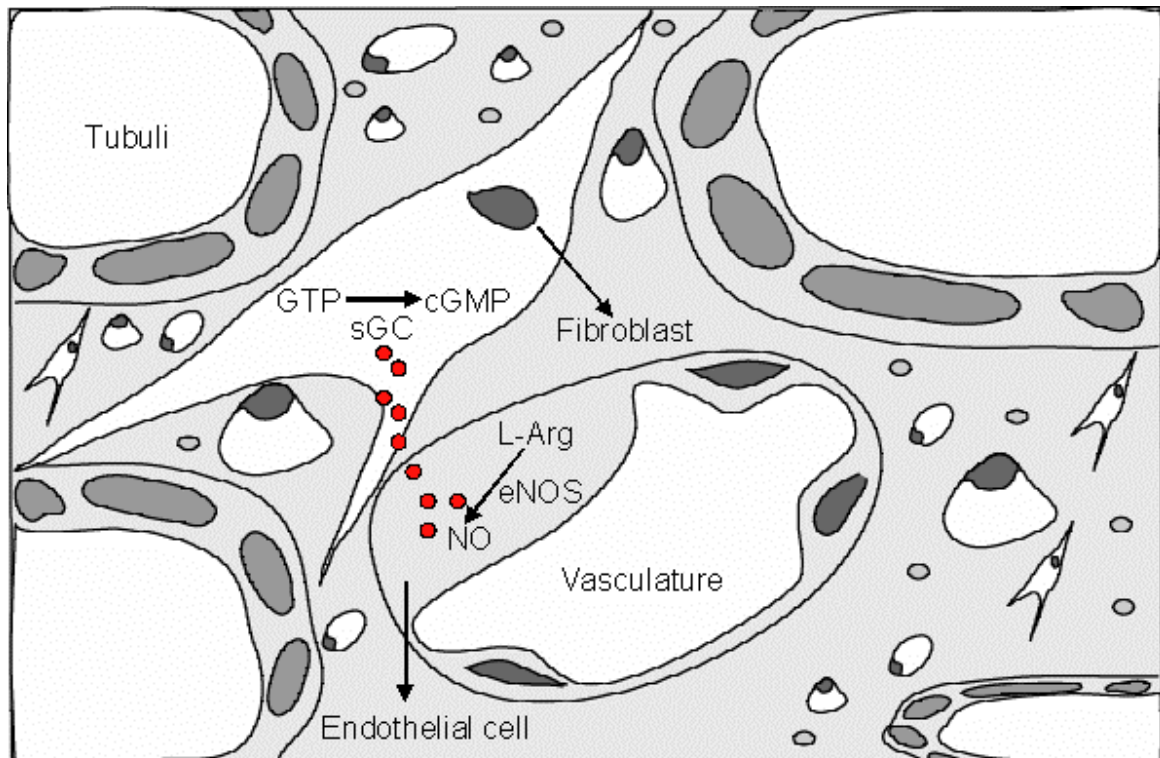


Figure 2: Distribution of NO-cGMP signaling in the tubulointerstitium. L-Arginine (L-Arg), NO (Nitric oxide), Endothelial NO synthase (eNOS), Neuronal NOS (nNOS), cGMP (Cyclic guanosine monophosphate), GTP (Guanosine 5'-triphosphate), sGC (Soluble guanylate cyclase).

sGC has not been found in endothelial cells. A heterogeneous distribution of NOS

and sGC in the renal tissues suggests that NO acts through paracrine diffusion to its target for cGMP generation, rather than by intracellular signaling [31]. The anatomic features of these cells in renal tissue have also proved this, since in the kidney the endothelial cell is closely linked to the vasculature and the mesangium, and the macula densa is adjacent to the extraglomerular mesangium. This is supported by the coincident histochemical localization of PKG and sGC, implying that cGMP is a second messenger acting through intracellular signaling.

1.3.2 The physiology of NO-cGMP signaling

It was established by the mid-1970s that GC exists in membrane-bound and soluble forms in most cells [33]. In general, particulate GC does not respond to NO, since it has no heme prosthetic group in its structure. Purification of GC from the cytosolic compartment revealed the soluble isoform was a heterodimer composed of alpha- and beta-subunits and containing heme as a prosthetic group [34]. The most abundant subunits are alpha1 and beta1, which are found in many tissues [35]. NO binds to the enzyme's prosthetic heme group that is linked to His-105 residue of the beta1-subunit induces conformational changes leading to an up to 400-fold increase in catalytic activity [36]. In vivo, sGC is activated at a low level of NO in the range of 5-100 nM; for NO >200 nM, nearly all of the binding sites for sGC are bound with NO [37]. Activated sGC catalyzes the conversion of GTP to cGMP and pyrophosphate [38].

PKG, PDE and the ion channel are the three main downstream effectors of the NO-cGMP pathway. PKGI can decrease cytosolic calcium and lead to smooth muscle relaxation [39]. Activation of PKG phosphorylates the thromboxane A2 receptor of platelet and then decreases platelets aggregation [40]. Furthermore, PKGI can phosphorylate vimentin, which is involved in neutrophil activation [41]. In contrast to PKGI, PKGII recently has been found in juxtaglomerular renin-secreting cells and in several nephron segments, contributing to renin release and ion transport in the tubule [42]. Therefore, the NO-cGMP pathway plays an important role in vasodilatation, inhibition of platelet aggregation and neutrophil infiltration.

PDEs are enzymes which hydrolyze the 3'-phosphoester bond of cGMP to their biologically inactive noncyclic nucleotides 5'-GMP [43]. The cellular levels of cGMP are

defined by the balance between the activities of the synthesizing enzyme (sGC) and the catabolizing enzymes (PDEs). Investigations during recent years have revealed that PDEs are a critically important component of the NO-cGMP signal transduction. But the distribution of PDEs in the kidney is unclear. Studies of cultured rat mesangial cells show that atrial natriuretic peptide-induced cGMP accumulation is markedly decreased in the presence of angiotensin II, and this inhibition is abolished by IBMX [44]. Thus the PDE inhibitor might represent a novel class of pharmacologic agents suited for “signaling transduction pharmacotherapy” [45].

The action of cation channels regulated by cellular cGMP levels is involved in the molecular basis of sensory systems of visualization and olfaction [32].

1.3.3 The pathophysiology of NO-cGMP signaling

Only little is known about the regulation and expression of NO-cGMP signaling in renal fibrosis. Some data have shown that mechanisms behind the well known fibrogenic systems, such as the angiotensin system, the endothelin and the renal kallikrein-kinin system, are related to NO-cGMP signal transduction [46, 47, 48]. Angiotensin II inhibition could stimulate cGMP production and potentially contribute to renal protection in chronic nephritis [46]; and NO decreases secreted endothelin-1 due to the activation of sGC and increased cGMP generation [48]. In addition, nephrotoxic effects of cyclosporin A may result from the disruption of the bradykinin/sGC pathway [47]. It was shown that dexamethasone, one of several known selective inhibitors of iNOS, had a stimulatory effect on sGC in the glomeruli of rat kidney [49]. The contractile apparatus in the podocyte foot processes was proved to be a target of the cGMP signaling, which correlates with detachment of the cells from the glomerular basement membrane and is closely associated with many nephropathies [50]. Therefore, NO-cGMP signal transduction might take part in the regulation of the kidney functions and the progression of kidney diseases.

1.3.4 Pharmacological stimulators of sGC activity

In this study, the transcriptional regulation of the NO-cGMP pathway was investigated and the pathway was modified to further define its role in progressive renal fibrosis. From the above information, we know that sGC is the most important receptor

for the ubiquitous biological messenger NO and is intimately involved in many signal transduction pathways. Activators of sGC are therefore very desirable as both pharmacological tools and potential therapeutics to probe the NO-cGMP pathway. In the 1990s, YC-1, chemically 3-(5'-hydroxymethyl-2'-furyl)-1-benzylindazole, was identified as a moderate and ~tenfold sGC activator. The actions of YC-1 are heme-dependent, synergistic with NO and with the inhibition of PDE activity [51]. Recently, Stasch and colleagues reported on the discovery of a more potent sGC stimulator devoid of inhibiting PDE activity, Bay 41-2272, chemically 5-cyclopropyl-2-[1-(2-fluorobenzyl)-1Hpyrazolo(3,4-b)pyridin-3-yl]-pyrimidin-4-ylamine, which stimulates sGC up to 30-fold in an NO-independent manner by interacting with cysteines 238 or 243 of the alpha1 subunit, which is different from the binding site of NO [52]. Although Bay 41-2272 alone is not as strong a stimulator of sGC as NO, the specific activity of sGC could be 416-fold above the baseline through the combination of Bay 41-2272 and the NO donor [52]. These effects are probably mediated both by NO-independent stimulation of the enzyme and NO-dependent stimulation by sensitization of sGC towards endogenous NO. It has been demonstrated that, in a rat model of renin transgenic hypertension and spontaneously hypertensive rats (SHRs), oral administration of Bay 41-2272 lowered mean arterial pressure and showed antiplatelet activity, and enhanced survival in a low-NO rat model of hypertension [52]. In comparison to L-arginine, sGC stimulation with Bay 41-2272 avoids the potentially deleterious actions of the effector pathway of NO. A decrease in cGMP levels due to reduced sGC protein was found in the smooth muscle cells of SHRs, despite enhanced eNOS/NO production in the endothelium [53]. In this model, the sGC-cGMP pathway but not the eNOS/NO pathway was impaired, resulting in a decrease in cGMP production. So Bay 41-2272 was chosen to specifically enhance NO-cGMP signaling and further characterize the role of the sGC in renal pathological matrix accumulation.

1.4 Aim of the study

We tested the hypothesis that the NO signal transduction via sGC plays its own, transcriptionally regulated role in pathological renal matrix expansion and that a selective enhancement of the sGC activity by Bay 41-2272 will limit kidney fibrosis in a pressure-independent manner. To test these hypotheses, the following protocols were carried out in the model of anti-thy1 glomerulonephritis.

1. How is the glomerular NO-cGMP signal transduction regulated in the injury phase of acute anti-thy1 glomerulonephritis one day after antibody injection? How does this correlate with anti-thy1 antibody-induced inducible NO production and mesangial cell lysis? How will a pretreatment with Bay 41-2272 affect NO-induced glomerular injury? Bay 41-2272 treatment was started 6 days before disease induction.
2. How is the glomerular NO-cGMP signal transduction altered in the matrix expansion phase of acute anti-thy1 glomerulonephritis seven days after antibody injection? How do the activity and expression of the NO-cGMP signaling pathway relate to glomerular TGF-beta overexpression and matrix accumulation? Will the administration of Bay 41-2272 decrease glomerular matrix expansion? In this protocol, Bay 41-2272 treatment was started 24 hours after disease induction, so that the therapy began after the mesangial cell lysis had occurred.
3. How is the tubulointerstitial and glomerular NO-cGMP signal transduction changed in the progression phase of chronic anti-thy1-induced glomerulosclerosis 16 weeks after antibody injection? Is the signal pathway concordantly or discordantly expressed at the glomerular and tubulointerstitial level? How do the activity and expression of the NO-cGMP signaling pathway correlate with glomerulosclerosis, tubulointerstitial fibrosis and renal insufficiency? Will enhancement of sGC activity through Bay 41-2272 slow the progressive course of chronic anti-thy1-induced glomerulosclerosis? The actions of Bay 41-2272 were compared side-by-side to the sole vasodilator hydralazine. In this protocol, treatment with Bay 41-2272 or hydralazine was started 1 week after disease induction.

2 Materials and methods

2.1 Materials

2.1.1 Chemicals, tools and instruments

All materials used, chemicals and cell culture media, if not differently stated, were purchased from Sigma Chemical-Aldrich Co. (Taufkirchen, Germany).

The following table lists the tools and instruments that were used during the experiments:

Table 1: Tools and instruments used during the experiments.

Blood pressure monitor	Life Science Instruments, California, USA
Camera Polaroid	Polaroid GmbH, UK
Cell culture container	NUNC™ Brand Products, Denmark
Centrifuge 5417R	Eppendorf-Netheler-Hinz GmbH, Hamburg, Germany
Combitips plus, 0.5/2.5/5ml	Eppendorf AG, Hamburg, Germany
Cryo Tube™ Vials	NUNC™ Brand Products, Denmark
Electrophoresis Power Supply EPS 300	Pharmacia Biotech, Sweden
Electrophoresis camber	Hoefer Scientific Instruments, California, USA
Embed machine	Thermo electron corporation, Dreieich, Germany
Eppendorf pipette/Multipette	Eppendorf-Netheler-Hinz GmbH, Hamburg, Germany
Eppendorf tips	Eppendorf AG, Hamburg, Germany
Eppendorf tubes 0.5/1.5/2.0ml	Eppendorf AG, Hamburg, Germany
Exam Gloves	Kimberly-Clark, Roswell, USA
Filter Unit	Schleicher & Schuell GmbH, Dassel, Germany
HiTrap Protein G HP	Amersham Biosciences, Freiburg, Germany
Homogenizer	Labortechnik, Müllheim, Germany
Incubator "HERA Cell"	Heraeus Instruments, Hanau, Germany
Laminal flow	Heraeus Instruments, Hanau, Germany
LightCycler	Roche Diagnostic GmbH, Mannheim, Germany

2 Materials and methods

LightCycler™-Kapillaren	Boehringer Mannheim, Mannheim, Germany
Megafuge 2.0R	Heraeus Instruments, Hanau, Germany
Metabolic cages	3701M081, Tecniplast, Buguggiate, Italian
Metal sieves (ISO 3310-1 checked)	Merck, Darmstadt, Germany
Microplate Reader (MRX)	DYNEX Technologies, Sullyfield Circle, USA
Microscope	Leica Microscopie & Systeme GmbH, Wetzlar, Germany
Microscope Slides, Super Frost Plus	R. Langenbrinck, Emmendingen, Germany
Microscope Cover Glasses	Gerhard Menzel GmbH, Braunschweig, Germany
Microtiter plate shaker TITRAMAX 101	Heidolph Instruments, Schwabach, Germany
Microtome	Microm International GmbH, Walldorf, Germany
Minishaker MS1	IKA Works Inc. Wilmington, Germany
NONC-Immuno 96-Well shape plates	NUNC A/S, Roskilde, Denmark
Operation instruments: forceps, etc.	Medicalis Medizintechnologie, Garbsen, Germany
Parafilm	American National Can™, Greenwich, USA
Pipette 2, 5, and 25 ml	Greiner Bio-one GmbH, Frickenhausen, Germany
Microwave	Bosch, Germany
Multi-adapter for S-Monovette	Sarstedt, Nümbrecht, Germany
pH Meter	Wissenschaftlich Technische Werkstätten, Weilheim, Germany
Polypropylene Conical Tube, 15/50ml	Becton Dickinson, Franklin Lakes, USA
RNA/DNA-Calculator „Gene Quant“	Pharmacia Biotech. Sweden
S-Monovette 9ml with EDTA	Sarstedt, Nümbrecht, Germany
Scale	Sartorius, Göttingen, Germany
Shaker, “Big squid”	IKA-WERKE GmbH, Staufen, Germany
Single-use fine dosage syringe	B.Braun Melsungen AG, Melsungen, Germany
Sterile Syringe 1ml	Becton Dickinson GmbH, Heidelberg, Germany
Thermomixer Compact	Eppendorf AG, Hamburg, Germany

2 Materials and methods

Tissue culture Plates/Dishes	Becton Dickinson, Franklin Lakes, USA
TRIO-Thermoblock	Biotron GmbH, Germany
UV-20 light	Hoefer Pharmacia Biotech INC, San Francisco, USA
Vortex-2-Genie	Scientific Industries (SI), Bohemia, N.Y.USA

2.1.2 Computer and software

1. Measurements of ELISA and data analysis were carried out using BioLinx™ (Dynatech Laboratories, Inc, Sullyfield Circle, USA).
2. For the analysis of the *Real time*-PCR, *LightCycler 3.5.3* (*LightCycler*-Software, Roche, Mannheim, Germany) was used.
3. Statistical analysis was done using SPSS 11.0 (SPSS Inc. Chicago, USA) and Excel 2000 (Microsoft Corporation, USA).
4. Graphical representations were done using Excel 2000 and Sigma Plot™ (Systat Software GmbH, Scientific Graphic Software 7.0, Erkrath, Germany).
5. The final thesis was written using Word 2000 (under Windows NT, Microsoft Corporation, USA) and Reference Manager (Adept Scientific GmbH, Frankfurt, Germany).

2.2 Animal experiments

Animal care and experiments were in conformity with the guidelines of the American Physiological Society and were approved by local authorities (animal experiments register No. G 0240/02, Landesamt für Arbeitsschutz, Gesundheitsschutz und technische Sicherheit Berlin).

2.2.1 Animals

Male Wistar rats (initial weight of 180-250 g, Charles River, Sulzfeld, Germany) were used in this study. Animals were housed in the center of the animal laboratory (Tucholsky-Straße 2, 10117 Berlin, Germany), caged in pairs with free access to food and drinking water in a constant temperature room with a 12-hour dark/12-hour light cycle. The animals were visited daily, and the consumption of food and drinking water and body weight were monitored.

2.2.2 Production of monoclonal antibody OX-7 and mAb 1-22-3

2.2.2.1 Cell culture

Monoclonal mouse hybrid granny cells of the OX-7 (company center of Applied Microbiology & Research, Salisbury, UK) and mAb 1-22-3 (Gift from Fujio Shimizu, Nephrology, Niigata University Graduate School of Medical and Dental Sciences, Niigata, Japan) were used. The cells stored at -70°C were transferred under sterile conditions into the following culture medium (Biochrom AG, Berlin, Germany): RPMI 1640 supplemented with 9% fetal calf serum, 1.6% G-50 glucose solution, 0.3% HEPES, 100 U/ml Penicillin and 100 $\mu\text{g/ml}$ Streptomycin in a culture bottle, incubated at $37^{\circ}\text{C}/5\%$ CO_2 and passaged at confluence. The cells were microscopically controlled every 48 hours by means of Trypan Blue staining, which differentiates vital and non-vital cells. At the same time, the pH of the culture medium was determined. Every two days, the cell culture medium was changed and the cells proliferated. 35 ml cell suspension with 0.5×10^6 /ml cells were transferred into a miniPERM cell culture module (Heraeus Instruments, Hanau, Germany) and put on a lathe fixture (Heraeus Instruments, Hanau, Germany) for being mixed to achieve a better oxygen supply to the cells. When the cells in the culture module reached a density of 8×10^6 /ml, the contents of the culture modules were divided into 4 miniPERM culture modules. After incubation for 24 and/or 48 hours, the medium was changed according to cell growth and the pH of medium. If cell density reached 11.5×10^6 /ml, 17 ml were taken out of the culture module and stored at 4°C for later purification. The cell culture module was filled up with culture medium again to a total volume of 35 ml.

2.2.2.2 Purification of the monoclonal antibody OX-7/mAb 1-22-3

To purify the IgG fraction, the cell culture suspension was mixed with binding buffer (20 mM sodium phosphate, pH 7.0). The mixture was filled to a pre-equilibrated Protein G column at a flow velocity of 0.5 ml/min. There is a strong affinity between IgG and protein G at pH 7. Then the IgG was eluted with elution buffer (0.1 mol/l glycine-HCl, pH 2.7) and neutralized with 1 mol/l Tris-HCl (pH 9). After extensive dialysis against PBS (Biochrom AG, Berlin, Germany) (pH 7.4) for 24 hours, the antibody concentration was adjusted to 1 mg/ml by reading the absorbance at 280 nm and stored at -70°C until use.

2.2.3 Models of anti-thy1-induced renal disease

2.2.3.1 *Acute anti-thy1 glomerulonephritis*

The acute anti-thy1 glomerulonephritis (aGN) model was induced by tail vein injection of monoclonal antibody OX-7 (1 mg/kg body weight in PBS) under light ether (Chinosolfabrik, Seelze, Germany) anesthesia. Control animals were injected with equal volumes of PBS.

2.2.3.2 *Chronic anti-thy1-induced glomerulosclerosis*

In the anti-thy1-induced chronic glomerulosclerosis (cGS) model, before antibody injection, unilateral nephrectomy was performed under anesthesia of 0.1 mg ketanest/0.01 mg xylazin per 100 g body weight (ketamin 10%, WDT, Garbsen, Germany; Rompun 2%, Bayer Vital GmbH, Leverkusen, Germany). A small flank incision was made, then the right kidney was separated and removed after the right renal artery, vein and ureter were ligated at the renal pedicle. The monoclonal antibody mAb 1-22-3 was injected at a high dose of 5 mg/kg body weight in PBS three days after uni-nephrectomy. Control animals with and without uni-nephrectomy were injected with equal volumes of PBS.

2.2.4 Food and drinking water intakes

All animals were fed a normal protein diet (Altromin No.1311, Altromin, Lage, Germany) for at least three days before the start of the experiment to allow equilibration. Dependent on body weight, the drugs were added to the food or the drinking water of treated animals. The calculated amount of the drugs was added to 1 kg flour of the standard rat food stated as above and mixed evenly. Then 600 ml water were added to the mixture and mixed, until a homogeneous dough developed. The dough was strongly rolled out about 1 cm thick and shaped by means of biscuit mold. The biscuits were dried with the help of a warm air fan. The average food and water consumptions of the animals from preliminary tests were about 25 g/day and 50 ml/day. The active substance quantity given is based on this consumption. In order to ensure that the calculated active substance quantity was actually ingested, the food and water consumptions of the treated group were controlled daily.

Table 2: Contents of the food (average content in 1 kg diet).

Contents of breeding diet	
Raw protein	22.50%
Lysine	1.20%
Raw fat	5%
Raw fiber	4.50%
Raw ash	6.50%
Calcium	0.90%
Phosphorus	0.70%
Vitamin A	15000 IE
Vitamin D ₃	600 IE
Vitamin E	75 mg
Copper	5 mg

2.2.5 Drug administration

Bay 41-2272 (10 mg/kg body weight/day) was added to the food meal. This dose has previously been reported to reduce sufficiently the blood pressure in spontaneously hypertensive rats [52]. Bay 41-2272 was generously provided by Dr. Johannes-Peter Stasch, Pharma Research Center, Bayer AG, Wuppertal, Germany.

Hydralazine was given with the drinking water in a dose of 15 mg/kg body weight/day. The dosage was adjusted according to the blood pressure, which in the hydralazine-treated rats should be the same as that of Bay 41-2272-treated rats. Although the precise mechanism of action of hydralazine is not fully understood, it apparently lowers blood pressure by exerting a peripheral vasodilating effect through a direct relaxation of vascular smooth muscles, which might result from the inhibition of the release of Ca²⁺ from the sarcoplasmic reticulum [54].

2.3 Experimental design

The NO-cGMP signaling cascade was separately analyzed in the injury phase of acute anti-thy1 glomerulonephritis (protocol 1), the matrix expansion phase of acute anti-thy1 glomerulonephritis (protocol 2) and the anti-thy1-induced chronic

glomerulosclerosis (protocol 3). The expression analysis of the NO-cGMP cascade included mRNA expression of eNOS and alpha1 and beta1 sGC. The activity of sGC was determined at basal level and in response to a defined amount of NO in freshly isolated glomeruli and cortical tissues *ex vivo*.

2.3.1 Protocol 1: NO-cGMP signal transduction in the injury phase of acute anti-thy1 glomerulonephritis (day 1 after antibody injection)

Six days before antibody injection, male Wistar rats were divided into the following groups:

- A) PBS-injected controls (Control, n=6);
- B) anti-thy1 antibody-injected animals, no treatment (aGN, n=10);
- C) anti-thy1 antibody-injected animals plus Bay 41-2272 (aGN+Bay 41-2272, n=10).

Treatment with Bay 41-2272 was started 6 days before and continued until 24 hours after OX-7 injection. On the fifth day, systolic blood pressure was measured. On the sixth day, glomerulonephritis was induced and 24-hour urine specimens were collected. The animals were sacrificed 24 hours after disease induction, when mesangial cell lysis develops and inducible glomerular NO production is markedly elevated [55]. In the injury protocol, urinary protein, glomerular cell number, NO production and iNOS mRNA expression were analyzed as indicators of mesangial cell injury.

2.3.2 Protocol 2: NO-cGMP signal transduction in the matrix expansion phase of acute anti-thy1 glomerulonephritis (day 7 after antibody injection)

One day after antibody injection, male Wistar rats were assigned to the following groups:

- A) PBS-injected controls (Control, n=6);
- B) anti-thy1 antibody-injected animals, no treatment (aGN, n=10);
- C) anti-thy1 antibody-injected animals plus Bay 41-2272 (aGN+Bay 41-2272, n=12).

Bay 41-2272 treatment was started 24 hours after anti-thy1 antibody injection for 6 days, when mesangial cell lysis is complete and the fibrotic response begins [56]. On

the fifth day, systolic blood pressure was measured. On the sixth day, 24-hour urine specimens were collected. The animals were sacrificed seven days after disease induction, when the fibrotic response peaks [16]. In this protocol, urinary protein and parameters of glomerular matrix expansion, including glomerular matrix score and expression of TGF-beta1, fibronectin and PAI-1, were measured. In addition, mRNA expression of P-selectin and immunohistological detection of glomerular macrophage infiltration and fibrinogen deposition were also analyzed.

2.3.3 Protocol 3: NO-cGMP signal transduction in anti-thy1-induced chronic glomerulosclerosis (progression phase)

A 24-hour proteinuria was measured one week after anti-thy1 antibody injection. On the basis of the actual 24-hour proteinuria achieved, the diseased animals were randomized and assigned to the following groups:

- A) non-nephrectomized, PBS-injected controls (2-K Control, n=5);
- B) uni-nephrectomized, PBS-injected controls (1-K Control, n=4);
- C) uni-nephrectomized, anti-thy1-injected animals, no treatment (cGS, n=18);
- D) uni-nephrectomized, anti-thy1-injected animals treated with Bay 41-2272 (cGS+Bay 41-2272, n=18);
- E) uni-nephrectomized, anti-thy1-injected animals treated with hydralazine (cGS+Hydralazine, n=12).

To avoid interference with the induction of the disease, Bay 41-2272 and hydralazine treatments were started one week after antibody injection. Systolic blood pressure was assessed in week 8 and the days before sacrifice. 24-hour proteinuria was measured after 1, 4, 8, 12 and 16 weeks. The animals were sacrificed 16 weeks after disease induction. Proteinuria, blood pressure, tissue fibrosis, macrophage infiltration and kidney function were determined. Glomerular and tubulointerstitial changes were analyzed separately. Glomeruli were isolated by a graded sieving technique. Since renal cortex consists mainly of tubulointerstitial tissue (>95%), it was used as representative of the tubulointerstitium. Analysis of fibrosis involved a histological scoring of the matrix accumulation and molecular analysis of the expression of the key fibrosis marker and mediator TGF-beta1, the matrix protein fibronectin and

the matrix degradation inhibitor PAI-1. Tubulointerstitial and glomerular macrophage infiltrations were analyzed by immunohistochemistry using an ED1-antibody. In addition, mRNA expression of the adhesion molecule P-selectin was measured. Blood creatinine and urea concentrations, calculated creatinine clearance and blood hematocrit served as markers of renal function.

2.4 Harvesting of materials

2.4.1 Urine collection

For urine collection, the animals were individually housed in metabolic cages for 24 hours. The metabolic cages are equipped with a special funnel and cone design that effectively separates urine from feces, food remainder and water. To avoid excessive bacterial growth and an associated change of some examined parameters, 100 µl penicillin/Streptomycin (10000 U/10000 µg/ml) were pipetted into the urine collection tube. During their accommodation in metabolic cages, the animals had free access to food and drinking water. After 24 hours, urine was collected, centrifuged for 10 min at 10000 rpm to remove particulate matter and frozen for later measurements at -25°C.

2.4.2 Removal of kidney and blood and further processing

2.4.2.1 *Removal of kidney and blood*

At the end of the experiment, the rats were anaesthetized with ketamine and Xylazine and sacrificed. The animals were fixed in an upside-down position. Then the abdominal cavity was opened with a u-shaped cut from penis to both rib elbows endings. Blood was drawn from the lower abdominal aorta until the heartbeat stopped. Ice-cold sterile PBS was then injected, until the heart beat again. Under the liver, the large body artery and the lower vein were clamped and then the lower vein was cut. The kidney was perfused with 40 ml ice-cold sterile PBS under stable pressure. The blood-empty kidneys were then removed and stored in 50 ml ice-cold sterile PBS until further processing. The blood was filled into EDTA-coated tubes, centrifuged at 3000 rpm and 4°C for 10 min, aliquot according to measured parameters, e.g. urea, creatinine and cGMP [20 µl 5 mM IBMX (Alexis GmbH, Grünberg, Germany) was added to 980 µl of plasma to block cGMP degeneration], and they were frozen at -25°C.

2.4.2.2 *Isolation of glomeruli*

The kidneys were separated from fats and capsules. A fifth of the total kidney was separated at a kidney pole. Different parts of the kidney pole were divided for fixing in 10% neutral buffered formalin (Merk, Darmstadt, Germany) and shock-frozen by liquid nitrogen for RNA investigation and then kept at -80°C. Then the remaining kidney tissue was halved and the renal pelvis was cut out with small curved shears. The kidney tissue was chopped up with a blade on an ice-cold glass until a homogeneous viscous mass developed, which was then passed through metal sieves and mechanically broken down to yield glomeruli. The tissue mass was transferred to the highest sieve with the mesh size of 160 µm, pressed by means of glass spatulas and washed with PBS. Tissues accumulated on the second sieve with the mesh size of 125 µm. The tissues were collected and flushed directly and vigorously with PBS several times. The glomeruli accumulated on the lowest sieve with the mesh size of 71 µm and were collected by means of indirect 300 ml PBS washing. The isolated glomeruli were then transferred into a 50 ml PBS tube and centrifuged for 5 min at 1900 rpm and 4°C.

2.4.2.3 *Preparation of tubulointerstitial tissue*

Since renal cortex consists mainly of tubulointerstitial tissue (>95%), it was used as representative of the tubulointerstitium. The kidney cortex was chopped up with a blade on an ice-cold glass, and then 60 mg chopped cortex were taken into 6 ml culture medium at a density of 10 mg/ml for the cortical cell culture.

2.4.3 Cell culture

In protocol 1 (injury phase), basal and LPS-stimulated nitrite production of glomeruli was measured in glomerular culture with or without LPS. In protocol 2 (matrix expansion phase), glomerular TGF-beta1, fibronectin and PAI-1 production and basal and NO-stimulated sGC activity were measured in glomerular culture with or without DEA/NO; in addition, glomerular TGF-beta1 production in vitro in the presence of Bay 41-2272 was also analyzed. In protocol 3 (progression phase), TGF-beta1, fibronectin and PAI-1 production and basal and NO-stimulated sGC activity were measured in glomerular and tubulointerstitial culture with or without DEA/NO. Two or three samples from each animal were analyzed.

2 Materials and methods

The culture medium was made from DMEM supplemented with 0.1 U/ml insulin, 100 U/ml penicillin and 100 µg/ml streptomycin (Biochrom AG, Berlin, Germany). Cortical cell cultures were set as described above. The isolated and centrifuged glomeruli were resuspended in 5 ml culture medium. 10 µl were taken and extended on a Petri dish in the form of a line. Then glomeruli were microscopically counted and the concentration of glomeruli was adjusted to 2000 per ml. Glomerular concentrations were determined to achieve the comparability of different samples. After 48 hours of incubation at 37°C/5% CO₂, supernatants were harvested and stored at -25°C until analysis of TGF-beta1, fibronectin or PAI-1 contents.

In order to prove the direct regulation of TGF-beta1 production by stimulated sGC independent of blood pressure, glomeruli from 6 normal and 8 nephritic rats (protocol 2) were resuspended in DMEM culture medium at a density of 2000 per ml. The sGC stimulator Bay 41-2272 was added in increasing concentrations: 0, 0.1, 1, 5 and 10 µM. After 48 hours of incubation at 37°C/5% CO₂, supernatants were harvested and stored at -25°C until analysis of glomerular TGF-beta1 production.

In protocol 1 (injury), glomeruli were cultured at a density of 2000 per ml for 48 hours (basal NO glomerular production). Additional samples were cultured in the presence of 10 µg LPS from *Escherichia. Coli* (serotype 0127:B8) to stimulate inducible NO production (stimulated glomerular NO production). Nitrite served as indicator of NO production and was determined by the Griess reaction in glomerular culture supernatants.

150 µl cortical cells and glomeruli in DMEM were pipetted into a 96-well microplate for further cGMP assessment. The microplate with samples was first prewarmed at 37°C/5% CO₂ for one hour, then was added 20 µl 5 mM IBMX and incubated for 10 min to inhibit cGMP degradation. NO-mediated stimulation was studied by addition of 20 µl 1 mM DEA/NO (Alexis GmbH, Grünberg, Germany). After 10 min of incubation, the microplate was put on ice to stop the reaction and added 20 µl 5% dodecyltrimethylammonium bromide to facilitate cell lysis. A microscopic evaluation with Trypan blue was carried out to check whether the cells were lysed. Lysed cells were stored at -80°C for cGMP ELISA.

The remaining glomeruli were homogenized in Trizol™ Reagent (Invitrogen life technologies, Carlsbad CA, USA). After 5 min of incubation at room temperature, the samples were stored at -80°C until RNA isolation.

2.5 Measurements

2.5.1 Systolic blood pressure

Systolic blood pressure was measured in trained conscious animals by a tail cuff method with plethysmography [57]. The animals were fixed in a dark acrylic glass pipe. This pipe was kept at a moderate temperature in an ambient chamber. After 5 min acclimatization, a seal with an integrated sensor was put around the rats' tails about 1 cm before the tail root, and in each case three measurements were made, whose values were averaged. Before the actual beginning of the experiment, the animals were accustomed to the procedure, in order to avoid misleadingly high values caused by stress.

2.5.2 Renal function

Plasma creatinine and urea levels and creatinine clearance were determined as markers of the excretory kidney function and blood hematocrit was analyzed as the renal endocrine, erythropoietin-producing capacity. Plasma and urine creatinine and plasma urea were determined with the analyzer Hitachi 747-400 (Diamond Diagnostic Inc., Holliston, USA). For the determination, the method of Jaffé is used in this equipment, in which creatinine in alkaline solution and picrate form a yellow-orange colored complex which can be photometrically measured. The color of the complex relates directly to the concentration of creatinine. The creatinine clearance was calculated on the basis of: $(\text{Urinary creatinine} \times \text{urine volume}) / (\text{serum creatinine} \times \text{collecting time } 1440 \text{ min})$. Urea is measured with a kinetic UV test. At first urea reacts with water and is converted by urease into ammonium and carbon dioxide. Then the produced ammonium reacts with α -Ketoglutarat and NADH (nicotine amide adenine dinucleotid hydrogen). The conversion of NADH is afterwards kinetically measured. Hematocrit was determined by the percentage of blood cells in blood plasma after a 10 min/ 3000 rpm centrifugation.

2.5.3 Rat tail bleeding time

Shortly before the anesthetized rats were sacrificed, the dorsal part of the tail was cut with a standardized incision (10 mm long, 1 mm deep) with a sterile razor blade. The bleeding time was then measured [58].

2.5.4 Urinary protein

The total urinary protein was determined by the Pyrogallol red method in a colorimetric terminator point with the Pyrogallol-Red method kit (Biocon Diagnostik, Marienhagen, Germany). The Pyrogallol-red-molybdate complex used is bound to proteins. The binding causes a shift of the absorbance peak to 600 nm. The color intensity can directly reflect the total protein concentration [59]. Due to the presence of detergents in the reagents, different types of proteins give similar recoveries [60]. The sample concentration could be read by a standard curve consisting of six dilutions with protein concentrations from 0 to 5 g/l. 10 µl standard and/or sample were added to a 96-well microplate. Then 350 µl ready for use reagent were pipetted into each well. Standard dilutions, samples and empty value were measured in duplicate. After 10 min response time, the developed color product could be read photometrically with a wavelength of 570 nm on the plate reader. The protein concentrations of samples were calculated: $A \text{ (absorbance) sample} / A \text{ standard} \times \text{urine volume} \times \text{dilution} = \text{proteins in mg/day}$.

2.5.5 Basal and LPS-stimulated nitrite production

Nitrites are stable oxidative end products of NO and served as indicators of endogenous NO synthesis [3]. Nitrite levels in cell culture supernatants were measured by the Griess reaction [61]. 10 standard samples (50, 25, 20, 15, 10, 7.5, 5, 2.5, 1, 0 µM) were prepared with sodium nitrite. 50 µl of sample were then mixed with 100 µl Griess reagent [0.05% N-(1-naphthyl) ethylene diamine dihydrochloride, 0.5% sulfanilamide in 45% glacial acetic acid] in 96-well plates. After 10-min incubation in the dark, absorbance was read at 570 nm in an automated plate reader. Then basal and LPS-stimulated glomerular NO production were analyzed.

2.5.6 Histology

Kidney tissue was fixed with 10% neutral buffered formalin for 12 hours and then embedded in paraffin. The tissue was transferred to an embed automat after initial drainage in paraffin. The paraffin-impregnated tissue was poured in block and cut 2-3 μm thick with the microtome after hardening. All slides were dried afterwards for 24 hours at 37°C in the reheating furnace. The slides were deparaffinized before the stain procedure.

Uncoated slides were used for PAS staining. The slides were brought into xylene (J.T.Baker, Deventer, Holland) twice for 10 min and transferred afterwards for 2 min into the descending alcohol row (Herbeta-Arzneimittel, Berlin, Germany) (ethanol 100%, 100%, 96%, 96%, 80%, 50%, and distilled water).

For the immunohistological staining, the slides were transferred into fresh xylene twice for 10 min and into each unit of the descending alcohol row for 10 min. Subsequently, the deparaffinized slides were cooked in a pot with citrate buffer by pH 6.5 at 96°C for 10 min and kept in distilled water after cooling until the subsequent procedure. For the immunohistology, the slides remained in distilled water before the embedment with ImmuMount (Thermo Shandon, USA).

2.5.6.1 PAS staining

For this staining, the following solutions were first set:

- A) Alcoholic periodic acid solution: 1 g periodic acid was dissolved in 30 ml distilled water. Then 70 ml 100% ethanol were mixed in the solution.
- B) Alcoholic disulphide solution: 0.5 g potassium disulphide were dissolved in 30 ml distilled water, and then 70 ml 100% ethanol were added.
- C) Schiff reagent commercial mixture (Merk, Darmstadt, Germany).

After deparaffinization, the slides were placed in 1% periodic acid for 10 min. Then they were washed in running tap water for 5 min and afterwards briefly in disulphide solution. The slides were then brought into the Schiff reagent warmed to 40°C and incubated at 40°C for 20 min. Then the slides were dipped briefly in disulphide solution again and washed in running tap water for 10 min. After 5 min's counterstain in Meyer's

hematoxylin (Merk, Darmstadt, Germany), the slides were blued for 10 min in running tap water. Then the slides were transferred into the ascending alcohol row for 1 min (in distilled water, and ethanol 50%, 80%, 96%, 96%, 100%, 100%, and twice xylene) and covered up with Corbit-Balsam (R.Langensbrink, Emmendingen, Germany) (37°C). Stain result: Connective tissue: blue, Cytoplasm: pink, Nucleus: blue-black and Acidic Mucopolysaccharide: bright magenta.

2.5.6.2 ED1 staining

Before the staining, tris-buffered saline (TBS) had to be manufactured. At first two master solutions were set. Master solution A: 0.5 mol/l Tris-solution, consisting of 60.55 g Tris (hydroxymethyl)-aminomethan /1 l distilled water. Master solution B: 1.5 mol/l NaCl solution, consisting of 87.66 g NaCl/1 l distilled water. The master solutions were kept at 4°C. TBS was set before use in the ratio of 1 part solution A +1 part solution B +8 parts distilled water, and then adjusted to pH 7.6 with 0.5 mol/l HCl.

The immunohistological staining of ED1 was accomplished with the paraffin slides in a humidified chamber. The slides were first deparaffinized and brought into the descending alcohol row and cooked in citrate buffer as described above. Then the sections on the slides were circled with a tallow pencil (DAKO Cytomation, Hamburg, Germany) and placed in TBS buffers. Then the sections were blocked with inactivated fetal calf serum for 30 min. The sections were incubated with the primary antibody Mouse anti-Rat ED1 (Serotec GmbH, Düsseldorf, Germany) for 30 min. The antibody was diluted 1:100 with an antibody dilution medium (1 part inactivated fetal calf serum, 1 part RPMI medium, 8 parts distilled water). There were three cuts on each slide. One cut served as negative control and was incubated only with antibody dilution medium instead of the primary antibody. They were rinsed with TBS buffer after the incubation. Then incubation with the secondary antibody Rabbit anti-Mouse-Ig (DAKO) followed for 30 min. After 30 min incubation with APAAP Mouse-Ig (DAKO), the sections were rinsed again with TBS buffer and incubated with the substrate fast red (DAKO) about 5 min. The color was microscopically controlled. Then the sections were rinsed with distilled water and placed in Mayer's Hematoxylin as counterstaining for 1min. Then they were washed with running tap water for 10 min and covered up with ImmuMount.

Stain result: cell nucleus: blue-black, immunocomplexes: bright red.

2.5.6.3 *Fibrinogen staining*

The immunohistological staining of fibrinogen was accomplished with the paraffin slides in a humidified chamber. The slides were first deparaffinized and brought into the descending alcohol row and cooked in citrate buffer as described above. Then the sections on the slides were circled with a tallow pencil and placed in TBS buffers. Then the sections were blocked with 3% bovine albumin for 30 min. The sections were incubated with the primary antibody Rabbit anti-Human fibrinogen (DAKO Cytomation, Hamburg, Germany) for 30 min. The antibody was diluted 1:200 with an antibody diluent. There were three cuts on each slide. One cut served as negative control and was incubated only with antibody diluent instead of the primary antibody. They were rinsed with TBS buffer after the incubation. Then incubation with the secondary antibody Mouse anti-Rabbit-Ig (DAKO) followed for 30 min. And then incubation with the third antibody Rabbit anti-Mouse-Ig was executed for 30 min after TBS rinsing. After 30 min incubation with APAAP Mouse-Ig, the sections were rinsed again with TBS and incubated with the substrate fast red about 5 min. The color was microscopically controlled. Then the sections were rinsed with distilled water again and placed in Mayer's Hematoxylin as counterstaining for 1 min. Then they were washed with running tap water for 10 min and covered up with ImmuMount. Stain result: cell nucleus: blue-black, immunocomplexes: bright red.

2.5.6.4 *Histological evaluation*

All microscopic examinations were performed in a blinded fashion. Three μm sections of paraffin-embedded tissue were stained with PAS. In protocol 1, the number of cell nuclei was counted in 15 glomeruli of 80-100 μm diameter from each animal for calculation of mesangial cell lysis [55]. In protocol 2, the histological evaluation was made by means of light microscopy according to the semiquantitative procedure [56]. The percentage of mesangial matrix-occupying area in 20 glomeruli from each rat was graded as: 0=0%, 1=0-25%, 2=26-50%, 3=51-75% and 4=76-100%. In protocol 3, glomerular matrix expansion was evaluated by rating the mesangial matrix-occupying area in 15 glomeruli from each rat, using the same scoring system as above.

Tubulointerstitial matrix deposition was determined in 15 randomly selected cortical areas per sample observed at x200 magnification, using the following scale: 0=normal, 1=lesions involving less than 10% of cortical area, 2=involving 10-30%, 3=involving 31-50% and 4=involving more than 50%, respectively. ED1 staining representing glomerular macrophage infiltration was counted in at least 15 glomerular sections from each rat, tubulointerstitial macrophage infiltration in at least 15 randomly selected cortical areas per sample observed at x200 magnification, respectively. Due to glomerular deposition of platelets as platelet-fibrinogen aggregates, glomerular fibrinogen staining was used as indirect indicator for glomerular platelet deposition, and glomerular fibrinogen deposition is expressed as the percentage of fibrinogen-positive areas in 15 glomeruli from each rat (0-100%) [58].

2.5.7 Enzyme-linked immunosorbent assay (ELISA)

An ELISA technology was used for the assessment of the cytokine TGF-beta1, PAI-1, protein fibronectin and cGMP. TGF-beta1 was determined by an ELISA sandwich methodology. The sample is incubated in a microplate precoated with a capture antibody. The antigen in the sample binds with the capture antibody and becomes immobilized. After removal of the unbound antigen, enzyme conjugate is added and then binds with the immobilized antigen to form a sandwich of antibody-antigen-antibody/enzyme bound to the microplate. After the unbound antigen or antibody and free conjugate are washed off, a chromogenic enzyme substrate is added, and reacts with the bound enzyme and produces a color reaction. A quantitative determination of antigen or antibody concentrations is obtained by absorbance measurement of the colored reaction product using a spectrophotometric microwell reader.

PAI-1, fibronectin and cGMP were determined by competitive ELISA. In competitive ELISA of PAI-1 and fibronectin, the antigen is coated onto the inside wall of the microplate. The antigen from the test sample and the antigen coated on the microplate compete for a limited number of primary antibody-binding sites. An enzyme-labeled secondary antibody is added afterwards. In cGMP ELISA, the antibody is coated onto the inside wall of the microplate. The antigen from the test sample and the enzyme-labeled antigen conjugate compete for a limited number of immobilized antibody-binding sites. The amount of antigen-antibody-enzyme complex bound to the solid

phase (microplate) is inversely related to the concentration of antigen present in the sample. After the unbound enzyme antigen conjugate is washed off, chromogenic substrate is added. The bound enzyme conjugate reacts with the chromogenic substrate and produces a color reaction. A quantitative determination of antigen or antibody concentrations is obtained by absorbance measurement of the colored reaction product using a spectrophotometric microplate reader.

2.5.7.1 *TGF-beta1*

The TGF-beta1 concentrations were determined in the cell culture supernatant with a commercially available ELISA kit (TGF-beta1 DuoSet™, R&D Systems, Wiesbaden, Germany). A 96-well microplate was coated with 100 µl capture antibody of mouse anti-TGF-beta1 (2 µg/ml) per well and left overnight at room temperature. Each well was aspirated and washed with wash buffer PBST (0.05% Tween20, Boehringer Ingelheim, Heidelberg, Germany, in PBS) and blotted against clean paper towels. The plate was then blocked by adding block buffer (5% Tween20, 5% Sucrose in PBS) and incubated at room temperature for 1 hour. Then the plate was washed again and ready for sample addition. Latent TGF-beta1 in the samples should be first activated to the immunoreactive form. 100 µl samples were acidified with 20 µl 1 mol/l HCl (Merck, Darmstadt, Germany), mixed thoroughly at room temperature for 10 min and then neutralized with 20 µl 1.2 mol/l NaOH/0.5 mol/l HEPES buffer. A standard solution of recombinant human TGF-beta1 (2000 pg/ml) was diluted with Reagent Diluent (1.4% delipidized bovine serum, 0.05% Tween20 in PBS) to form a seven-point standard curve using 2-fold serial dilutions from 2000 pg/ml to 0 pg/ml. 100 µl standard and the activated sample were pipetted into the precoated microplate and incubated for 2 hours at room temperature. Then the aspiration and wash of the microplate were repeated again. 100 µl detection antibody (300 ng/ml), chicken anti-human TGF-beta1, were added to each well and incubated for 2 hours at room temperature. Then the microplate was washed again. 100 µl streptavidin-HRP were added to each well and incubated 20 min at room temperature in the dark. After washing the microplate, 100 µl substrate solution (a mixture of H₂O₂ and Tetramethylbenzidine) (Biochrom AG, Berlin, Germany) were added to each well and incubated for 20 min at room temperature. Finally, 50 µl 0.18 mol/l H₂SO₄ (Merck, Darmstadt, Germany) were added to stop the reaction. And

the absorbance of each well was determined at a wavelength of 450 nm immediately. The measured values of the samples were computed according to the standard curve.

2.5.7.2 *Fibronectin*

A 96-well microplate was coated and left overnight at 4°C with rat fibronectin antigen (200 µg/ml, Sigma, USA), which was dissolved in PBS. Then each well was aspirated and blocked by block buffer (10% bovine serum albumin in PBST) and incubated for 1 hour at 37°C. Then the plate was washed with PBST and ready for the addition of samples and standards. The samples can be diluted with DMEM. The fibronectin standard was diluted to concentrations of 2667, 1334, 667, 333, 167, 83, 42, 21, 10, 5, 3 and 0 ng/ml. 50 µl standards and samples were incubated with 50 µl rabbit anti-rat primary antibody (0.6 µg/ml, Chemicon International, Inc. Temecula, Canada) on another non-coated microplate for 1 hour at 37°C. Then 95 µl of the mixture were transferred onto the precoated plate and incubated for 1 hour at 37°C. After a wash phase, 100 µl peroxidase-conjugated secondary antibody (0.3 µg/ml peroxidase-conjugated Affini goat anti-rabbit IgG, Dianova, Hamburg, Germany) were added and incubated at 37°C for 1 hour. After washing, the OPD substrate-complex was added and incubated at room temperature in darkness for 30 min. Finally, the absorbance of each well was measured photometrically at a wavelength of 450 nm, and the concentrations were computed according to the standard curve.

2.5.7.3 *PAI-1*

In the same way as with the fibronectin ELISA, a 96-well microplate was first coated with 100 µl rat PAI-1-antigen (3.6 µg/ml, American Diagnostica Inc. Greenwich, USA) and left overnight at 4°C in PBS. After aspiration of each well, block buffer was added and incubated for 1 hour at 37°C. Then the plate was washed with PBST and ready for the addition of samples and standards. The samples can be diluted with DMEM. Standards were manufactured with concentrations of 1143, 846, 625, 463, 342, 254, 188, 139, 103, 76, 56, and 0 pg/µl. 50 µl standards and samples were incubated with 50 µl rabbit anti-rat primary antibody (100 µg/ml, Oxford Biomedical Research, Michigan, USA) on another non-coated microplate for 1 hour at 37°C. Then 95 µl of the mixture were transferred onto the antigen-coated plate and incubated for 1 hour at 37°C. After a

wash phase 100 μ l peroxidase-conjugated secondary antibody were added and incubated for 1 hour. After washing, the OPD substrate-complex was added and incubated at room temperature in darkness for 30 min. Finally, the absorbance of each well was measured photometrically at a wavelength of 450 nm, and the concentrations were computed according to the standard curve.

2.5.7.4 *cGMP*

The *cGMP* competitive enzymeimmunoassay system (Amersham, Freiburg, Germany) was used in the research. The kit includes novel lysis reagents in order to facilitate simple and rapid extraction of *cGMP* from cells. Lysis reagent 1 hydrolyses cell membranes to release intracellular *cGMP*. Lysis reagent 2 sequesters the key component in lysis reagent 1 and ensures *cGMP* is free for subsequent analysis. The assay is based on competition between unlabelled *cGMP* (from samples) and a fixed quantity of peroxidase-labeled *cGMP* for a limited number of binding sites on a *cGMP*-specific antibody.

2.5.7.4.1 Plasma *cGMP*

The assay buffer working solutions and working standards (0, 2, 4, 8, 16, 32, 64, 128, 256, 512 fmol/well) were prepared as shown in kit. 10 μ l of the acetylation reagent were added to 100 μ l standards and samples. 100 μ l rabbit anti-*cGMP* antibody were added to all wells precoated with donkey anti-rabbit IgG except the blank and NSB (non-specific binding) wells. Then 50 μ l standards and samples were pipetted into the appropriate wells. 150 μ l of assay buffer were pipetted into the NSB wells. The plate was incubated at 3-5°C for 2 hours. Then 100 μ l diluted peroxidase-labeled *cGMP* conjugate were added to all wells except the blank. The plate was incubated at 3-5°C for 1 hour. Then all wells were aspirated and washed with wash buffer. Immediately, 200 μ l Tetramethylbenzidine substrate were pipetted into all wells. The plate was mixed on a microplate shaker for exactly 30 minutes at room temperature. Finally 100 μ l of 1 mol/l H₂SO₄ were added to all wells to halt the reaction prior to end point determination. The optical density can be read at 450 nm within 30 minutes. Finally, the concentrations were computed according to the standard curve.

2.5.7.4.2 Basal and NO-stimulated cGMP production

Before the assay, cells would be lysed. After the incubation of culture cells, 20 µl 5% dodecyltrimethylammonium bromide were added to the cell culture and mixed on a microplate shaker for 10 min to facilitate cell lysis. This enabled the total (intra- and extracellular) cGMP to be measured. A microscopic evaluation with Trypan blue was carried out to check whether the cells were lysed. Lysed cells were then ready for the assay. The assay buffer working solutions and working standards (0, 2, 4, 8, 16, 32, 64, 128, 256, 512 fmol/well) were prepared as shown in kit. 10 µl of the acetylation reagent were added to 100 µl standards and samples. 100 µl rabbit anti-cGMP antibody were added to all wells precoated with donkey anti-rabbit IgG except the blank and NSB wells. Then 50 µl standards and samples were pipetted into the appropriate wells. 50 µl diluted lysis reagent 1 and 100 µl diluted lysis reagent 2 were pipetted into the NSB wells. The plate was incubated at 3-5°C for 2 hours. Then 100 µl diluted peroxidase-labeled cGMP conjugate were added to all wells except the blank. The plate was incubated at 3-5°C for 1 hour. All wells were aspirated and washed with wash buffer. Immediately, 200 µl Tetramethylbenzidine substrate were pipetted into all wells. The plate was mixed on a microplate shaker for exactly 30 minutes at room temperature. Finally 100 µl of 1 mol/l H₂SO₄ were added to all wells to halt the reaction prior to end point determination. The optical density can be read at 450 nm within 30 minutes. Finally, the concentrations were computed according to the standard curve.

2.5.8 mRNA analysis

2.5.8.1 *RNA isolation by Trizol*

Total RNA was extracted by using Trizol Reagent according to the manufacturer's instructions. 50-100 mg tissue were transferred into 1 ml Trizol reagent and homogenized with homogenizer for 30 sec. The samples were then incubated at room temperature for 5 min. 200 µl chloroform (Merck, Darmstadt, Germany) were added. After 15 sec vigorous vortex of samples, the mixture was incubated at room temperature for 3 min and then centrifuged at 14000 rpm and 4°C for 15 min. RNA remains exclusively in the upper aqueous phase. The aqueous phase was transferred carefully into a fresh tube (about 400-500 µl), and the remainder was discarded. 500 µl

2 Materials and methods

isopropyl alcohol (J. T. Baker, Deventer, Holland) were added. The sample was mixed by gentle inversion and incubated for 10 min at room temperature. Then the sample was centrifuged again at 14000 rpm and 4°C for 10 min. The supernatant was removed and the remaining RNA pellet was washed with 1 ml 75% ethanol (Merck, Darmstadt, Germany), and then centrifuged at 14000 rpm and 4°C for 5 min. The supernatant was removed. The RNA pellet was dried in Laminar Flow for 5-10 min. Then the RNA pellet was dissolved in DEPC-treated water and incubated at 60°C in the thermal mixer for 10 min to ensure total resuspension.

Two investigation procedures to examine the quality and concentration of the isolated RNA content followed. The quality of the RNA was checked on 2% agarose gel electrophoresis. 1 µl RNA was dissolved in 9 µl DEPC-treated water. Then 8 µl bromine-phenol-blue (Carl Roth GmbH, Karlsruhe, Germany) were added and the sample was transferred into gel. The gel was run at 100 volts for 1 hour. Two bands, 18S and 28S ribosomal RNA bands, can be seen under ultraviolet light. The RNA was also spectrophotometrically quantified. 1 µl RNA was mixed with 99 µl DEPC-treated water. The zero value attitude of the spectrometer was made with DEPC-treated water. The sample was measured at a wavelength of 260 nm against zero. The RNA concentration was adjusted to 1 µg/µl with DEPC-treated water. Then the RNA was kept at -80°C until further analysis.

2.5.8.2 Reverse transcription-polymerase chain reaction (RT-PCR)

RT-PCR is a highly sensitive method for determining gene expression at the RNA level and for quantifying the strength of gene expression. “Two-step” RT-PCR was used in this research. A cDNA copy is created with reverse transcriptase from the RNA PCR Core kit (Roche, Applied Biosystems, New Jersey, USA).

Table 3: Mixture of reverse transcription components.

Components	Volume (µl)
MgCl ₂	4
10xPCR Buffer	2
DEPC-treated water	2
dGTP	2

dATP	2
dTTP	2
dCTP	2
RNase Inhibitor	1
MuLV Reverse Transcriptase	1
Random Hexamers	1
RNA	1 (conc. 1 µg/µl)

The reverse transcription is carried out in a thermocycler using the following conditions. The cDNA obtained in this reaction is then used for the subsequent PCR.

Table 4: Procedure for reverse transcription.

25°C	10 min
42°C	45 min
95°C	5 min
4°C	endlessly

2.5.8.3 Polymerase chain reaction

PCR is a method for oligonucleotide primer-directed enzymatic amplification of a specific DNA sequence of interest. The PCR product is amplified from a DNA template using a heat-stable DNA polymerase and an automated thermocycler to put the reaction through 30 or more cycles of denaturing, annealing of primers and polymerization. Quantitative analysis of changes in molecular targets with PCR plays a key role in scientific research.

The amount of PCR product increases logarithmically in the first few PCR cycles before reaching a plateau. To ensure accurate quantification of the sample concentration, only these first cycles should be considered. The later PCR cycles, which are usually run to ascertain the final amount of PCR product, do not easily permit to drawn conclusions as to starting concentrations. In conventional PCR, an endpoint analysis is carried out in the plateau phase of the PCR by examining the products by the staining of the sample separated by gel electrophoresis. In this research, PCR was checked with a LightCycler System called Real-time PCR [62, 63]. Real-time PCR

2 Materials and methods

refers to the continuous monitoring of the progress of the amplification during the whole PCR reaction and allows measurements to be made during the log-linear phase of a PCR. Utilization of a dsDNA-binding dye, SYBR Green I (Roche Diagnostics GmbH, Mannheim, Germany), is more specific since it only fluoresces when bound to dsDNA. The LightCycler System typically measures fluorescence once every cycle, to monitor the increase in PCR product formation.

The LightCycler System is capable of providing sequence confirmation of the amplified product through an innovative function called melting curve analysis. Each dsDNA product has its own specific melting temperature (T_m). Checking the T_m of a PCR product can thus be compared with analyzing a PCR product by length in gel electrophoresis to examine the purification.

A relative quantification was used, which is based on the relative expression of a target gene versus a reference gene, GAPDH in this study. Amplification is described as $N=N_0 \cdot E^{\Delta CP}$ (N: number of amplified molecules; N_0 : initial number of molecules; E: amplification efficiency; ΔCP : crossing point deviation expressing as $\Delta CP = CP_{\text{target}} - CP_{\text{GAPDH}}$) [64]. In this quantification method, CP is defined as the point at which the fluorescence rises appreciably above the background fluorescence. Finally the N_0 of samples were calculated and compared.

A mastermix of the following reaction components was prepared:

Table 5: Mixture of PCR components.

Components	Volume (μl)
MgCl ₂	1.6
DEPC-treated water	11.4
Template (sense)	1.5
Template (antisense)	1.5
SYBR Green	2.0 (Conc. 0.5 $\mu\text{g}/\mu\text{l}$)
cDNA	2.0

The template used (TIB Molbiol, Berlin, Germany):

Table 6: Templates of PCR.

Template	Sequence	Annealing/Melting Temperature
GAPDH sense antisense	5'-CCATCTTCCAGGAGCGAGAT-3' 5'-GATGACCTTGCCCACAGCCT-3'	59°C/86°C
eNOs sense antisense	5'- TCCAGTAACACAGACAGTGC -3' 5'- CAGGAAGTAAGTGAGAGCCTG -3'	61°C/88°C
iNOS sense antisense	5'- GCAGAATGTGACCATCATGG -3' 5'- ACAACCTTGGTGTGTTGAAGGC -3'	60°C/86°C
alpha1sGC sense antisense	5'- CCACATCAACACAGGCTAAT -3' 5'- GAAGTGCAAGGTTTCAGTCTC -3'	62°C/86°C
beta1sGC sense antisense	5'- CGGATGCCACGGTATTGTCT -3' 5'- CTCCTGGCTTGACGCACATT -3'	62°C/84°C
P-selectin sense antisense	5'- ACCATGACGTGTATCCAGCC -3' 5'- CCTTCGTCACACATGAACTG -3'	61°C/79°C
TGF-beta1 sense antisense	5'-GGTGGCAGGCGAGAGCGCTGA-3' 5'-GGCATGGTAGCCCTTGGGCT-3'	64°C/86°C
PAI-1 sense antisense	5'-CAGCATGTGGTCCAGGCCTCCAAA-3' 5'-TGTGCCGCTCTCGTTCACCTCGATCT-3'	64°C/84°C
Fibronectin sense antisense	5'-GGTCCAAATCGGTCATGTTCCCA-3' 5'-CGTAATGGGAAACCGTGTAAGGG-3'	64°C/86°C

2.6 Statistical analysis

All values are expressed as mean \pm standard error of the mean (SEM). Statistics were analyzed with SPSS 11.0. For normal distributive data analysis, one-way analysis of variance (ANOVA) and an unpaired student's *t*-test were used. Regarding the abnormal distributive data, statistical analysis was performed using a Mann-Whitney-*U*-test. A p value <0.05 was considered significant.

3 Results

3.1 Blood pressure, bleeding time and plasma cGMP levels in acute anti-thy1 glomerulonephritis (injury phase and matrix expansion phase)

In this study, similar results were found in blood pressure, bleeding time and plasma cGMP levels of the injury phase and the matrix expansion phase in acute anti-thy1 glomerulonephritis. In the interest of simplicity, they are presented together.

3.1.1 Systolic blood pressure

As shown in Figure 3, systolic blood pressure was normal in the control (123 ± 1 mmHg) and untreated aGN groups (118 ± 2 mmHg). The intake of Bay 41-2272 significantly decreased systolic blood pressure (101 ± 3 mmHg).

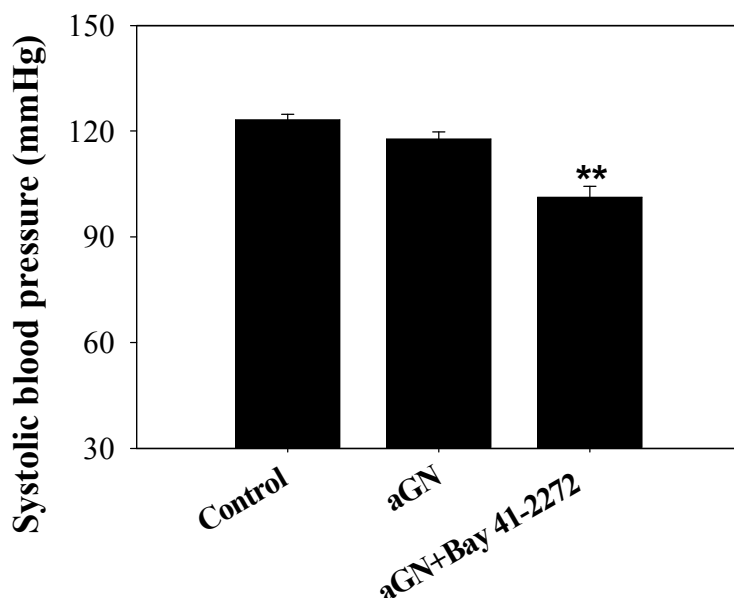


Figure 3: Effects of Bay 41-2272 (+Bay 41-2272) on systolic blood pressure in acute anti-thy1 glomerulonephritis (aGN). Normal control animals (Control) were injected with PBS. Blood pressure was measured in conscious rats using tail cuff. (** $p < 0.01$ vs. aGN and Control)

3.1.2 Bleeding time

As shown in Figure 4, the bleeding time was significantly prolonged by Bay 41-2272 treatment (471 ± 41 sec) as compared to the control and the aGN groups (268 ± 21 sec and 298 ± 36 sec, respectively).

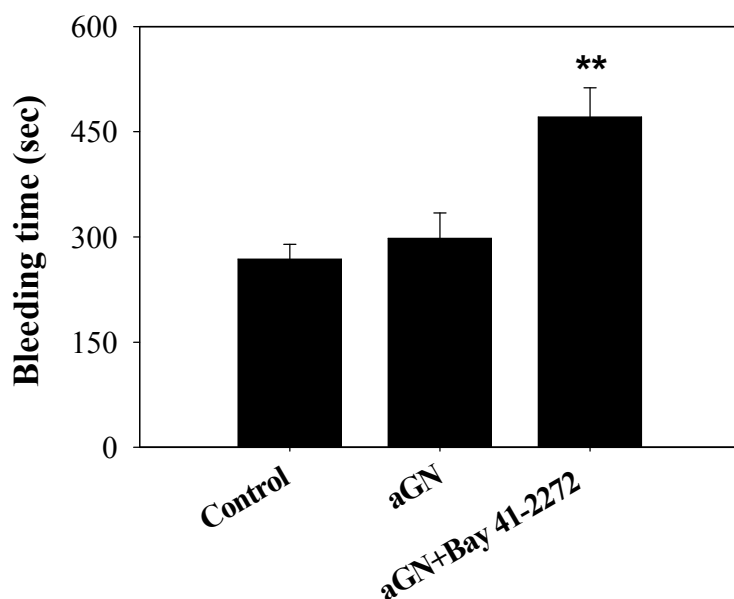


Figure 4: Effects of Bay 41-2272 (+Bay 41-2272) on bleeding time in acute anti-thy1 glomerulonephritis (aGN). Bleeding was induced by a standard tail incision (10 mm long and 1 mm deep) in anesthetized animals. (** $p < 0.01$ vs. aGN and Control)

3.1.3 Plasma cGMP levels

As shown in Figure 5, plasma cGMP levels were significantly higher in the untreated aGN group than those in the normal controls (4130 ± 650 fmol/ml vs. 2120 ± 260 fmol/ml), and were elevated significantly further by Bay 41-2272 treatment (6610 ± 810 fmol/ml).

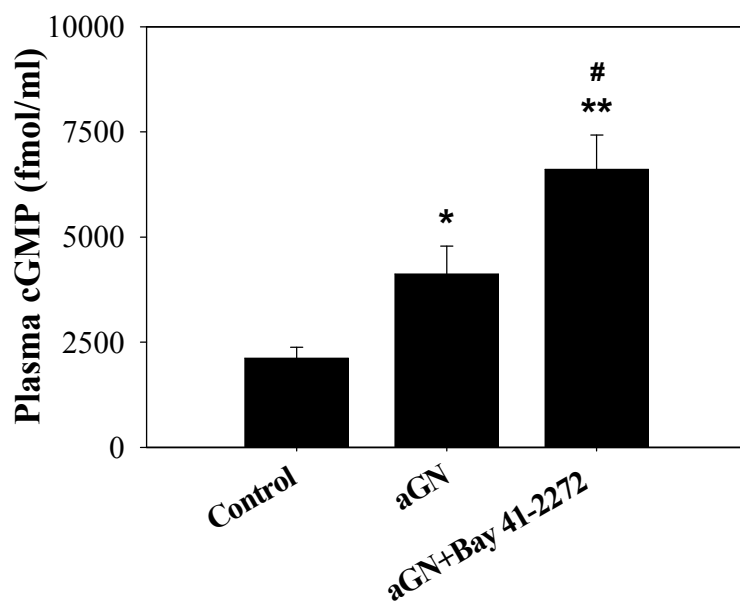


Figure 5: Effects of Bay 41-2272 (+Bay 41-2272) on plasma cGMP levels in acute anti-thy1 glomerulonephritis (aGN). Normal control animals (Control) were injected with PBS. (**p<0.01 and *p<0.05 vs. Control, #p<0.05 vs. aGN)

Summing up, Bay 41-2272 treatment caused a decrease in systolic blood pressure, a prolongation of bleeding time and an increase in the plasma cGMP levels, which proves the in vivo bioavailability of the drug through stimulating cGMP synthesis.

3.2 Protocol 1: NO-cGMP signaling in the injury phase 1 day after induction of acute anti-thy1 glomerulonephritis

3.2.1 Body weight

The aGN+Bay 41-2272 group was treated for 6 days before and 1 day after the induction of acute anti-thy1 glomerulonephritis. The experiment was ended 1 day after disease induction. There was no difference in the body weight at the end of the experiment among the three groups (Control 253±3 g, aGN 250±5 g and aGN+Bay 41-2272 255±7 g).

3.2.2 Proteinuria

The proteinuria of diseased rats was significantly higher than that in the control group (14±2 mg/day, p<0.01 vs. aGN and aGN+Bay 41-2272). Treatment with Bay 41-2272 before anti-thy1 antibody-induced mesangial cell lysis reduced proteinuria slightly, but not significantly, when compared to the aGN group (31±4 mg/day vs. 53±10 mg/day, p>0.05).

3.2.3 Mesangial cell lysis

As shown in Figure 6, anti-thy1 antibody injection resulted in a rapid drop in glomerular cell number. Cell nuclei counts averaged 56.3±1.1 per glomerular section in the control group, whereas the aGN group's and the aGN+Bay 41-2272 group's cell counts were significantly reduced to 44±1.1 and 44.3±1.1 per glomerular section, respectively. There was no difference between the aGN group and the aGN+Bay 41-2272 group. This result indicates that Bay 41-2272 has no effect on mesangial cell injury 1 day after anti-thy1 glomerulonephritis induction.

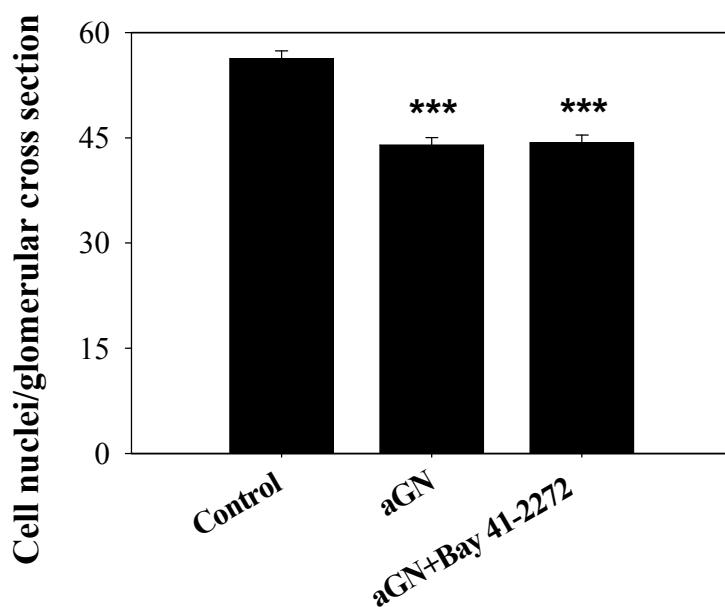


Figure 6: Effects of Bay 41-2272 (+Bay 41-2272) on glomerular nuclei count indicating mesangial cell lysis 1 day after induction of acute anti-thy1 glomerulonephritis (aGN). Normal control rats (Control) were injected with PBS. (***) $p < 0.001$ vs. Control)

3.2.4 Glomerular iNOS-NO pathway

As shown in Figure 7, glomerular iNOS mRNA expression increased significantly in the aGN group ($263 \pm 38\%$) as compared to the control group ($100 \pm 28\%$). This increase was not significantly changed in the Bay 41-2272 treated group ($226 \pm 26\%$).

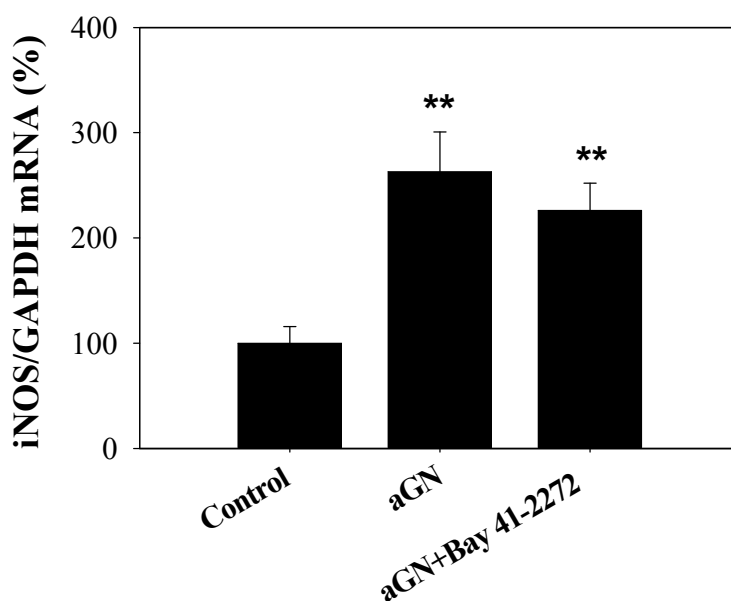


Figure 7: Effects of Bay 41-2272 (+Bay 41-2272) on glomerular iNOS mRNA expression 1 day after induction of acute anti-thy1 glomerulonephritis (aGN). Normal control animals (Control) were injected with PBS. mRNA was analyzed by a real-time PCR method using GAPDH as housekeeping gene. mRNA is shown as a percentage of the normal control group. (**p<0.01 vs. Control)

As shown in Figure 8, glomerular NO production was in line with the iNOS mRNA expression. Compared to the control group (2.1 ± 0.3 nmol/ml), the basal NO synthesis of isolated glomeruli was significantly elevated in the aGN group (6.9 ± 0.5 nmol/ml) and the aGN+Bay 41-2272 group (6.9 ± 1.7 nmol/ml) 1 day after disease induction. LPS stimulated the glomerular NO production significantly in the aGN group (49.1 ± 4.7 nmol/ml) and the aGN+Bay 41.2272 group (50.6 ± 8.8 nmol/ml), in contrast to the control group (9.3 ± 0.9 nmol/ml). And there was no difference between the aGN and the Bay 41-2272-treated aGN group.

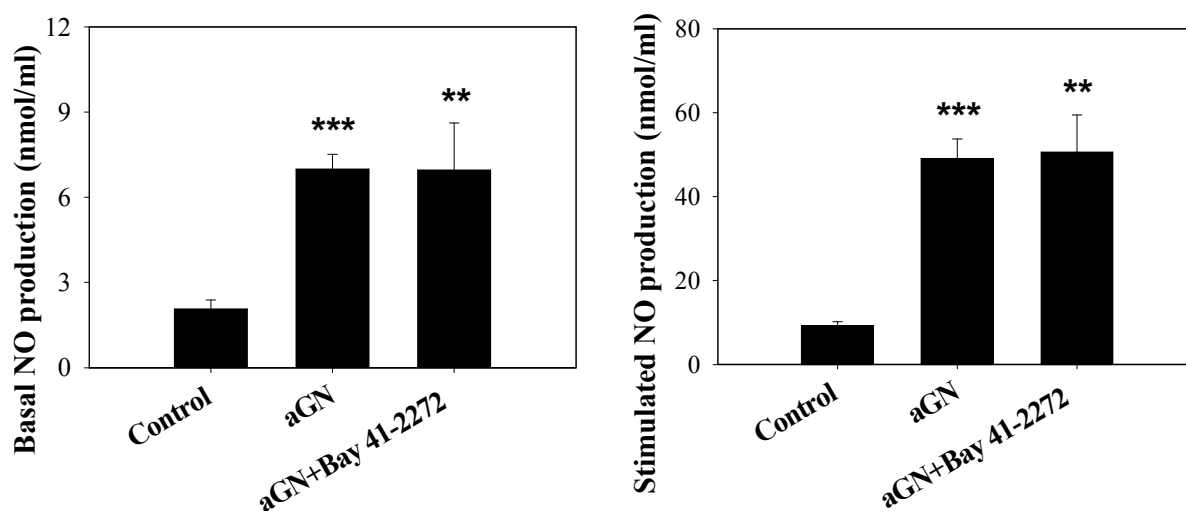


Figure 8: Effects of Bay 41-2272 (+Bay 41-2272) on glomerular basal and LPS-stimulated NO production 1 day after induction of acute anti-thy1 glomerulonephritis (aGN). Normal control animals (Control) were injected with PBS. Nitrite as indicator of NO production was determined by the Griess reaction. Glomeruli were harvested from individual animals and cultured at a density of 2000 per ml for 48 hours. (***)p<0.001 and **p<0.01 vs. Control)

3.2.5 Glomerular eNOS-NO-cGMP signaling cascade

As shown in Figure 9, there was no difference in eNOS mRNA expression among the three groups (control $100\pm 15\%$, aGN $145\pm 23\%$, aGN+Bay 41-2272 $100\pm 14\%$, $P>0.05$). The induction of anti-thy1 glomerulonephritis did not significantly change eNOS expression.

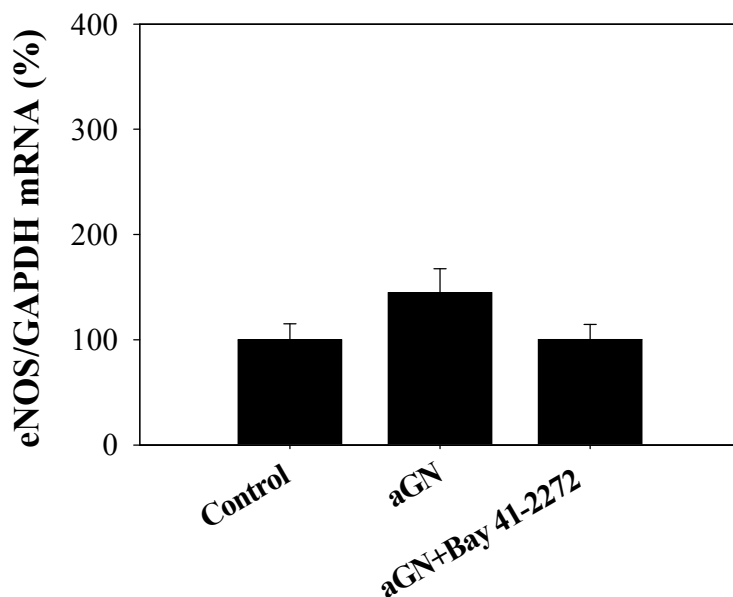


Figure 9: Effects of Bay 41-2272 (+Bay 41-2272) on glomerular eNOS mRNA expression 1 day after induction of acute anti-thy1 glomerulonephritis (aGN). Normal control animals (Control) were injected with PBS. mRNA was analyzed by a real-time PCR method using GAPDH as housekeeping gene. mRNA is shown as a percentage of the normal control group.

As shown in Figure 10, compared to the control group (alpha1 sGC $100\pm 21\%$ and beta1 sGC $100\pm 22\%$), sGC mRNA expression was reduced significantly by 90% after anti-thy 1 antibody injection (aGN: alpha1 sGC $10\pm 2\%$ and beta1 sGC $13\pm 2\%$, aGN+Bay 41-2272: alpha1 sGC $6\pm 2\%$ and beta1 sGC $10\pm 2\%$).

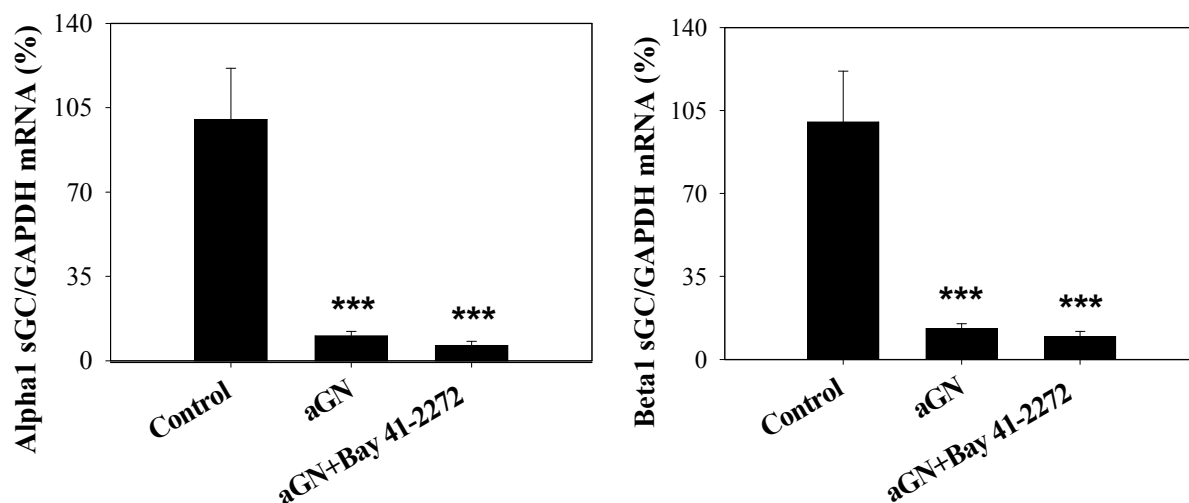


Figure 10: Effects of Bay 41-2272 (+Bay 41-2272) on glomerular alpha1 sGC and beta1 sGC mRNA expression 1 day after induction of acute anti-thy1 glomerulonephritis (aGN). Normal control animals (Control) were injected with PBS. mRNA was analyzed by a real-time PCR method using GAPDH as housekeeping gene. mRNA is shown as a percentage of the normal control group. (***) $p < 0.001$ vs. Control)

As shown in Figure 11, corresponding to sGC mRNA expression, basal and NO-stimulated glomerular cGMP levels were significantly depressed in the untreated diseased animals as compared to normal controls (basal cGMP levels: 10 ± 1 fmol/well vs. 27 ± 5 fmol/well, NO-stimulated cGMP levels: 34 ± 11 fmol/well vs. 143 ± 23 fmol/well, both $p < 0.01$ vs. Control). Treatment with Bay 41-2272 had no significant influence on the glomerular cGMP levels (basal cGMP production 12 ± 1 fmol/well and NO-stimulated cGMP production 25 ± 3 fmol/well).

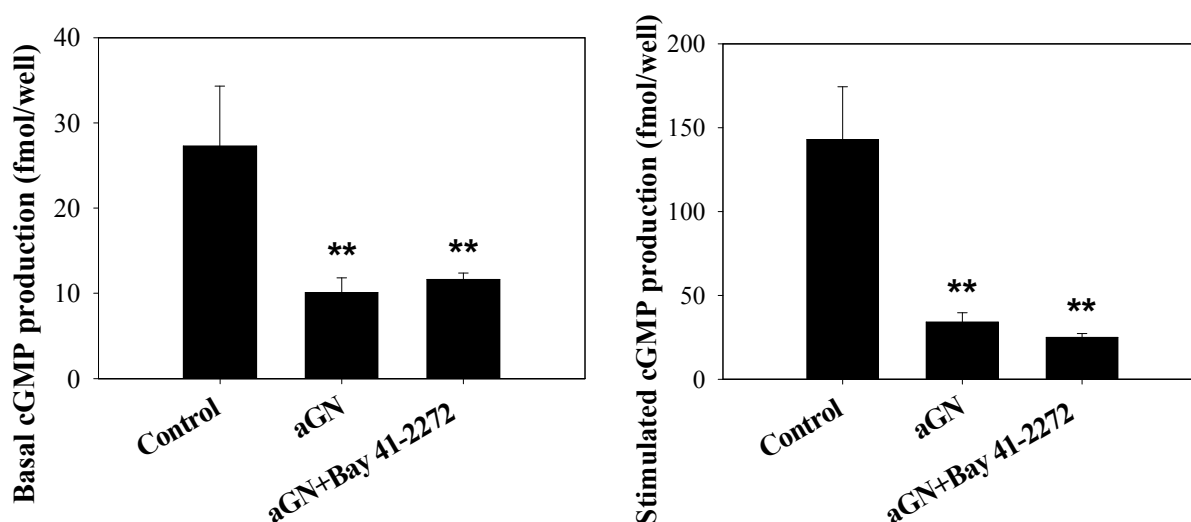


Figure 11: Effects of Bay 41-2272 (+Bay 41-2272) on basal and DEA/NO stimulated glomerular cGMP production 1 day after induction of acute anti-thy1 glomerulonephritis (aGN). Normal control animals (Control) were injected with PBS. cGMP generation was measured by ELISA in glomeruli harvested from individual animals in the presence or absence of the NO donor DEA/NO. (** $p < 0.01$ vs. Control)

Taken together, the results from protocol 1 consistently demonstrate that the expression and activity of the NO-cGMP pathway are dramatically impaired one day after anti-thy1 glomerulonephritis induction. Treatment with Bay 41-2272 could not stimulate glomerular cGMP synthesis and hence was unable to affect the mesangial cell lysis in the injury phase of acute anti-thy1 glomerulonephritis.

3.3 Protocol 2: NO-cGMP signaling in the matrix expansion phase 7 days after induction of acute anti-thy1 glomerulonephritis

3.3.1 Body weight

Bay 41-2272 treatment was begun 1 day after and continued 7 days after the induction of acute anti-thy1 glomerulonephritis. The experiment ended 7 days after disease induction. There was no difference in the body weight at the end of the experiment among the three groups (Control 231 ± 14 g, aGN 240 ± 11 g and aGN+Bay 41-2272 240 ± 12 g).

3.3.2 Proteinuria

As shown in Figure 12, in contrast to the normal controls (16 ± 4 mg/day), proteinuria was significantly elevated in the diseased rats (aGN 165 ± 10 mg/day, aGN+Bay 41-2272 110 ± 18 mg/day). Bay 41-2272 treatment significantly reduced proteinuria as compared to untreated nephritic rats.

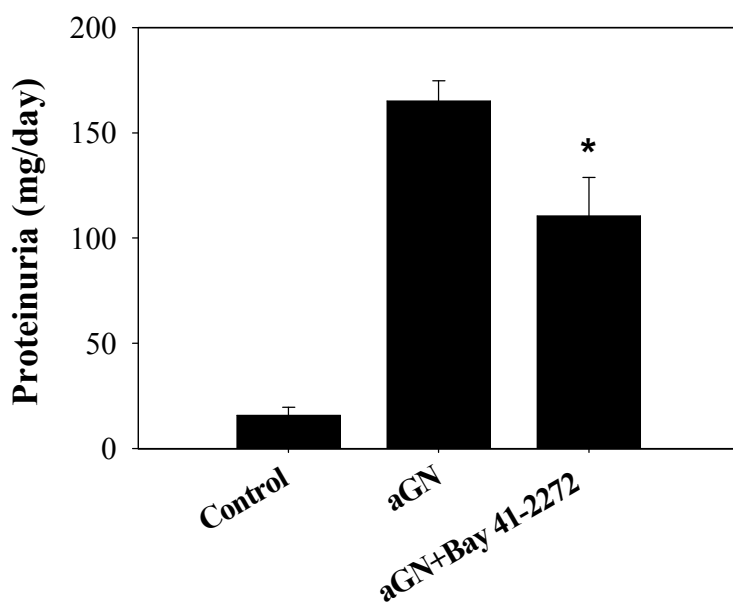


Figure 12: Effects of Bay 41-2272 (+Bay 41-2272) on proteinuria 7 days after induction of acute anti-thy1 glomerulonephritis (aGN). Normal control animals (Control) were injected with PBS. Urine was collected for 24 hours using metabolic cages. (* $p < 0.05$ vs. aGN)

3.3.3 Markers of glomerular matrix expansion

As shown in Figure 13, compared to the control group (Control: matrix score 1.1 ± 0.1 , TGF-beta1 78 ± 13 pg/ml, fibronectin 7766 ± 497 ng/ml and PAI-1 399 ± 29 ng/ml), diseased animals in the matrix expansion phase were characterized by significant glomerular matrix expansion and TGF-beta1 overexpression (aGN: matrix score 2.9 ± 0.1 , TGF-beta1 817 ± 66 pg/ml, fibronectin 69587 ± 2886 ng/ml and PAI-1 1368 ± 40 ng/ml). Treatment with Bay 41-2272 limited glomerular matrix expansion significantly (aGN+Bay 41-2272: matrix score 2.6 ± 0.1 , TGF-beta1 603 ± 49 pg/ml, fibronectin 45668 ± 2513 ng/ml and PAI-1 1156 ± 53 ng/ml, $p < 0.05$ vs. aGN for all parameters).

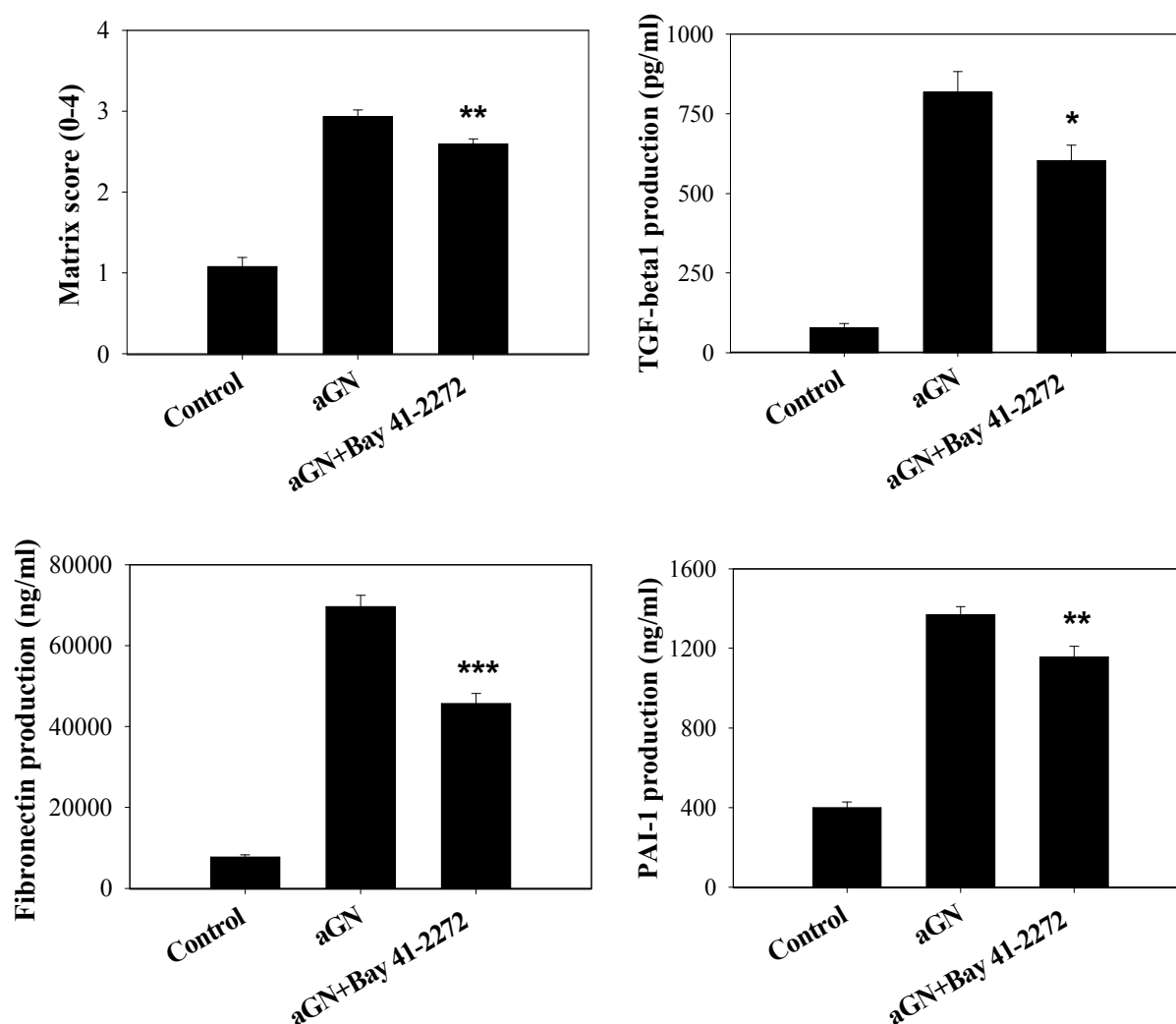


Figure 13: Effects of Bay 41-2272 (+Bay 41-2272) on markers of glomerular matrix expansion, including matrix score, TGF-beta1, fibronectin and PAI-1 production, 7 days after induction of acute anti-thy1 glomerulonephritis (aGN). Normal control animals (Control) were injected with PBS. Matrix expansion was scored on PAS-stained slides. Glomeruli were harvested from individual animals and cultured at a density of 2000 per ml for 48 hours. (** $p < 0.001$, ** $p < 0.01$, * $p < 0.05$ vs. aGN)

3.3.4 Glomerular eNOS-NO-cGMP signaling cascade

As shown in Figure 14, compared to the aGN group ($72 \pm 10\%$), Bay 41-2272 treatment significantly up-regulated eNOS mRNA expression ($125 \pm 20\%$). There was no significant difference in eNOS mRNA between the control group ($100 \pm 10\%$) and the untreated aGN group.

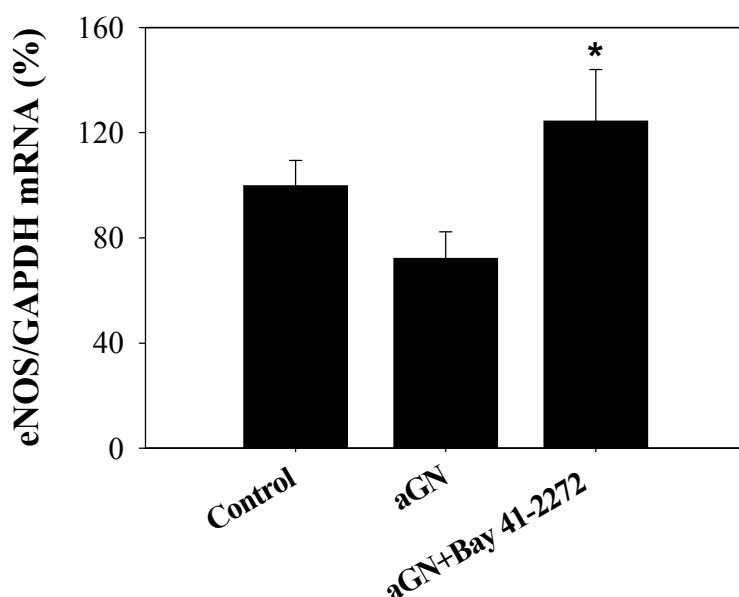


Figure 14: Effects of Bay 41-2272 (+Bay 41-2272) on glomerular eNOS mRNA expression 7 days after induction of acute anti-thy1 glomerulonephritis (aGN). Normal control animals (Control) were injected with PBS. mRNA was analyzed by a real-time PCR method using GAPDH as housekeeping gene. mRNA is shown as a percentage of the normal control group. (* $p < 0.05$ vs. aGN)

As shown in Figure 15, compared to the normal controls (alpha1 sGC $100 \pm 14\%$ and beta1 sGC $100 \pm 15\%$), sGC mRNA expression in the untreated aGN group (alpha1 sGC $563 \pm 76\%$ and beta1 sGC $330 \pm 31\%$) increased significantly after disease induction.

Treatment with Bay 41-2272 further up-regulated sGC mRNA expression (alpha1 sGC $1758 \pm 544\%$ and beta1 sGC $1218 \pm 463\%$) to a greater extent than in the aGN group. As is consistent with the sGC mRNA expression, basal and NO-stimulated glomerular cGMP production was significantly elevated in nephritic animals (382 ± 156 fmol/well and 38011 ± 17528 fmol/well) as compared to normal controls (basal cGMP production: 16 ± 3 fmol/well, NO-stimulated cGMP production: 195 ± 33 fmol/well). Although basal glomerular cGMP production was similar in treated (381 ± 98 fmol/well) and untreated nephritic animals, glomerular NO-stimulated cGMP production was significantly further increased in the Bay 41-2272-treated animals (181969 ± 114910 fmol/well).

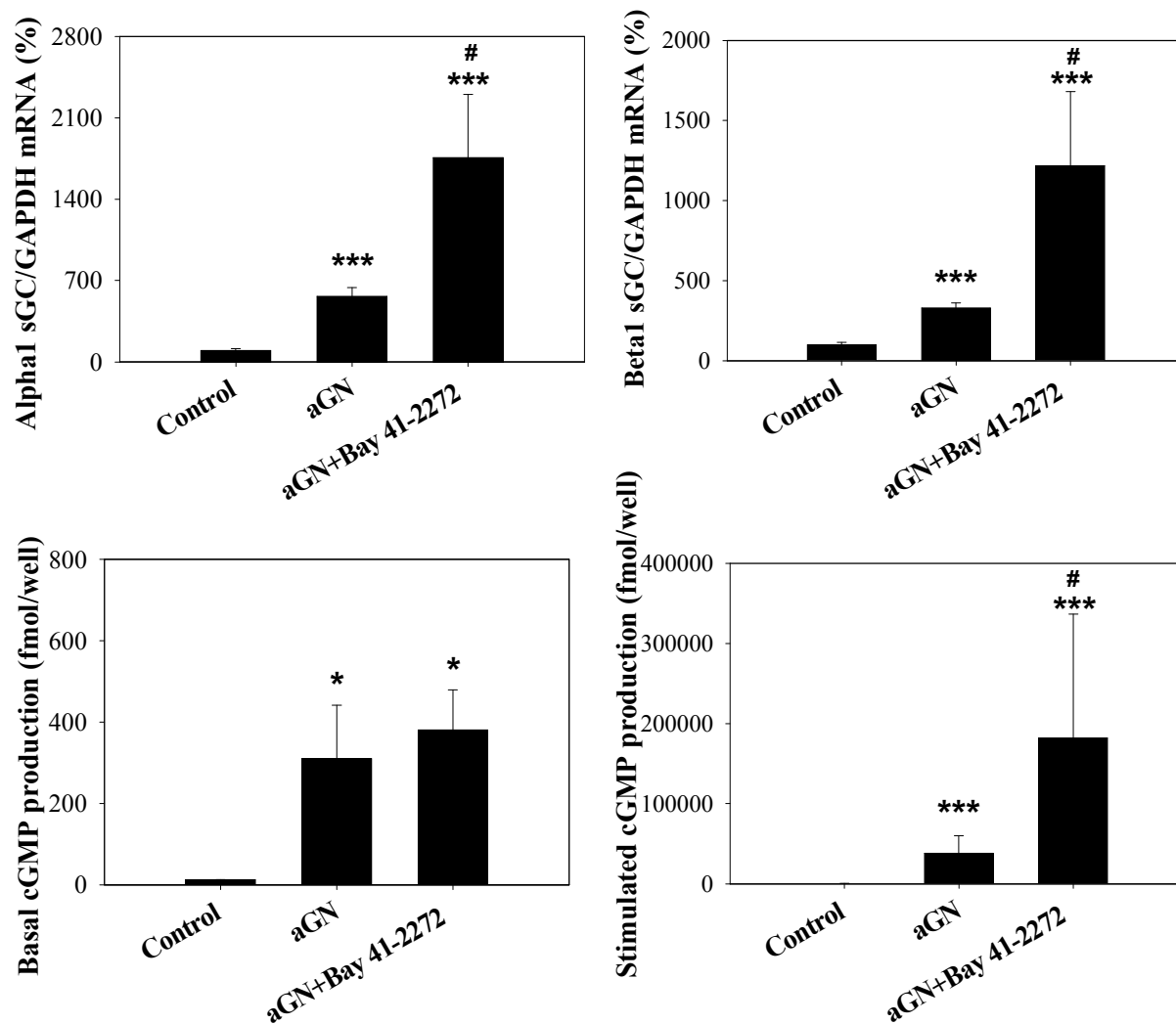


Figure 15: Effects of Bay 41-2272 (+Bay 41-2272) on glomerular sGC mRNA expression and sGC activity to produce cGMP 7 days after induction of acute anti-thy1 glomerulonephritis (aGN). Normal control animals (Control) were injected with PBS. mRNA was analyzed by a real-time PCR method using GAPDH as housekeeping gene. mRNA is shown as a percentage of the normal control group. cGMP generation was measured by ELISA in glomeruli harvested from individual animals in the presence or absence of the NO donor DEA/NO. (** $p < 0.001$ and * $p < 0.05$ vs. Control, # $p < 0.05$ vs. aGN)

3.3.5 Mechanisms of Bay 41-2272's renoprotective effects

3.3.5.1 Blood pressure

As shown in Figure 3, Bay 41-2272 reduced systolic blood pressure significantly, as compared to control and untreated nephritic animals.

3.3.5.2 TGF-beta1 production in vitro

As shown in Figure 16, 48 hours of exposure of glomeruli to Bay 41-2272 induced a dose-dependent decrease in glomerular TGF-beta1 production. In normal glomeruli, 0.1 μ M, 1 μ M, 5 μ M and 10 μ M Bay 41-2272 reduced TGF-beta1 production by 16%, 24%, 28% and 26%, and in day 7 anti-thy1 nephritic glomeruli, TGF-beta1 production were reduced by 10%, 15%, 25% and 21%, respectively.

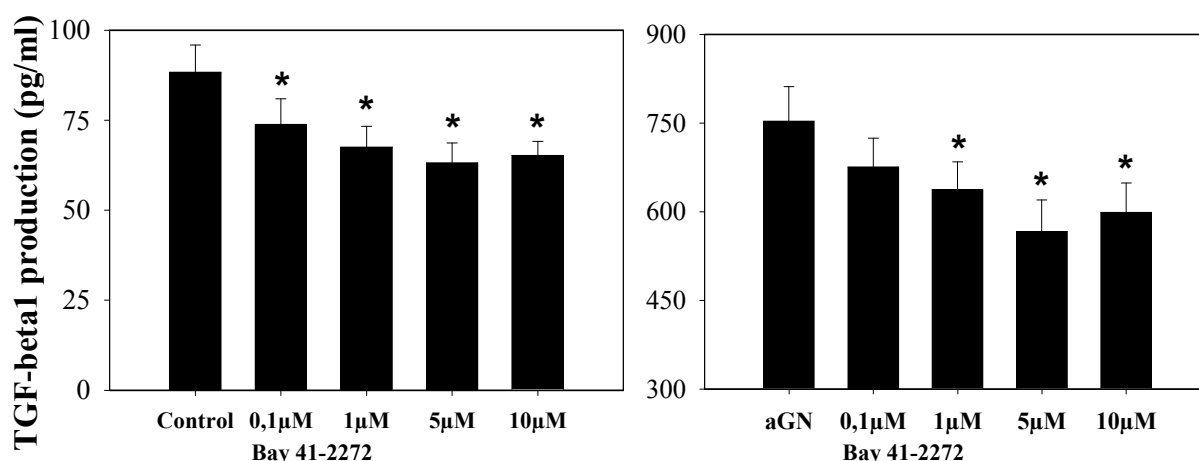


Figure 16: In vitro effects of Bay 41-2272 on TGF-beta1 production in glomeruli isolated from control and nephritic rats 7 days after induction of acute anti-thy1 glomerulonephritis (aGN). Normal control animals (Control) were injected with PBS. Glomeruli were cultured at a density of 2000 per ml for 48 hours in the presence of Bay 41-2272 in a concentration sequence of 0.1 μ M, 1 μ M, 5 μ M and 10 μ M. (* p <0.05 vs. glomeruli of Control and aGN without Bay 41-2272)

3.3.5.3 Glomerular platelet deposition

As shown in Figure 17, fibrinogen staining was hardly found in the control group. In contrast to the untreated aGN group (45 \pm 6% staining-positive area per glomerulus), Bay 41-2272 treatment (29 \pm 3% staining-positive area per glomerulus) significantly reduced fibrinogen deposition, which indicates platelet aggregation in the glomeruli. Combined with the prolonged bleeding time, this indicates that Bay 41-2272 has an anti-platelet effect through elevated cGMP synthesis.

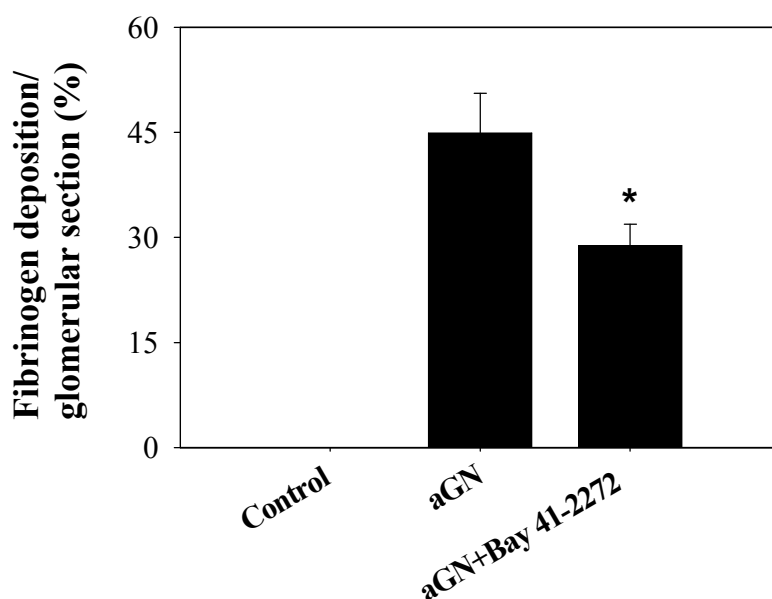


Figure 17: Effects of Bay 41-2272 (+Bay 41-2272) on glomerular fibrinogen deposition 7 days after induction of acute anti-thy1 glomerulonephritis (aGN). Normal control animals (Control) were injected with PBS. Glomerular fibrinogen deposition is expressed as the percentage of fibrinogen-positive area per glomerular cross-section. (* p <0.05 vs. aGN)

3.3.5.4 Glomerular macrophage infiltration

As shown in Figure 18, the nephritic groups had more glomerular macrophage infiltration than the control group (0.8 ± 0.2 cells per glomerular section). Glomerular macrophage infiltration was significantly inhibited by Bay 41-2272 treatment (6.2 ± 0.5 cells per glomerular section), in contrast to the aGN group (9.2 ± 1.2 cells per glomerular section). Although there was no significant difference in P-selectin mRNA expression among the three groups, Bay 41-2272 treatment ($85 \pm 12\%$) slightly inhibited glomerular P-selectin mRNA expression, as compared to the aGN group ($132 \pm 25\%$).

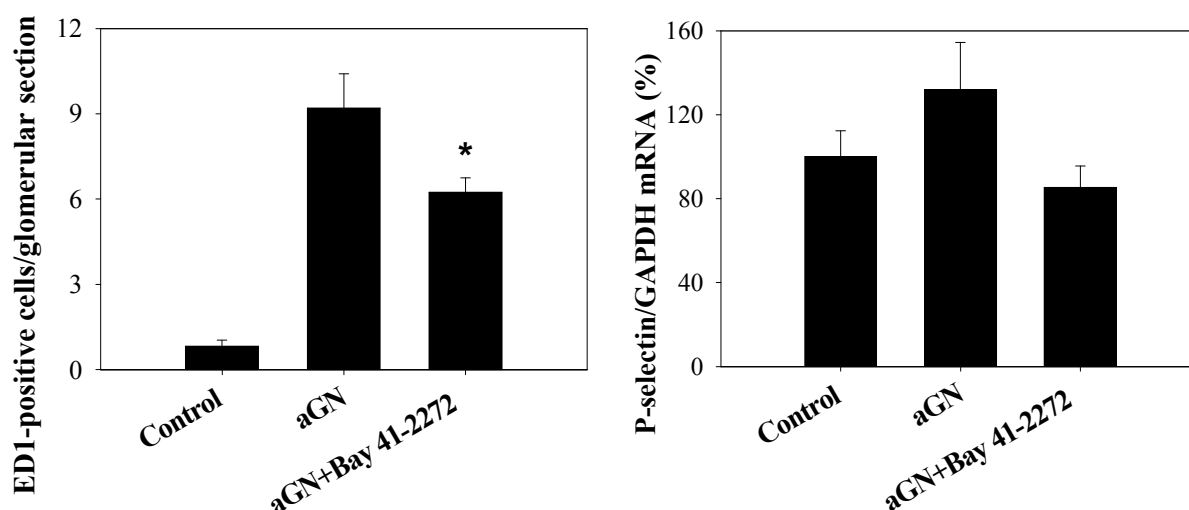


Figure 18: Effects of Bay 41-2272 (+Bay 41-2272) on glomerular ED1-positive cell infiltration and P-selectin mRNA expression 7 days after induction of acute anti-thy1 glomerulonephritis (aGN). Normal control animals (Control) were injected with PBS. Glomerular macrophage infiltration is expressed as number of ED1-positive cells per glomerular cross-section. mRNA was analyzed by a real-time PCR method using GAPDH as housekeeping gene. mRNA is shown as a percentage of the normal control group. (* $p < 0.05$ vs. aGN)

Taken together, the results of protocol 2 show that the NO-cGMP pathway is significantly up-regulated in the matrix expansion phase of acute anti-thy1 glomerulonephritis. Bay 41-2272 treatment further increased sGC expression and activity to produce cGMP, which limited the fibrotic parameters characterized in the matrix expansion phase of acute anti-thy1 glomerulonephritis.

3.4 Protocol 3: NO-cGMP signaling 16 weeks after induction of anti-thy1-induced chronic glomerulosclerosis (progression phase)

3.4.1 Body weight

Treatments with Bay 41-2272 and hydralazine were started 7 days after the induction of chronic-progressive anti-thy1 glomerulosclerosis (cGS). The experiment ended 16 weeks after disease induction. There was no difference in body weights at the beginning and the end of the experiment among the three cGS groups. At the end of the experiment, the final body weights in all diseased groups were significantly lower than those in the control groups.

Table 7: Effects of Bay 41-2272 (+Bay 41-2272) and hydralazine (+Hydralazine) on rats' body weights at the beginning and the end of chronic-progressive anti-thy1 glomerulosclerosis (cGS). Treatments were started 7 days after injection of anti-thy1 antibody into uni-nephrectomized rats. Non-diseased animals without (2-K Control) or with uni-nephrectomy (1-K Control) received a PBS injection. (* $p < 0.05$ vs. Control)

Groups	2-K Control	1-K Control	cGS	cGS+Bay 41-2272	cGS+Hydralazine
Begin	256±3 g	230±8 g	220±2 g	224±2 g	219±3 g
End	575±21 g	570±24 g	488±15 g*	482±11 g*	464±13 g*

3.4.2 Systolic blood pressure

As shown in Figure 19, the model of anti-thy1-induced chronic glomerulosclerosis was characterized by a significant increase in systolic blood pressure 8 weeks and 16 weeks after disease induction (134±2 mmHg and 135±1 mmHg, respectively), compared to 2-K Control (129±2 mmHg and 122±4 mmHg) and 1-K Control (122±4 mmHg and 122±5 mmHg). Bay 41-2272 treatment lowered blood pressure significantly to 116±3 mmHg in week 8 and 116±2 mmHg in week 16 after anti-thy1 antibody-injection, in comparison to the untreated cGS groups. Hydralazine administration reduced also systolic blood pressure significantly to 109±4 mmHg and 110±3 mmHg, respectively. Due to the absence of a significant difference between the Bay 41-2272-treated group and the hydralazine-treated group, hydralazine was a good control drug to observe the blood pressure-independent effect of Bay 41-2272.

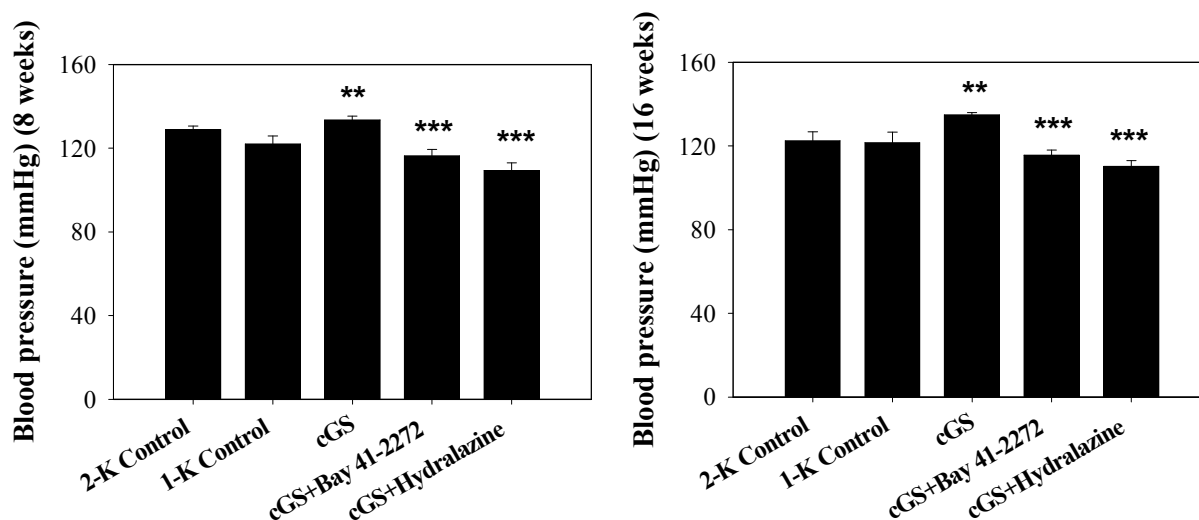


Figure 19: Effects of Bay 41-2272 (+Bay 41-2272) and hydralazine (+Hydralazine) on systolic blood pressure 8 weeks and 16 weeks after induction of chronic-progressive anti-thy1 glomerulosclerosis (cGS). Treatments were started 7 days after injection of anti-thy1 antibody into uni-nephrectomized rats. Non-diseased animals without (2-K Control) or with uni-nephrectomy (1-K Control) received a PBS injection. Blood pressure was measured in conscious animals using a tail cuff method. (** $p < 0.01$ vs. Control, *** $p < 0.001$ vs. cGS)

3.4.3 Proteinuria

As shown in Figure 20, all diseased rats were randomized at the beginning of the protocol, so that every diseased group had similar proteinuria (cGS 148 ± 8 mg/day, cGS+Bay 41-2272 146 ± 7 mg/day, cGS+Hydralazine 148 ± 10 mg/day), and proteinuria was significantly elevated in all diseased groups, in contrast to the 2-K and 1-K Controls (20 ± 4 mg/day and 17 ± 2 mg/day). During the experiment, proteinuria gradually increased in the three diseased groups, indicating a progressive chronic glomerulosclerosis model. At the end of the protocol, proteinuria was reduced slightly by Bay 41-2272 treatment (cGS+Bay 41-2272 422 ± 42 mg/day, $p > 0.05$ vs. cGS 476 ± 56 mg/day and cGS+Hydralazine 451 ± 70 mg/day), although not significantly.

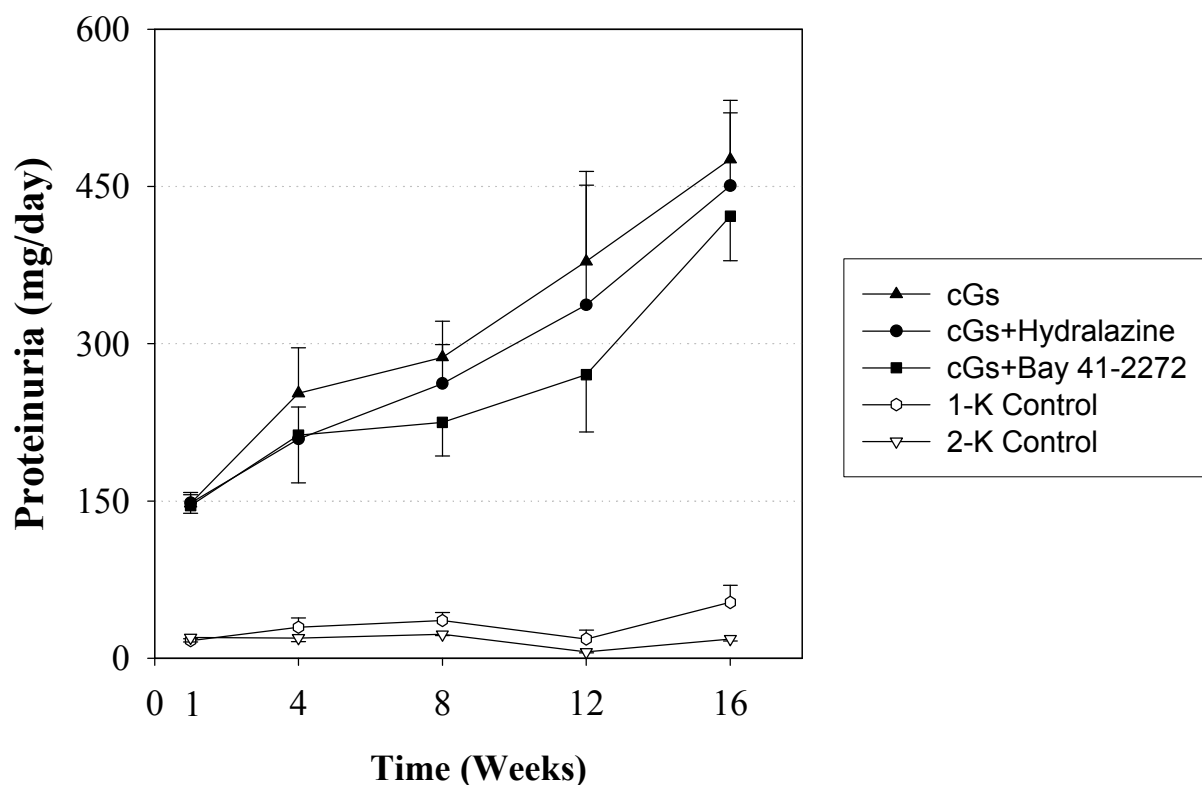


Figure 20: Effects of Bay 41-2272 (+Bay 41-2272) and hydralazine (+Hydralazine) on time course of proteinuria after induction of chronic-progressive anti-thy1 glomerulosclerosis (cGS). Treatments were started 7 days after injection of anti-thy1 antibody into uni-nephrectomized rats. Non-diseased animals without (2-K Control) or with uni-nephrectomy (1-K Control) received a PBS injection. Urine was collected for 24 hours using metabolic cages.

3.4.4 Markers of tubulointerstitial matrix accumulation

3.4.4.1 Matrix score

As shown in Figure 21, compared to the 2-K (0.04 ± 0.004) and the 1-K Control (0.1 ± 0.02), injection of anti-thy1 antibody induced significant tubulointerstitial matrix protein deposition in the cGS group (2.49 ± 0.22). Bay 41-2272 treatment reduced tubulointerstitial matrix protein accumulation significantly (-35.1%), in contrast to hydralazine treatment, which lowered matrix protein accumulation only slightly but not significantly (-9.2%), suggesting that Bay 41-2272 had a blood pressure-independent

effect on tubulointerstitial matrix protein accumulation.

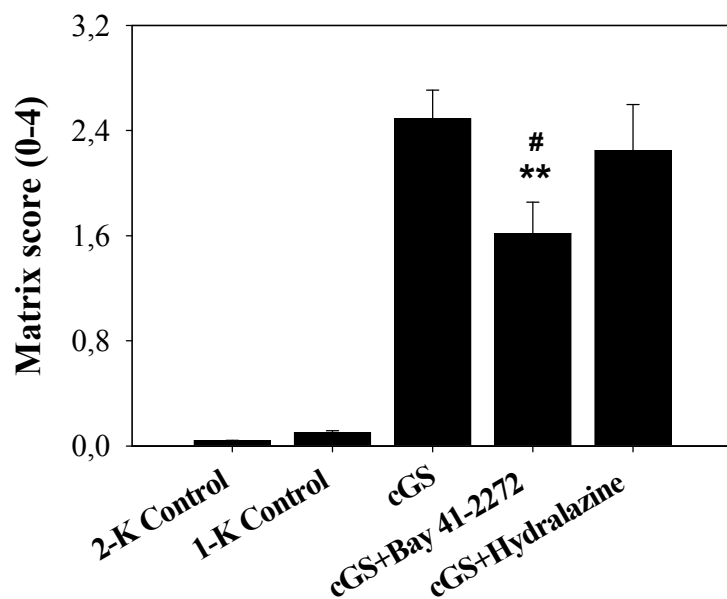


Figure 21: Effects of Bay 41-2272 (+Bay 41-2272) and hydralazine (+Hydralazine) on tubulointerstitial matrix protein accumulation 16 weeks after induction of chronic-progressive anti-thy1 glomerulosclerosis (cGS). Treatments were started 7 days after injection of anti-thy1 antibody into uni-nephrectomized rats. Non-diseased animals without (2-K Control) or with uni-nephrectomy (1-K Control) received a PBS injection. Matrix expansion was scored on PAS-stained slides. (** $p < 0.01$ vs. cGS, # $p < 0.05$ vs. cGS+Hydralazine)

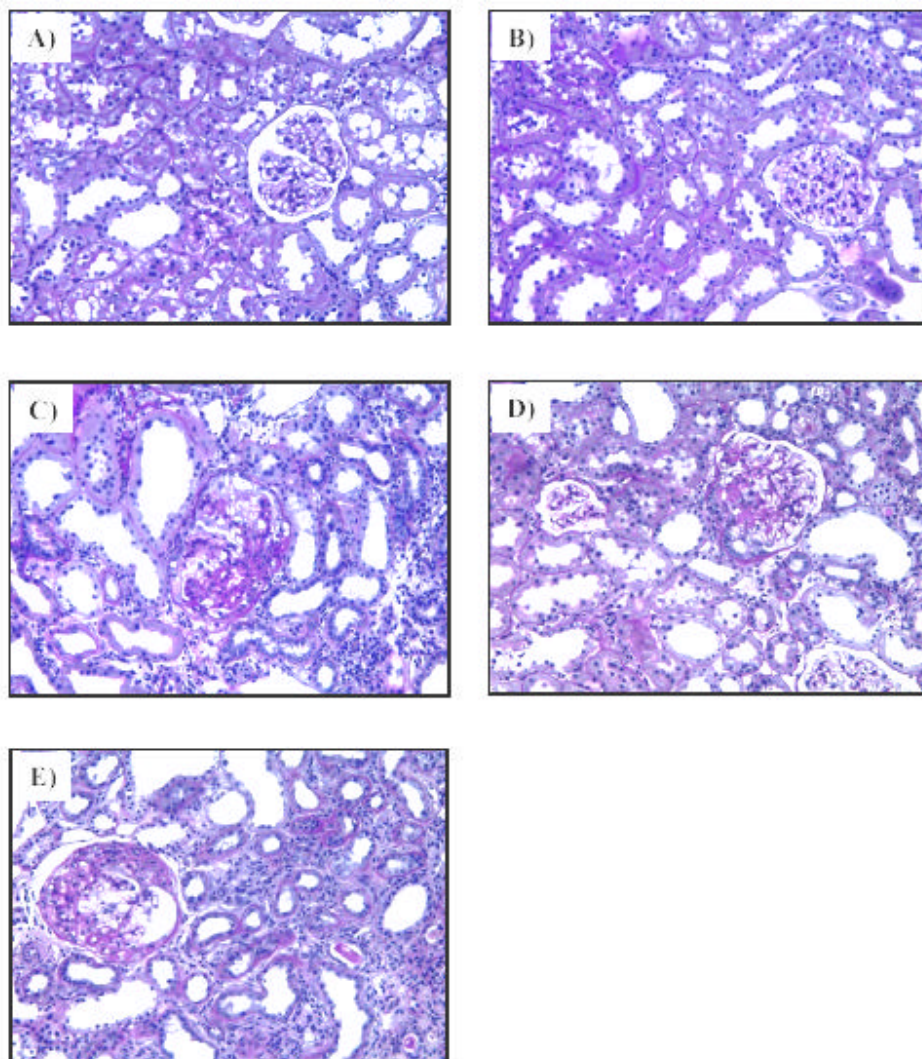


Figure 22: Effects of Bay 41-2272 and hydralazine on the histological picture 16 weeks after induction of chronic-progressive anti-thy1 glomerulosclerosis (cGS). Treatment was started 7 days after injection of anti-thy1 antibody into uninephrectomized rats. Shown are characteristic PAS-stained renal sections from A) a non-diseased animal without (2-K Control) and B) with uni-nephrectomy (1-K Control), and C) an animal with anti-thy1-induced chronic glomerulosclerosis without treatment and with Bay 41-2272 (D) or with hydralazine treatment (E) (Magnification x200).

3.4.4.2 Protein and mRNA expression of TGF-beta1, fibronectin and PAI-1

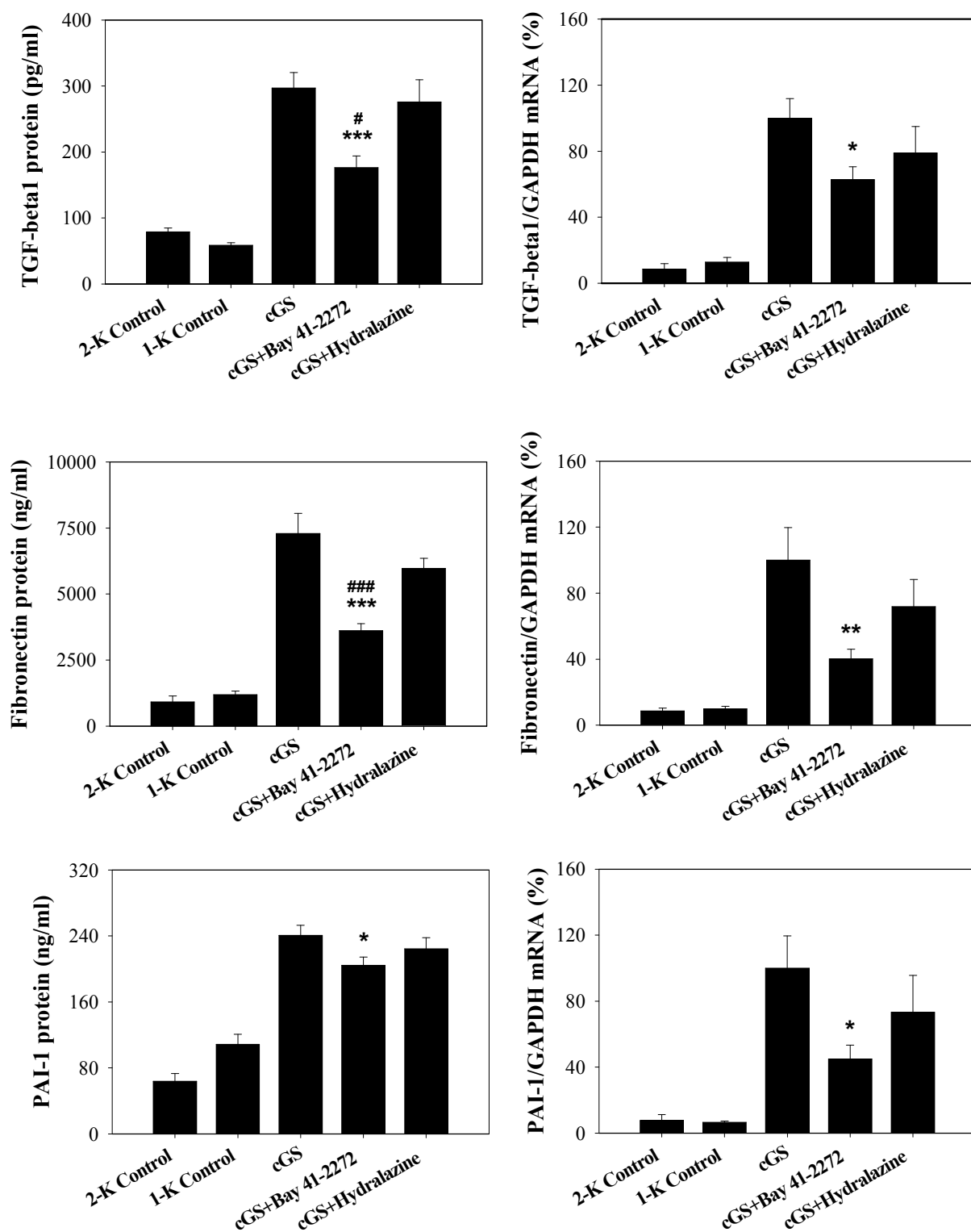


Figure 23: Effects of Bay 41-2272 (+Bay 41-2272) and hydralazine (+Hydralazine) on tubulointerstitial TGF-beta1, fibronectin and PAI-1 protein and mRNA expression 16 weeks after induction of chronic-progressive anti-thy1 glomerulosclerosis (cGS). Treatments were started 7 days after injection of anti-thy1 antibody into uninephrectomized rats. Non-diseased animals without (2-K Control) or with uninephrectomy (1-K Control) received a PBS injection. Matrix protein production was determined in extensively minced individual cortical tissues cultured at a density of 10 mg/ml for 48 hours. mRNA was analyzed by a real-time PCR method using GAPDH as housekeeping gene. mRNA is shown as a percentage of the untreated chronic anti-thy1 animals. (**p<0.001, *p<0.01 and #p<0.05 vs. cGS, ###p<0.001 and #p<0.05 vs. cGS+Hydralazine)

As shown in Figure 23, tubulointerstitial TGF-beta1, fibronectin and PAI-1 expression closely followed the changes seen in histological matrix deposition. Compared to 1-K Control animals (TGF-beta1 58±4 pg/ml, fibronectin 1182±145 ng/ml and PAI-1 108±12 ng/ml), the untreated cGS group was characterized by marked increases in the tubulointerstitial protein expression of TGF-beta1 (297±24 pg/ml), fibronectin (7296±760 ng/ml) and PAI-1 (240±12 ng/ml). The mRNA expression of TGF-beta1, fibronectin and PAI-1 was elevated 9.4-, 10.9- and 13.1-fold, respectively, in contrast to 1-K Control animals (TGF-beta1 12.84±2.79%, fibronectin 9.88±1.49% and PAI-1 6.58±0.69%). Treatment with Bay 41-2272 significantly reduced tubulointerstitial protein and mRNA expression of TGF-beta1 (-40.6%, -37.3%), fibronectin (-50.6%, -59.7%) and PAI-1 (-15.1%, -55.2%), respectively, while treatment with hydralazine only slightly and not significantly lowered the tubulointerstitial protein and mRNA expression of TGF-beta1 (-7.1%, -21%), fibronectin (-18.2%, -28%) and PAI-1 (-6.6%, -26.8%) in the chronic anti-thy1 animals.

3.4.5 Markers of glomerular matrix accumulation

As shown in Figure 24, the glomerular matrix protein expression in anti-thy1-induced chronic glomerulosclerosis was characterized by a significant increase in the histological matrix score (1.95±0.14) and protein expression of TGF-beta1 (173±24 pg/ml), fibronectin (11229±1255 ng/ml) and PAI-1 (351±32 ng/ml), compared to the 1-K Control (matrix score 0.86±0.03, TGF-beta1 53±9 pg/ml, fibronectin 2372±511 ng/ml

and PAI-1 208 ± 25 ng/ml). While Bay 41-2272 significantly lowered histological matrix accumulation (-35.4%) and TGF-beta1 (-28.3%) and fibronectin protein expression (-50.3%), treatment with hydralazine did not significantly affect glomerular matrix protein expression and accumulation (matrix score -4.6%, TGF-beta1 -1.7%, fibronectin -1.8% and PAI-1 +0.3%). Glomerular PAI-1 protein expression was also reduced by Bay 41-2272 (-14.8%), but this did not reach statistical significance.

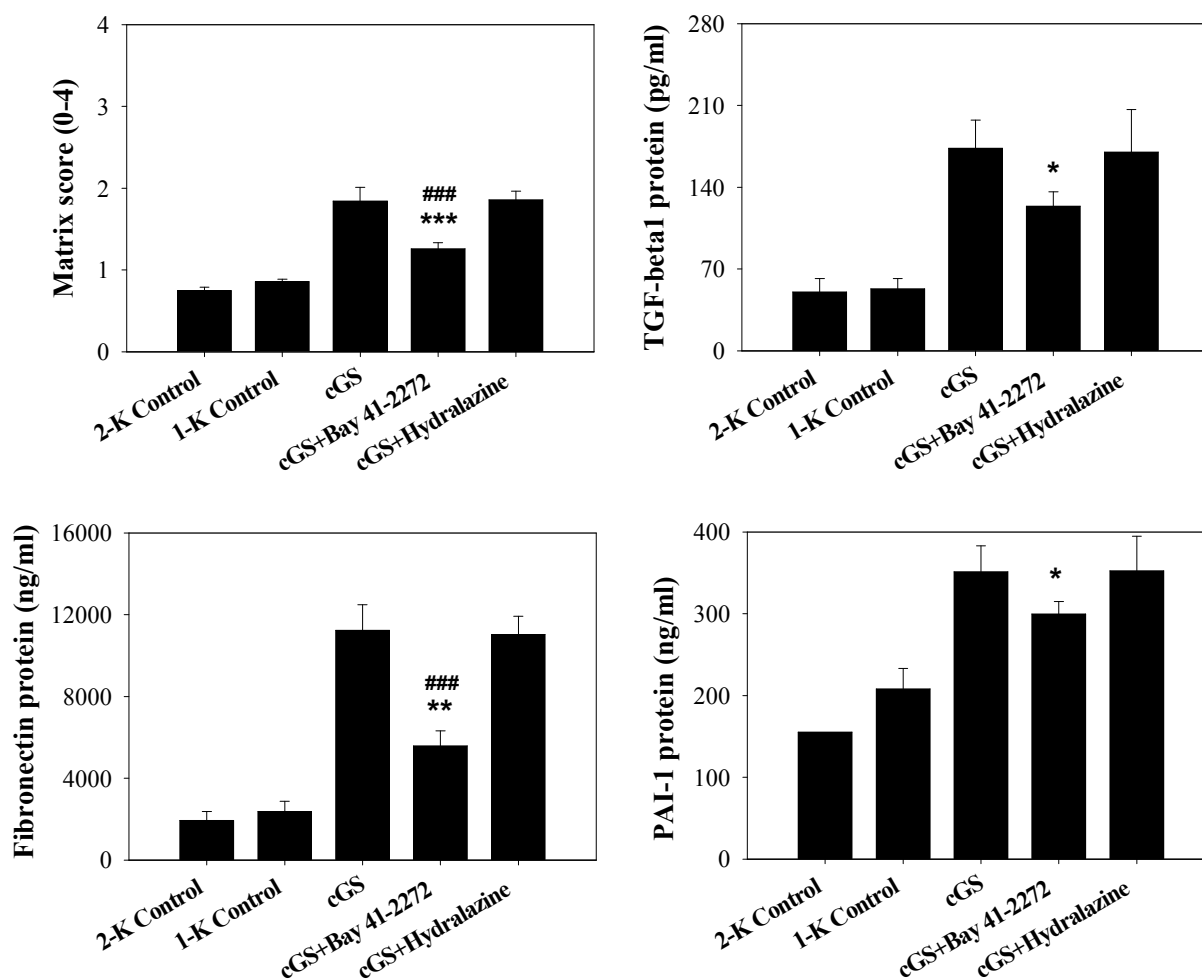


Figure 24: Effects of Bay 41-2272 (+Bay 41-2272) and hydralazine (+Hydralazine) on glomerular matrix protein accumulation and TGF-beta1, fibronectin and PAI-1 protein expression 16 weeks after induction of chronic-progressive anti-thy1 glomerulosclerosis (cGS). Treatments were started 7 days after injection of anti-thy1 antibody into uni-nephrectomized rats. Non-diseased animals without (2-K Control) or with uni-nephrectomy (1-K Control) received a PBS injection. Matrix expansion was scored on PAS-stained slides. Glomeruli were harvested from individual animals and cultured at a density of 2000 per ml for 48 hours. (**p<0.01, ***p<0.001 and *p<0.05 vs. cGS, ###p<0.001 vs. cGS+Hydralazine)

3.4.6 Markers of renal function

As shown in Figure 25, plasma creatinine, urea levels, creatinine clearance and hematocrit were analyzed as markers of renal function. Animals with chronic anti-thy1 glomerulosclerosis showed significant increases in plasma creatinine (cGS: 1.89 ± 0.38 vs. 1-K Control: 0.47 ± 0.01 mg/dl) and urea levels (cGS: 187 ± 45 vs. 1-K Control: 51 ± 3 mg/dl), while creatinine clearances (cGS: 0.25 ± 0.04 vs. 1-K Control: 0.52 ± 0.02 ml/min/100g body weight) and blood hematocrit levels (cGS: $41 \pm 2\%$ vs. 1-K Control: $48 \pm 1\%$) were significantly decreased. Corresponding to the histological and molecular results on renal matrix expansion, treatment with Bay 41-2272 significantly lowered plasma creatinine levels (0.74 ± 0.08 mg/dl) and urea levels (85 ± 10 mg/dl), while creatinine clearances (0.48 ± 0.06 ml/min/100g body weight) and blood hematocrit levels ($46 \pm 1\%$) were preserved. In contrast, renal function was not significantly affected by hydralazine treatment (plasma creatinine 1.51 ± 0.42 mg/dl, plasma urea 139 ± 25 mg/dl, and creatinine clearance 0.34 ± 0.05 ml/min/100 g body weight and hematocrit $40 \pm 2\%$).

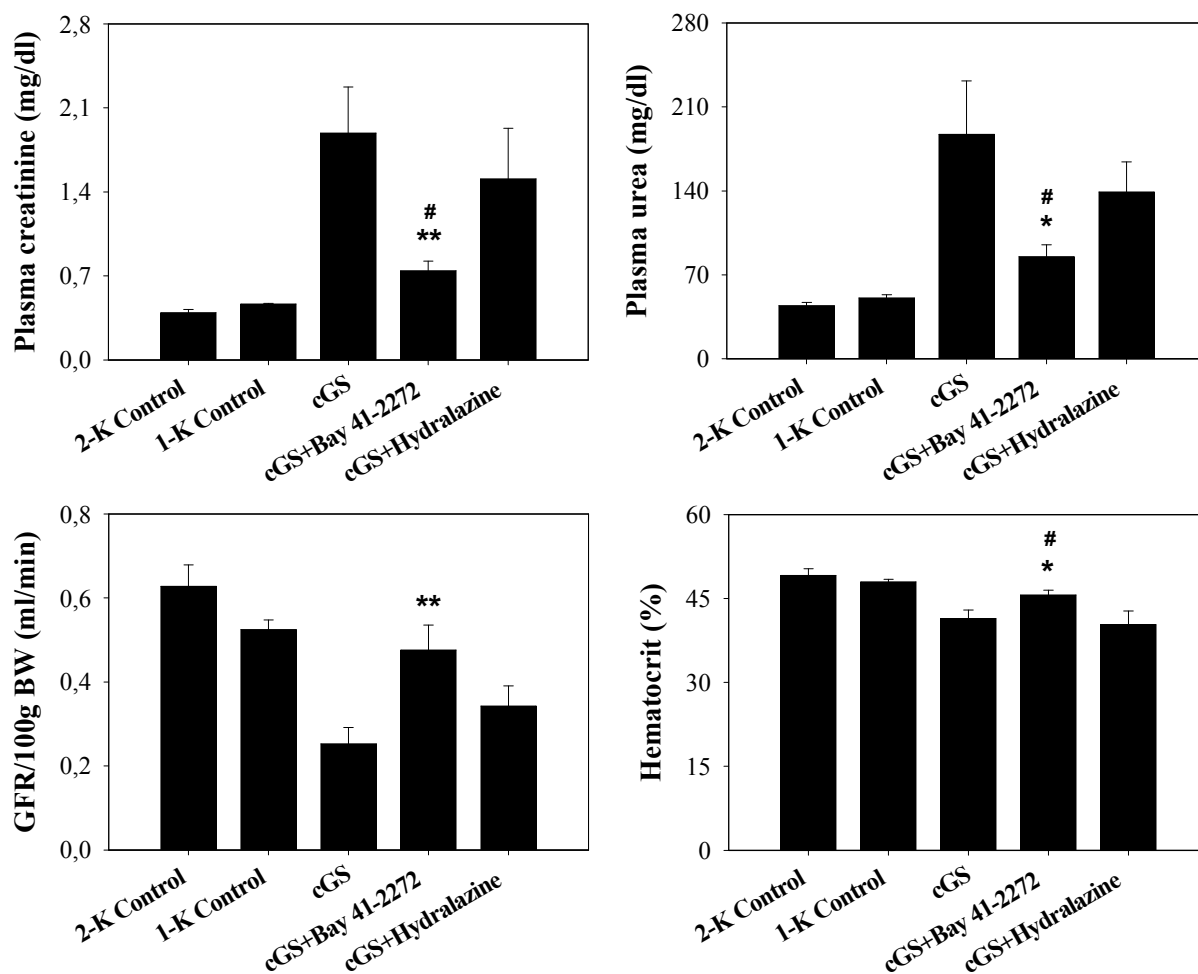


Figure 25: Effects of Bay 41-2272 (+Bay 41-2272) and hydralazine (+Hydralazine) on markers of renal function 16 weeks after induction of chronic-progressive anti-thy1 glomerulosclerosis (cGS). Treatment was started 7 days after injection of anti-thy1 antibody into uni-nephrectomized rats. Non-diseased animals without (2-K Control) or with uni-nephrectomy (1-K Control) received a PBS injection. (** $p < 0.01$ and * $p < 0.05$ vs. cGS, # $p < 0.05$ vs cGS+Hydralazine)

3.4.7 Tubulointerstitial eNOS-NO-cGMP signaling cascade

As shown in Figure 26, although there was no significant difference among the three diseased groups (cGS: $100 \pm 7\%$, cGS+Bay 41-2272: $132 \pm 14\%$ and cGS+Hydralazine: $100 \pm 15\%$), in comparison to the 1-K and 2-K Control groups ($70 \pm 12\%$ and $73 \pm 9\%$), eNOS mRNA expression was elevated in diseased animals, especially in the cGS+Bay

41-2272 group.

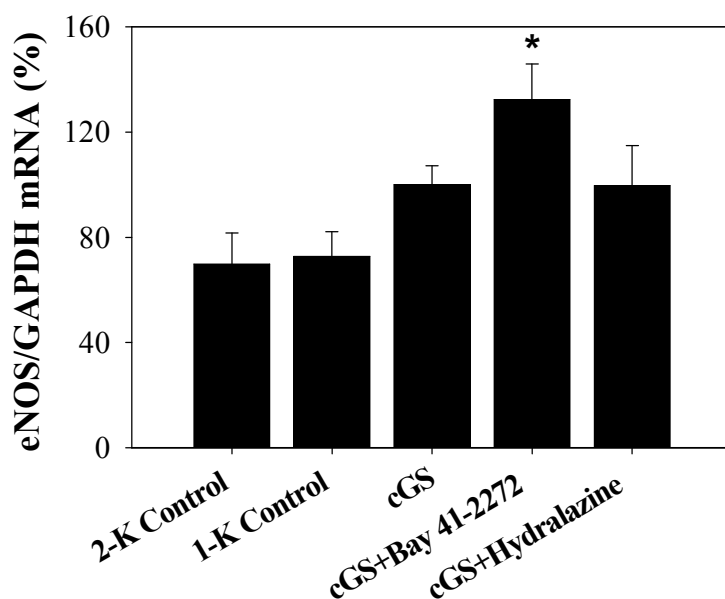


Figure 26: Effects of Bay 41-2272 (+Bay 41-2272) and hydralazine (+Hydralazine) on tubulointerstitial eNOS mRNA expression 16 weeks after induction of chronic-progressive anti-thy1 glomerulosclerosis (cGS). Treatments were started 7 days after injection of anti-thy1 antibody into uni-nephrectomized rats. Non-diseased animals without (2-K Control) or with uni-nephrectomy (1-K Control) received a PBS injection. mRNA was analyzed by a real-time PCR method using GAPDH as housekeeping gene. mRNA is shown as a percentage of the untreated chronic anti-thy1 animals. (* $p < 0.05$ vs. Control)

As shown in Figure 27, in comparison to the 2-K ($32 \pm 16\%$ and $34 \pm 7\%$) and 1-K ($39 \pm 16\%$ and $29 \pm 7\%$) Control groups, anti-thy1-induced chronic glomerulosclerosis showed a marked 2.8-fold and 3.2-fold increase in the mRNA expression of the tubulointerstitial $\alpha 1$ - and $\beta 1$ sGC. While basal tubulointerstitial cGMP production did not differ between the untreated diseased group (19 ± 1.48 fmol/well) and the control groups (2-K 24 ± 2 fmol/well and 1-K 22.5 ± 4.5 fmol/well), the NO-stimulated cGMP production was 2.7-fold higher in the chronic anti-thy1 group than in 2-K Control (115 ± 16 fmol/well) and 1-K Control group (92 ± 6 fmol/well). Compared to the untreated diseased animals, administration of Bay 41-2272 did not significantly alter the

3 Results

expression of the sGC (alpha1 $80 \pm 16\%$ and beta1 $95 \pm 17\%$), but resulted in a significantly higher NO-stimulated tubulointerstitial cGMP production (534 ± 126 fmol/well vs. 282 ± 41 fmol/well), while treatment with hydralazine did not significantly affect mRNA expression and activity of sGC (alpha1 $116 \pm 15\%$, beta1 $118 \pm 17\%$ and NO-stimulated cGMP levels 206 ± 37 fmol/well).

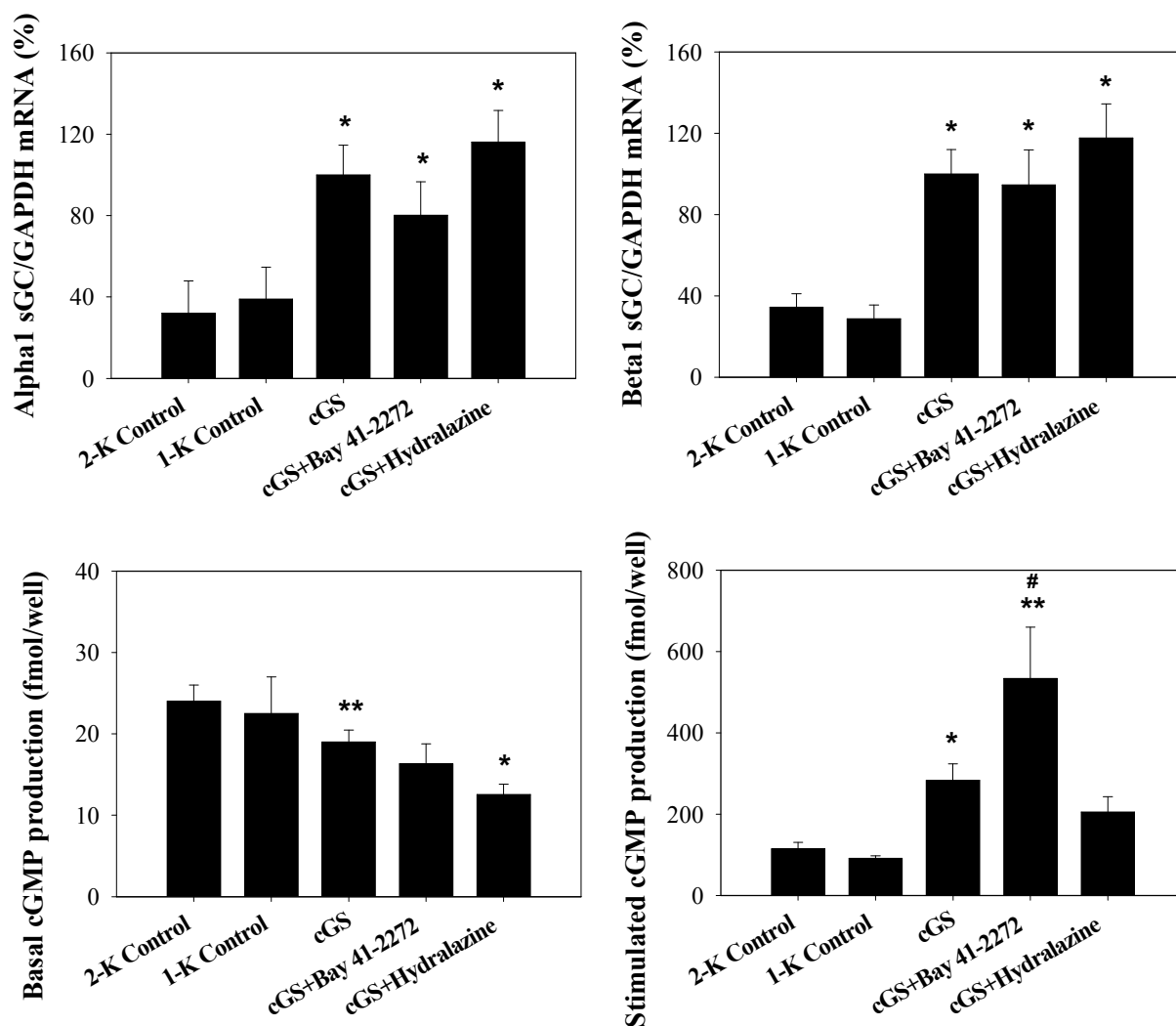


Figure 27: Effects of Bay 41-2272 (+Bay 41-2272) and hydralazine (+Hydralazine) on tubulointerstitial sGC mRNA expression and activity to produce cGMP 16 weeks after induction of chronic-progressive anti-thy1 glomerulosclerosis (cGS). Treatments were started 7 days after injection of anti-thy1 antibody into uni-nephrectomized rats. Non-diseased animals without (2-K Control) or with uni-nephrectomy (1-K Control) received a PBS injection. mRNA was analyzed by a real-time PCR method using GAPDH as housekeeping gene. mRNA is shown as a percentage of the untreated chronic anti-thy1 animals. cGMP generation was measured by ELISA in cortical tissue from individual animals in the presence or absence of the NO donor DEA/NO. (**p<0.01 vs. cGS+Hydralazine, *p<0.05 vs. Control, #p<0.05 vs. cGS)

3.4.8 Glomerular sGC activity

As shown in Figure 28, glomerular cGMP production was evaluated as sGC activity. In comparison to the normal control animals, basal and NO-stimulated glomerular cGMP production was lower in the untreated chronic anti-thy1 animals (-40%, $P>0.05$ and -58%, $p<0.05$ vs. 2-K Control 15 ± 1 fmol/well and 77 ± 7 fmol/well, respectively). Treatment with Bay 41-2272 increased basal (12 ± 2 fmol/well vs. cGS: 9 ± 1 fmol/well, $p=0.17$) and NO-stimulated cGMP production (59 ± 8 fmol/well vs. cGS: 32 ± 4 fmol/well, $p<0.01$), as compared to the untreated chronic anti-thy1 group, while hydralazine administration did not affect basal and NO-stimulated glomerular cGMP synthesis (8.64 ± 1.45 fmol/well and 29 ± 4 fmol/well, respectively).

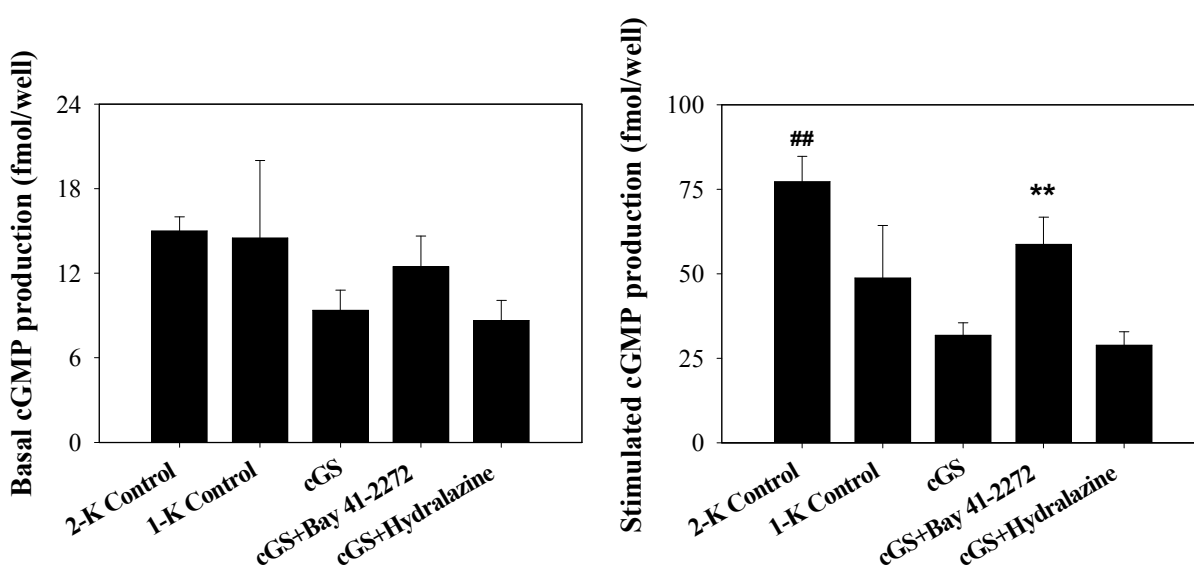


Figure 28: Effects of Bay 41-2272 (+Bay 41-2272) and hydralazine (+Hydralazine) on glomerular sGC activity to produce cGMP 16 weeks after induction of chronic-progressive anti-thy1 glomerulosclerosis (cGS). Treatments were started 7 days after injection of anti-thy1 antibody into uni-nephrectomized rats. Non-diseased animals without (2-K Control) or with uni-nephrectomy (1-K Control) received a PBS injection. cGMP generation was measured by ELISA in glomeruli harvested from individual animals in the presence or absence of the NO donor DEA/NO. (**p<0.01 and ###p<0.01 vs. cGS and cGS+Hydralazine)

3.4.9 Renal macrophage infiltration

As shown in Figure 29, the diseased groups had more cortical and glomerular macrophage infiltration than the 2-K (9.17 ± 0.4 and 0.7 ± 0.14 ED1-positive cells/section) and 1-K (7.86 ± 1.25 and 0.7 ± 0.21 ED1-positive cells/section) Control groups. Cortical and glomerular macrophage infiltration were significantly inhibited by Bay 41-2272 treatment (-39.7% and -46.7%), in contrast to cGS (58 ± 5 and 2.55 ± 0.33 ED1-positive cells/section), while hydralazine treatment did not affect macrophage infiltration (51 ± 5 and 2.58 ± 0.32 ED1-positive cells/section).

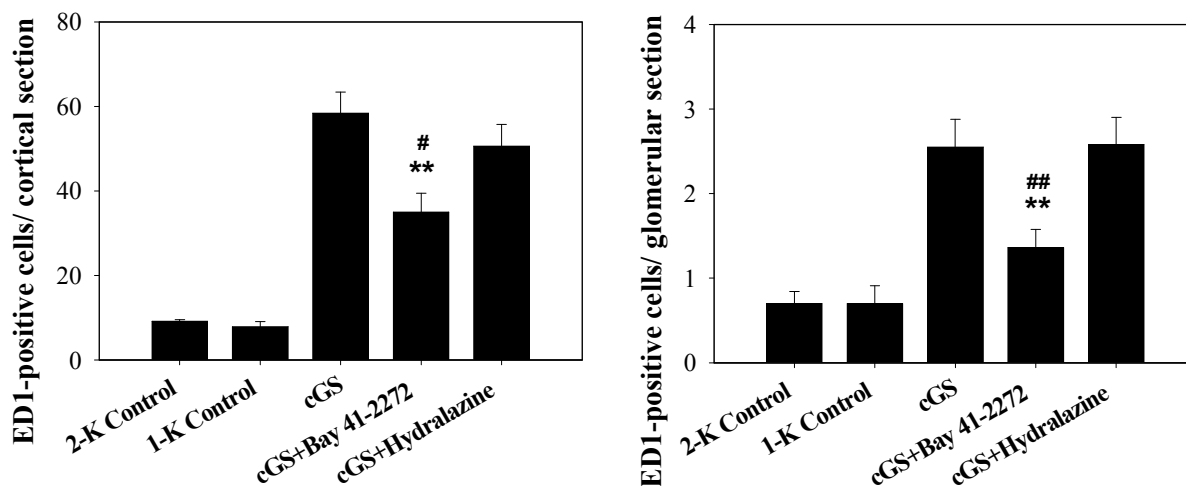


Figure 29: Effects of Bay 41-2272 (+Bay 41-2272) and hydralazine (+Hydralazine) on cortical and glomerular ED1-positive cells infiltration 16 weeks after induction of chronic-progressive anti-thy1 glomerulosclerosis (cGS). Treatments were started 7 days after injection of anti-thy1 antibody into uni-nephrectomized rats. Non-diseased animals without (2-K Control) or with uni-nephrectomy (1-K Control) received a PBS injection. Data are expressed as ED1-positive cells per cortical section observed at x200 magnification and per glomerular cross-section. (**p<0.01 vs. cGS, ##p<0.01 and #p<0.05 vs. cGS+Hydralazine)

As shown in Figure 30, and as it is consistent with macrophage infiltration, the untreated cGS group ($100\pm 15\%$) had significantly more tubulointerstitial P-selectin mRNA expression, which is important for macrophage infiltration, than the 2-K ($8\pm 1\%$) and 1-K ($13\pm 2\%$) Control groups. Bay 41-2272 administration inhibited tubulointerstitial P-selectin mRNA expression significantly (-47%) as compared to cGS, while hydralazine only slightly lowered P-selectin mRNA expression (-19%).

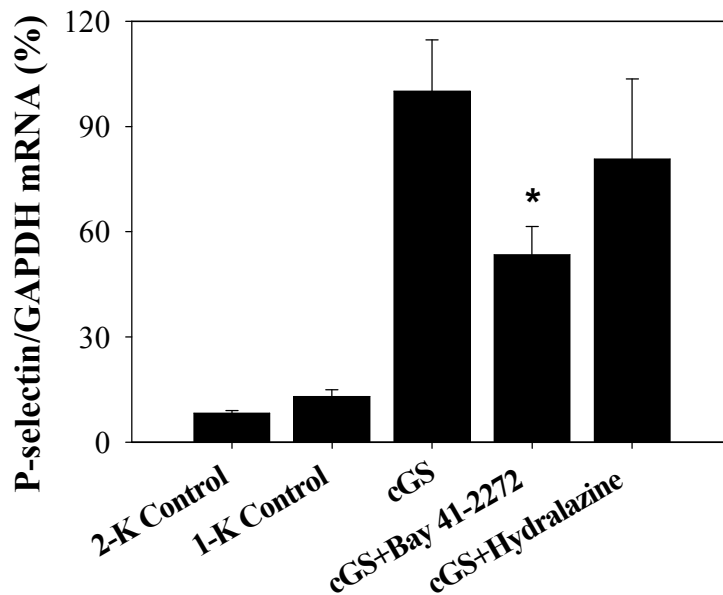


Figure 30: Effects of Bay 41-2272 (+Bay 41-2272) and hydralazine (+Hydralazine) on tubulointerstitial P-selectin mRNA expression 16 weeks after induction of chronic-progressive anti-thy1 glomerulosclerosis (cGS). Treatments were started 7 days after injection of anti-thy1 antibody into uni-nephrectomized rats. Non-diseased animals without (2-K Control) or with uni-nephrectomy (1-K Control) received a PBS injection. mRNA was analyzed by a real-time PCR method using GAPDH as housekeeping gene. mRNA is shown as a percentage of the untreated chronic anti-thy1 animals. (* $p < 0.05$ vs. cGS)

To sum up, in chronic progressive anti-thy1-induced glomerulosclerosis, tubulointerstitial sGC activity was significantly up-regulated, whereas glomerular sGC activity was diminished. Bay 41-2272 supplementation markedly increased both tubulointerstitial and glomerular sGC activity and subsequently slowed the progression of tubulointerstitial sclerosis and glomerulosclerosis in a blood pressure-independent manner.

4 Discussion

The aim of this study was to analyze the relation between the NO-cGMP cascade and the time course of renal fibrosis from injury to progressive matrix expansion. The results of the study show that the activity and expression of the NO-cGMP pathway are transcriptionally regulated during the injury, matrix expansion and progression phases in the rat model. Specific stimulation of NO-sGC signaling by Bay 41-2272 limits TGF-beta overexpression and matrix expansion, although it demonstrates no effects on mesangial cell lysis due to lack of the effector receptor sGC, suggesting its therapeutical differentiation between the beneficial and detrimental actions of the L-arginine-NO pathway. Before the results obtained will be discussed in detail, I would like to first evaluate the methodology used.

4.1 Critical evaluation of the methodology used

4.1.1 Animal model of anti-thy1-induced acute and chronic renal disease

A single injection of anti-thy1 antibody into normal or uni-nephrectomized rats causes a sequence of distinct phases of “injury”, “matrix expansion” and subsequent “progression”, which enable us to study the NO-cGMP pathway in different processes separately, while most renal disease models show no distinct injury phase and involve overlapping cycles of tissue injury and matrix expansion, such as the model of hypertension and diabetes. The injury phase is characterized by marked inducible NO production and mesangial cell lysis, which has also been found in IgA nephropathy, Wegener’s granulomatosis, lupus nephritis, acute tubular necrosis and kidney transplant rejection. The subsequent fibrosis is characterized by matrix protein accumulation, which is similar to human mesangioproliferative glomerulonephritis and IgA nephropathy. All these histological features can be found in many experimental and human renal diseases [65]. Hence the model was chosen to interpret the relevant role of the NO-cGMP pathway and its modification in human renal disease. Renal mesangial cells are specialized smooth muscle cells that play an important role in the structural support of the glomerulus and in the control of glomerular filtration rate [66]. In the same way as shown in our model, they contribute also to the pathological processes of the

glomerulus, particularly in glomerulonephritis and glomerulosclerosis. The NO-cGMP pathway plays an important role in mesangial cells [31], which might indicate an important role of NO-cGMP signal transduction in kidney diseases, such as mesangial proliferative glomerulonephritis. Therefore, we tested the hypothesis in anti-thy1 glomerulonephritis, an animal model for mesangial proliferative glomerulonephritis, which is ideal for studying the NO-cGMP pathway in vivo in comparison to the in vitro studies on the mesangial cell.

The common final pathway of chronic renal disease, independent of the primary disorder, suggests that a self-progressing mechanism and a common intrarenally determined program are operating, since the ongoing deterioration of organ function occurs even if the initial disease has been removed [9]. In the present study, anti-thy1-induced chronic glomerulosclerosis was produced through an injection of anti-thy1 antibody and a persistent hyperfiltration injury of the remaining kidney, which is consistent with a self-perpetuating and intrarenal common final pathway in many chronic renal diseases, while the ongoing and extrarenal injuries obliterate the decrease in renal function in the diabetic and hypertensive nephropathy models. Therefore, anti-thy1-induced glomerulosclerosis provides a good in vivo method to characterize the intrarenally self-progressing pathway contributing to chronic renal fibrosis. Because the molecular mechanisms of matrix expansion in various renal diseases, such as diabetic and hypertensive nephropathy, are rather common, the findings of this study may be relevant for fibrotic renal disease in general.

4.1.2 Analysis of markers of renal fibrosis

In the anti-thy1 glomerulonephritis animal model, the progressive renal disease is glomerular in origin. Thus, the measurements of sclerotic parameters in glomeruli are very important for this research. However, glomeruli occupy only 3-4% of the kidney volume compared to the >90% comprised by tubules and the interstitium [67]. Therefore, the metal sieves technique was used to yield glomeruli. Many studies have shown that tubulointerstitial injury and fibrosis correlate best with renal disease progression and insufficiency and develop independently no matter whether they originate from primarily glomerular or vascular lesions [68]. In anti-thy1-induced chronic glomerulosclerosis, the TGF-beta overexpression and matrix expansion spread from

the glomeruli into the tubulointerstitium. Thus, the parameters of tubulointerstitial fibrosis are very important in the evaluation of chronic progression. Since renal cortex consists mainly of tubulointerstitial tissue (>95%), it was used as representative of the tubulointerstitium. The separation of glomeruli and cortical cell enables us to study the fibrogenic responses of the glomeruli and the tubulointerstitium of every individual animal separately, including the production of TGF-beta, fibronectin and PAI-1 at protein level in cell culture and at mRNA level.

There were preliminary studies in our work group, which showed that the production of TGF-beta1, fibronectin and PAI-1 by isolated glomeruli and cortical cells is constant for 48 hours in culture. The 48-hour harvesting of culture supernatant was chosen on the basis of these data and the fact that the quantities of these molecules are sufficient to get accurate ELISA measurements and correlate to ECM accumulation in vivo [69]. As shown in the results, there is a big difference in disease parameters, such as glomerular and cortical TGF-beta1, fibronectin and PAI-1 expression, between untreated diseased rats and normal controls, and these differences enable detection of small differences in therapeutic efficacy. ELISA data obtained from individual rats presented the fibrotic severity precisely, in contrast to quantization from PAS staining, which is variable in tissue sectioning, staining intensity and subjective scores.

4.1.3 TGF-beta1 as a key marker of matrix expansion

Determination of the key fibrosis mediator TGF-beta1 is a valid sensitive marker of renal matrix expansion [56, 70]. This concept is proved in the rat model of anti-thy1 glomerulonephritis. In animals with two kidneys, anti-thy1 antibody injection leads to acute and reversible mesangioproliferative glomerulonephritis, in which TGF-beta returns to normal after the resolution of mesangial cell injury; whereas in uninephrectomized rats, injection of anti-thy1 antibody results in persisting TGF-beta overexpression and progressive glomerulosclerosis and tubulointerstitial fibrosis. The analysis of PAI-1 and fibronectin levels can also be an important evaluation of the anti-fibrotic effect of a new therapy independent of TGF-beta, by reflecting the imbalance of ECM synthesis and degradation. In this study, it is shown that TGF-beta production had a close relation with fibronectin and PAI-1 production and ECM accumulation, indicating that the increase in matrix accumulation is likely to result from both elevated matrix

synthesis and inhibited matrix degradation.

4.1.4 Stimulation of sGC by Bay 41-2272

Due to the importance of NO-cGMP signal transduction, modulation of this signaling cascade has attracted much attention. L-arginine and NO donor administration have long been used to modulate the NO-cGMP pathway. However, experimental studies have shown both therapeutic and detrimental consequences of treatment with L-arginine and NO donor, since the effector molecular effects of NO have also contributed to it. The use of L-arginine is not only obstructed by the potential synthesis of cytotoxic amounts of NO via iNOS, but also by the generation of agmatine, proline and polyamines via alternative L-arginine-metabolizing pathways, which are involved in renal tissue repair through different, partly opposing mechanisms [5]. The use of pharmacological NO donors leads to a rather unspecific release of NO across the whole body, is prone to tachyphylaxis and has been linked to an unwanted pro-oxidant activity [71]. In contrast, the new class of sGC modulators, such as Bay 41-2272, has attracted particular interest as the target of the L-arginine-NO-cGMP signal transduction without the formation of by-products, NO oxidative effects and tolerance, since they amplify the cGMP levels exactly at the downstream effector of NO, where cGMP is naturally generated. Therefore, sGC stimulators represent useful pharmacological tools to differentiate between signal molecular and effector molecular effects of NO.

In order to further define the role of the NO-cGMP pathway in renal disease, the rat model with anti-thy1 glomerulonephritis was first used to study the in vivo effects of Bay 41-2272 on renal function, pathology and the expression of pro-inflammatory and pro-fibrogenic factors. Second, in vitro cultures of glomeruli were used to study the possible mechanisms for the renoprotective effect of Bay 41-2272. Finally, the effects of Bay 41-2272 on the renal disease progression in this rat model were compared with those of a vasodilator, hydralazine.

4.2 The NO-cGMP pathway in the injury phase of acute anti-thy1 glomerulonephritis

The predominant mechanism of the injury phase is mesangial cell lysis, which is dependent on the generation of cytotoxic NO through iNOS. The sustained and high-

output generation of NO by iNOS may result in a broad spectrum of consequences, such as lipid peroxidation, DNA damage and pro-apoptotic effects. In this protocol, we observed the regulation of glomerular NO-cGMP signal transduction, its relation to inducible NO production and mesangial cell lysis and the effects of pretreatment with Bay 41-2272 on the injury phase.

4.2.1 Regulation of NO-cGMP signal transduction

It was interesting to find that there was about 90% decrease in glomerular alpha1 sGC and beta1 sGC expression of nephritic rats shortly after anti-thy1 antibody-induced mesangial cell injury had occurred. Corresponding to the gene expression, nephritic rats had significantly lower basal glomerular cGMP, which additionally could hardly be stimulated by DEA/NO. Bay 41-2272 pretreatment failed to stimulate sGC expression and activity to exogenous NO stimulation, probably because of the loss of glomerular sGC. The disruption of the NO-cGMP cascade paralleled the mesangial cell lysis, consistent with a high degree of sGC distribution in mesangial cells [31]. It has been reported that pro-inflammatory cytokines, such as interleukin-1beta and TNF-alpha, decrease the half-life of the sGC subunit [72]. Prolonged incubation of smooth muscle cells with NO donors has been shown to decrease sGC activity, protein and mRNA [73]. This suggests that high-output NO derived from iNOS and cytokines may also modulate sGC subunit expression. In contrast to the traditional meaning of “NO deficiency”, resulting from reduction in L-arginine and eNOS, decreased cGMP was present in the injury model with high-output NO production and normal eNOS expression. These results have opened a new explanation for “NO deficiency”.

4.2.2 Effects of Bay 41-2272 on mesangial cell lysis

In rat nephrotoxic nephritis, macrophage infiltration was decreased by iNOS inhibition, accompanied by an increase in eNOS [74]. It has been shown that in human mesangial cells, iNOS mRNA half-life was reduced by the NO-cGMP pathway to regulate the toxic effects of high levels of NO [66]. Then I inquired if Bay 41-2272 might activate the L-arginine-eNOS-cGMP pathway to depress the L-arginine-iNOS-NO pathway in the injury phase. As shown in the results, the animals in protocol 1 displayed a typical manifestation of the injury phase in acute anti-thy1 glomerulonephritis: up-

regulation of iNOS mRNA expression with a high-output of NO and mesangial cell lysis. Pretreatment with Bay 41-2272 could not increase cGMP synthesis, perhaps due to the lack of the receptor sGC. With this in mind, it is not surprising that Bay 41-2272 had no effect on the degree of anti-thy1-induced mesangial cell injury, including proteinuria, mesangial cell counts, and NO output and iNOS mRNA expression. But it should be emphasized that unlike L-Arginine, which can increase mesangial cell injury due to pro-fibrogenic by-products and increased oxidative stress, Bay 41-2272 has no negative effects on the injury phase. It even slightly decreased proteinuria in our study. Hence, the deficiency of target receptor sGC in the injury phase is the reason for the lack of Bay 41-2272 effects in this phase of the disease.

4.3 The NO-cGMP pathway in the matrix expansion phase of acute anti-thy1 glomerulonephritis

In the matrix expansion phase following the injury phase, overexpression of TGF-beta and accumulation of ECM are the main features. In this protocol, we observed the alteration of the glomerular NO-cGMP signal transduction, its relation to glomerular TGF-beta1 overexpression and matrix accumulation and the effects of an administration of Bay 41-2272 on glomerular matrix expansion.

4.3.1 Regulation of NO-cGMP signal transduction

In contrast to the injury phase, a dramatic change of sGC was shown in the matrix expansion phase. Alpha1 sGC and beta1 sGC expression increased 5.6-fold and 3.3-fold in untreated nephritic rats. Although already up-regulated by the disease itself, Bay 41-2272 treatment further elevated the expression of alpha1 sGC and beta1 sGC 17.6-fold and 12.2-fold. The increase in sGC expression in the nephritic group is parallel to mesangial cell proliferation, indicating that sGC expresses significantly in mesangial cells, which is consistent with the disruption of sGC expression in the injury phase accompanied by mesangiolysis. Apart from increasing sGC expression, sGC activity to generate cGMP was also increased by the disease itself and significantly further amplified by Bay 41-2272, which is parallel to sGC mRNA expression. Of interest in this context is the finding that sGC enhancer treatment not only significantly increased glomerular NO-induced cGMP generation, but also the mRNA expression of both

subunits of the sGC. This may represent a self-reinforcement mechanism through which Bay 41-2272 can influence the expression of its effectors. However, it might as well be just a consequence of the improved glomerular wound repair in the treatment group. The increased sGC expression by Bay 41-2272 treatment, on the other hand, is a novel observation that has not been previously reported. It becomes important in pathophysiologic conditions, where deficient sGC expression is characterized. However, this is in contrast to the data from many cardiovascular studies, which have shown decreases in sGC expression and activity in hypertensive animal models [75, 76]. This may represent divergent regulatory mechanisms in the two different organs. In acute anti-thy1 glomerulonephritis, glomerular sGC expression and activity are compensatorily increased and relatively impaired, which may not suffice to counteract the fibrotic response, whereas Bay 41-2272 further elevated sGC expression and cGMP levels to limit matrix expansion. In addition, similar to the results in the injury phase, eNOS expression did not decrease in nephritic animals, which is consistent with no decrease in renal eNOS expression found in hypertensive rats [53], suggesting no eNOS-NO deficiency in the matrix expansion phase of acute anti-thy1 glomerulonephritis. Moreover, Bay 41-2272 increased eNOS expression transcriptionally. Further studies will be done to explore the mechanism of the up-regulation of eNOS expression by Bay 41-2272.

4.3.2 Antifibrotic effects of Bay 41-2272

In the present study, increases in glomerular production of 10.5-fold for TGF-beta1, 9-fold for fibronectin and 3.4-fold for PAI-1 were seen in the untreated nephritic group when compared to normal controls. These significant differences make it possible to observe the antifibrotic effects of Bay 41-2272. The cGMP levels further amplified by Bay 41-2272 significantly limited the fibrotic response of the matrix expansion phase, as shown by reductions in proteinuria, glomerular histological matrix accumulation and expression of TGF-beta1, fibronectin and PAI-1. Although all disease parameters prove the antifibrotic effects of Bay 41-2272, it remains unclear how enhanced NO-cGMP signal transduction results in the decrease in TGF-beta1 overexpression and the antifibrotic effect, which will be discussed later. It has been previously proved that L-arginine has antifibrotic action in anti-thy1 glomerulonephritis mediated by endogenous

production of NO through limiting TGF-beta overexpression [16]. Our findings further prove that the antifibrotic action of NO in renal fibrosis is mediated by cGMP through sGC modification.

4.4 The NO-cGMP pathway in anti-thy1-induced chronic glomerulosclerosis

In this study, increased blood urea and creatinine associated with marked reduction in the glomerular filtration rate and hematocrit were observed in anti-thy1-induced chronic glomerulosclerosis, indicating impaired renal function. In this protocol, we observed the change of the tubulointerstitial and glomerular NO-cGMP signal transduction in the progression phase of chronic anti-thy1-induced glomerulosclerosis 16 weeks after antibody injection, its correlation with glomerulosclerosis, tubulointerstitial fibrosis and renal insufficiency and the effects of the sGC enhancement by Bay 41-2272 on slowing the progressive course of chronic anti-thy1-induced glomerulosclerosis. In addition, the sole vasodilator hydralazine was used to investigate the blood pressure-independent effect of Bay 41-2272.

4.4.1 Regulation of NO-cGMP signal transduction

Very little is known about the long-term regulation of sGC in the kidney. sGC expression and activity showed contrary change in the glomeruli and the tubulointerstitium of the chronic model. In parallel to increased glomerular expression and activity of sGC in acute anti-thy1 glomerulonephritis, tubulointerstitial sGC mRNA expression and NO-dependent cGMP production were significantly up-regulated in the presence of marked tubulointerstitial fibrosis 16 weeks after induction of progressive anti-thy1 glomerulosclerosis. However, glomerular sGC expression and activity were significantly inhibited, in contrast to tubulointerstitial NO-cGMP signaling in the same model at the same time, but also to the strong up-regulated glomerular sGC activity in the matrix expansion phase of the acute model. Although Bay 41-2272 could not enhance sGC expression, sGC activity in response to NO stimulation in both depressed glomerular and elevated tubulointerstitial sGC expression was significantly enhanced by Bay 41-2272 treatment. Therefore, subsensitivity of sGC to NO stimulation, as observed in our results, could attenuate the efficacy of NO-cGMP signal transduction, contributing to the progression of renal disease. Compared to the relatively impaired

tubulointerstitial sGC, the glomerular sGC was completely impaired. The up-regulation of tubulointerstitial sGC expression in diseased rats might also be a self-compensatory effect to counteract the renal fibrosis.

Endothelium-independent NO-cGMP signaling by exogenous NO donor was blunted, indicating that dysfunction of sGC may be responsible for the blunted endothelium-independent NO-cGMP pathway. Considering slightly increased eNOS mRNA in diseased rats in the study, these alterations in the NO-cGMP system, namely, the enhanced eNOS-NO pathway and impaired sGC-cGMP pathway, seem to be the phenotypic character of renal fibrosis rats. Dysfunction of sGC-cGMP rather than eNOS-NO deficiency contributes to the impairment of NO-cGMP signal transduction in our animal model.

4.4.2 Antifibrotic effects of Bay 41-2272

Bay 41-2272 treatment increased cGMP generation and subsequently markedly limited the glomerular and tubulointerstitial progression in this model, as shown by reduced histological glomerular and tubulointerstitial fibrosis and expression of TGF-beta1, fibronectin and PAI-1. The inhibitory effects on TGF-beta1, fibronectin and PAI-1 protein and mRNA expression lead to a decrease in ECM synthesis and an increase in ECM protein degradation resulting in limiting renal fibrosis. In addition, administration of the sGC stimulator lowered blood creatinine and urea concentrations and increased creatinine clearance and hematocrit levels, underscoring that the morphological and molecular glomerular and tubulointerstitial benefits achieved went along with improved renal function. The present study in progressive anti-thy1-induced chronic glomerulosclerosis confirms the critical role of sGC and NO-dependent cGMP production in pathological renal matrix accumulation revealed in the acute anti-thy1 model. The important role of sGC in fibrotic kidney disease is thereby now expanded from glomerular to tubulointerstitial TGF-beta overexpression and matrix expansion, as well as from acute, reversible to chronic progressive renal disease.

However, at the glomerular level, Bay 41-2272 reduced TGF-beta1, fibronectin and PAI-1 as well, but the benefits are more moderate than those at the tubulointerstitial level. In addition, Bay 41-2272 treatment has no statistically significant effect on

proteinuria, which mainly reflects glomerular barrier impairment. It seems that Bay 41-2272 could reduce tubulointerstitial impairment more effectively than glomerular impairment. I think the possible reason is that Bay 41-2272 treatment was started as late as 7 days after induction of anti-thy1 glomerulosclerosis; at this point in time, the glomerular disease was already established. This view is supported by the results in the matrix expansion phase of acute anti-thy1 glomerulonephritis, in which Bay 41-2272 has significant effects on reducing glomerular TGF-beta1 overexpression, fibronectin, PAI-1 and proteinuria when begun as early as 24 hours after anti-thy1 glomerulonephritis induction. On the other hand, a late start of the therapy may result in more serious sGC impairment in the glomeruli than in the tubulointerstitium, which also leads to a less efficiency of Bay 41-2272 on proteinuria. In addition, it has been pointed out that proteinuria in anti-thy1-induced renal disease does not always follow the severity of the fibrotic response [77]. Thus, the finding that proteinuria is not significantly reduced in the chronic model is of interest, yet the reasons for it remain unclear.

4.5 Transcriptional regulation of NO-cGMP signal transduction from acute to chronic renal disease

As shown in the model of anti-thy1-induced renal disease, the NO-cGMP pathway displayed interesting changes from initial injury to the following matrix expansion phase and the final progressive fibrosis. It opened a new understanding of the pathogenesis of renal fibrosis. Previously, it had generally been assumed that the activity of this pathway is mainly dependent on the capability of eNOS to generate NO [3, 4, 5]. In this sense, impaired renal NO production has been linked to an insufficient supply with its main precursor L-arginine and the co-factor tetrahydrobiopterin as well as to increased deactivation of the NO produced, for example, by free radicals [5, 6, 78]. Therefore, the term NO deficiency has been mainly understood as deficiency in the synthesis of NO, and sGC has played a rather passive role. The sGC enzyme has been thought to be expressed constitutively and to transduce the NO signal without further modulation [79]. However, these findings in acute and chronic anti-thy1-induced renal diseases reveal that sGC can be the object of a marked transcriptional regulation as well and this relates directly to the subsequent ability of NO to produce cGMP.

In this study, there is no eNOS down-regulation in the acute and chronic

glomerulonephritis models, suggesting that NO deficiency from eNOS does not play a key role in the renal matrix expansion of our model. However, the dramatic down- and up-regulation of sGC expression and activity was found in this model. Hence, the impaired sGC activity may be the main reason for 'NO deficiency' in observed renal disease and NO-cGMP signal transduction impairment, indicating an impairment of NO-dependent signaling transduction either at the level of or downstream from sGC. This finding is evident in the injury phase. Despite glomerular NO production being markedly increased, the glomerular NO-cGMP pathway was disrupted due to the loss of the sGC enzyme. Similarly, a decrease in the expression or activity of vascular sGC has recently been reported in several disease models characterized by a functional NO deficiency, including spontaneously hypertensive rats, aging, myocardial infarction, angiotensin II infusion, lead-induced hypertension and diabetic Goto-Kakizata rats [53, 75, 80, 81, 82, 83]. In many of these studies, endothelial NO production was found to be normal or even increased as well. Thus, due to the uncoupling of the eNOS-NO and sGC-cGMP pathway, impaired expression or activity of sGC can functionally mimic "NO deficiency".

In acute anti-thy1 glomerulonephritis, glomerular sGC-cGMP signaling experienced dramatic and contrary alterations, from almost totally disrupted to markedly up-regulated expression and activity, consistent with the pathological change from mesangiolysis to mesangial cell proliferation and glomerular matrix expansion. Thus, it may be speculated that the change in glomerular sGC is related to the amount of its main host cells, mesangial cells, during the course of acute anti-thy1 glomerulonephritis. In progressive anti-thy1-induced chronic glomerulosclerosis, both glomerular and tubulointerstitial fibrosis contribute to the deterioration of renal function. Interestingly, it was found that the NO-cGMP pathway in the glomeruli was not consistent with the one in the tubulointerstitial tissue. Tubulointerstitial sGC activity after NO stimulation was markedly up-regulated, while the sGC activity of glomeruli was completely impaired. Compared to the glomeruli in the matrix expansion phase of acute anti-thy1 glomerulonephritis, glomerular cGMP production in response to NO was about 1187-fold down-regulated 16 weeks after disease induction, and tubulointerstitial cGMP synthesis stimulated by NO was 135-fold depressed. That is to say, the severity of the NO-sGC-cGMP impairment was in an ascending sequence: glomeruli in acute

glomerulonephritis, tubulointerstitium in chronic glomerulosclerosis and glomeruli in chronic glomerulosclerosis, which is consistent with the time course of chronic renal disease, from acute to chronic, with ongoing TGF-beta overexpression, from the glomerular compartment to the interstitial compartment, and from relative impairment to absolute insufficiency.

Because of the long period of disease in the chronic model, the mechanisms involved in the impairment of NO-cGMP are more complicated than those in the acute model. Several reasons are reported for the dysfunction of sGC in the kidney, such as a reduction in the enzyme's heme content and/or oxidation of the heme iron [83] and a mutation of prosthetic heme in sGC [84]. Metabolic changes, such as hypercholesterolemia, chronic hypertension, aging, oxidative factor and morphologic changes may contribute to the impairment of signaling downstream from NO, sGC expression or activity [75, 85, 86]. In this study, compared to old hypertensive chronic diseased rats, the glomerular sGC activity in response to NO stimulation of young normotensive acute nephritic rats was 1187-fold higher. All these reasons may be attributed to the subsensitivity of sGC cooperatively. The up-regulated sGC activity in the glomeruli of the acute model and the tubulointerstitium of the chronic model may reflect a self-compensatory mechanism for holding the disease progression. However, compensatorily increased cGMP levels cannot counteract the pathogenetic factors, otherwise fibrogenic factors could inhibit sGC compensation, resulting in relative insufficiency. But Bay 41-2272 treatment could go on stimulating sGC activity to improve renal disease. The impairment of the sGC-cGMP pathway could represent a mechanism by which pro-fibrotic agents reduce activation of the antifibrotic pathway.

4.6 Mechanisms of Bay 41-2272's antifibrotic effects

In order to further characterize the role of the NO-cGMP pathway in anti-thy1-induced renal disease, the specific sGC stimulator was used in this study. It showed that Bay 41-2272 ameliorates renal fibrosis via further increases in cGMP levels, resulting in the restoration of renal function in anti-thy1 glomerulonephritis, indicating a potential pharmacological target for the treatment of progressive renal fibrosis. There are several mechanisms that may be involved in antifibrotic effects via the increased cGMP.

4.6.1 Reduction in blood pressure

Systemic hypertension is a major risk factor that determines the rate of progression of renal disease [87, 88]. Transmission of the systemic blood pressure to the glomerulus may induce an adaptive glomerular hyperfiltration and an increase in glomerular capillary pressure leading to consequent glomerular hypertrophy and sclerosis [89, 90]. In addition, chronic hypertension may result in vascular narrowing, causing glomerular hypoperfusion and ischemic nephropathy [91]. This risk factor plays a more important role in anti-thy1 chronic glomerulosclerosis than in acute anti-thy1 glomerulonephritis, since the rats with anti-thy1-induced chronic glomerulosclerosis showed significantly high blood pressure, in contrast to the rats of acute anti-thy1 glomerulonephritis with normal blood pressure. Bay 41-2272 treatment reduced the systolic blood pressure of animals in the acute and the chronic models. Several mechanisms to decrease blood pressure via cGMP have been discussed in the literature. Activation of sGC in the vascular smooth muscle cell increases the conversion of GTP to cGMP, which regulates the intracellular Ca^{2+} and inhibits vasoconstricting factors, such as endothelin-1, and then decreases the blood pressure [48]. Therefore, sGC is an important target protein for regulating blood pressure. Due to the wide distribution of sGC in mesangial cells and vascular smooth muscle cells of the kidney, it is not surprising that Bay 41-2272 can reduce the glomerular hyperfiltration and hyperperfusion to prevent these hemodynamic adaptations as well as the subsequent complications via beneficial effects on systemic and intraglomerular blood pressure. Considering that renal vasoconstriction may contribute to the progression of chronic renal diseases, improved renal function could be explained by an effect of Bay 41-2272 upon renal circulation.

4.6.2 Blood pressure-independent effects of Bay 41-2272

Bay 41-2272 can significantly decrease systolic blood pressure by increasing cGMP, which leads to the question if the antifibrotic action of Bay 41-2272 is mediated by reduced glomerular blood pressure. However, there was a Bay 41-2272 dose-dependent reduction in TGF-beta1 protein synthesis in cultured normal and nephritic glomeruli, an environment where blood pressure plays no role. In addition, acute anti-thy1 glomerulonephritis is a normotensive model, and it has been found that systemic

hypertension and treatment with high doses of β -blocker does not influence the excess of the mesangial matrix deposition in this model [92], and renovascular hypertension did not influence healing of the glomerular lesions in the acute anti-thymocyte serum nephritis [93]. These findings suggest that sGC stimulation to increase cGMP can inhibit TGF-beta1 expression via a direct and blood pressure-independent mechanism in the model with acute glomerulonephritis.

In the chronic glomerulosclerosis model, the sole vasodilator hydralazine did not significantly alter the degrees of glomerulosclerosis, tubulointerstitial fibrosis and renal insufficiency, despite a comparable blood pressure decrease having been achieved, while only Bay 41-2272 significantly reduced pro-fibrotic factors, such as TGF-beta1, fibronectin and PAI-1, inflammatory cell infiltration and histological signs of glomerulosclerosis. This suggests that Bay 41-2272 slowed the progressive course of anti-thy1-induced glomerulosclerosis and appeared to be at least in part independent of blood pressure reduction. Renal TGF-beta1 overexpression and matrix accumulation were also reduced by blood pressure-independent mechanisms. The superiority of Bay 41-2272 over conventional antihypertensive therapies may result from elevated cGMP levels. Therefore, enhancement of cGMP production probably has antifibrotic effects that are independent of the reduction in blood pressure, which includes the following three mechanisms.

4.6.2.1 *Direct reduction in TGF-beta1 expression*

The renal pathology of anti-thy1 glomerulonephritis is characterized by ongoing TGF-beta1 overexpression, progressive glomerulosclerosis and interstitial fibrosis. These pathological changes were ameliorated by Bay 41-2272. A variety of mediators, including TGF-beta1, fibronectin and PAI-1, which are important growth factors for ECM production, were down-regulated by elevated cGMP. Therefore, one of the possible mechanisms for renoprotection may be linked to the direct effect of cGMP against pro-fibrotic factors and the subsequent inhibition of matrix protein deposition in the kidney.

4.6.2.2 *Inhibition of renal platelet deposition*

Platelet aggregation is important for the progression of glomerulonephritis through release of fibrogenic growth factors such as TGF-beta and platelet-derived growth

factor and can participate in the synthesis of the mesangial matrix [94]. It is assumed that the effects of NO on modulating platelet reactivity are mediated via the activation of sGC, the formation of cGMP and the subsequent activation of PKG, which can phosphorylate several proteins to decrease the intraplatelet free calcium levels and inhibit platelet activation and aggregation [95]. It has been shown that platelet inhibition via clopidogrel limited TGF-beta overexpression and matrix accumulation in the matrix expansion phase of acute anti-thy1 glomerulonephritis [58]. Bay 41-2272 supplementation increased plasma cGMP levels, prolonged the bleeding time and decreased glomerular fibrinogen deposition, indicating a reduction of platelet aggregation and glomerular platelet deposition via sGC-cGMP pathway stimulation, which correlated with reduced proteinuria, pro-fibrotic factors and renal fibrosis. Hence, inhibiting the pathological platelet activation may be another mechanism to slow down the progression of renal diseases.

4.6.2.3 *Inhibition of renal macrophage infiltration*

In the injury phase, macrophages produce NO, reactive oxygen species and proteases mediating mesangiolytic [14]. Later, macrophages can release cytokines and growth factors including TGF-beta which are important stimuli to the production of ECM [14]. During glomerular inflammation, cytokines and chemokines synthesized by mesangial cells modulate the expression of adhesion molecules involved in the infiltration, activation and differentiation of inflammatory cells within the glomeruli [96]. In the present study, infiltrating glomerular and interstitial macrophages, ED1-positive cells, were reduced by Bay 41-2272 treatment. Furthermore, P-selectin, an important adhesion molecule for leukocyte recruitment, was down-regulated by Bay 41-2272, indicating that the mechanism of Bay 41-2272 in reducing inflammation is due to inhibition of macrophage adhesion through an increase in cGMP content. This is consistent with a recent study, in which Bay 41-2272 and NO donor could stimulate the NO-cGMP pathway to inhibit P-selectin expression, leukocyte recruitment and inflammation in postcapillary venules [97]. In addition, Bay 41-2272 has vasodilatory properties and inhibits platelet aggregation to prevent adherence of leucocytes and platelets to the endothelium. They can result in the reduction of renal inflammation and renal fibrosis. This implies that elevated cGMP levels through Bay 41-2272, a sGC

stimulator, can directly reduce macrophage infiltration and adhesion molecule expression to slow the progression of anti-thy1-induced renal disease.

Specific stimulation of sGC signaling by Bay 41-2272 significantly limits pathological matrix expansion in the kidney and the course of progressive renal disease at least partially in a manner independent of blood pressure via direct inhibition of renal TGF-beta1 overexpression, platelet deposition and macrophage infiltration.

4.7 To differentiate the beneficial and detrimental actions of the L-arginine-NO pathway

Using L-arginine supplementation and NO donation to modify the L-arginine-NO pathway has been studied as a novel therapy to slow the rate of progressive renal disease. However, as outlined before, L-arginine or NO donation have the potential both to protect and to harm the kidney [16, 55, 69]. It has been asked if the beneficial effect of L-arginine is indeed mediated through NO, and how we can mimic its therapeutic potential. In the injury phase of anti-thy1 glomerulonephritis, due to the loss of the sGC enzyme, Bay 41-2272 cannot elevate the disrupted cGMP production, and then the detrimental action of the L-arginine-NO pathway is dominant. In contrast, markedly increased cGMP levels in the matrix expansion and progression phases through Bay 41-2272 administration resulted in an antifibrotic effect. These data expand our understanding of previous investigations of anti-thy1 glomerulonephritis using L-arginine supplementation or NO donation. Given the L-arginine-NO-cGMP signaling cascade, the very similar beneficial effects on TGF-beta overexpression and inhibition of ECM accumulation achieved by the sGC stimulator indicate that L-arginine and NO donation mediate its antifibrotic actions via cGMP signaling.

Furthermore, this study suggests that pharmacological enhancement of the NO-cGMP pathway may be a reasonable strategy to overcome important limitations of L-arginine supplementation or NO donation in treating progressive renal fibrosis, including the production of cytotoxic NO, the generation of endogenous L-arginine metabolites and unwanted pro-oxidant activity. Therefore, sGC stimulators can differentiate between the beneficial and detrimental actions of the L-arginine-NO pathway. The new class of sGC enhancers, such as Bay 41-2272, acts in a functionally very specific

manner on the L-arginine-NO-cGMP signaling to amplify the cGMP signal exactly at that sub-cellular place where further cGMP effector pathways are already lined up.

5 Summary

The expression and activity of the NO-cGMP signal transduction were analyzed during the injury, matrix expansion and progression phases in the rat model of anti-thy1-induced renal disease. In order to further characterize the role of NO-cGMP signaling, the activity of sGC and subsequent cGMP production were specifically enhanced with the novel orally applicable compound Bay 41-2272.

Acute anti-thy1 glomerulonephritis was induced by anti-thy1 antibody injection into rats with two kidneys, while anti-thy1-induced chronic glomerulosclerosis was produced by injecting anti-thy1 antibody into uni-nephrectomized rats. In protocol 1 (injury phase, day 1), Bay 41-2272 treatment was begun 6 days before and continued until one day after antibody injection. In protocol 2 (matrix expansion phase, day 7), Bay 41-2272 treatment was started one day after antibody injection and was continued until day 7. In protocol 3 (progression phase, week 16), treatments with Bay 41-2272 or hydralazine as sole vasodilator control were started one week after disease induction and lasted until week 16.

In the injury phase, glomerular expression and activity of the sGC were markedly down-regulated, while NO-cGMP signaling was highly up-regulated during the subsequent matrix expansion phase. During the progression phase, the glomerular and tubulointerstitial sGC pathways were discordantly altered, showing markedly up-regulated sGC expression and activity in tubulointerstitial fibrosis and depressed NO-cGMP signaling in persisting glomerulosclerosis. These data show that the sGC activity is highly regulated at the transcriptional level during the course of renal fibrosis, and correlates closely with the pathological changes from the injury over the matrix expansion toward the final progression phase. The results indicated that the sGC enzyme plays an active and independent role in NO signaling and that the pathophysiologic phenotype of “NO deficiency” results not only from reduced synthesis of NO, but also from the impaired subsequent production of its signaling molecule cGMP.

The sGC stimulator Bay 41-2272 significantly enhanced renal NO-stimulated cGMP production and thereby limited TGF-beta overexpression and matrix protein

accumulation in the matrix expansion phase of acute anti-thy1 glomerulonephritis. In the injury phase, Bay 41-2272 failed to improve NO-cGMP signaling due to a complete loss of sGC expression and thus could not interfere with the anti-thy1 antibody-induced glomerular mesangial cell damage. In the progression phase, treatment with Bay 41-2272 significantly slowed the progressive course of the anti-thy1-induced chronic glomerulosclerosis model towards glomerular sclerosis, tubulointerstitial fibrosis and impaired renal function. The sole vasodilator hydralazine did not affect NO-cGMP signaling and the progressive fibrosis and insufficiency, suggesting an at least partially blood pressure-independent mode in the renoprotective action of Bay 41-2272. Further analyses revealed that these pressure-independent effects of Bay 41-2272 were related to a direct reduction in the expression of the key fibrosis mediator TGF-beta1 and to a decrease in renal platelet deposition and macrophage infiltration. Taken together, these results indicate that pharmacological stimulation of sGC activity represents a novel, blood pressure-independent approach to limiting renal matrix accumulation and to slowing the progressive loss of function in chronic renal disease.

The use of L-arginine supplementation to increase renal NO synthesis has previously been shown to have both beneficial and detrimental consequences in experimental kidney disease. The findings of this study indicate that the beneficial L-arginine actions are likely to be mediated via subsequent NO-cGMP signaling and that specific stimulation of sGC activity is a feasible mode of separating the positive and negative effects of L-arginine administration in renal disease. Beyond the models of anti-thy1-induced renal disease, the results presented here are likely to open new perspectives in the understanding and treatment of renal disease in general. Ongoing TGF-beta overexpression and progressive renal matrix accumulation are hallmarks of most, if not all, chronic experimental and human kidney disorders. Thus, further studies are warranted in order to analyze whether the sGC enzyme also plays an independent role in other chronic renal diseases, such as experimental and human hypertensive and diabetic nephropathy, and whether enhancement of NO-cGMP signaling will limit their course towards progressive renal fibrosis and insufficiency.

6 Zusammenfassung

Im Rattenmodell der Anti-Thy1-induzierten Nierenfibrose wurde die Expression und Aktivität der NO-cGMP-Signaltransduktionskaskade während der Schädigungs-, Matrixexpansions- und Progressionsphase untersucht. Zur weiteren Charakterisierung der Rolle der NO-cGMP-Signaltransduktion wurden die Aktivität der löslichen Guanylatzyklase und die nachfolgende cGMP-Produktion spezifisch mit dem oral anwendbaren, neuen Wirkstoff Bay 41-2272 stimuliert.

Die akute Anti-Thy1-Glomerulonephritis wurde durch eine Anti-Thy1-Antikörperinjektion in Wistar-Ratten mit zwei Nieren induziert, während die chronische Anti-Thy1-Glomerulosklerose durch eine Anti-Thy1-Antikörperinjektion bei uninephrektomierten Ratten eingeleitet wurde. Im Protokoll 1 (Schädigungsphase, Tag 1) begann die Behandlung mit Bay 41-2272 sechs Tage vor und endet einen Tag nach der Antikörperinjektion. Im Protokoll 2 (Matrixexpansionsphase, Tag 7) wurde die Behandlung mit Bay 41-2272 einen Tag nach der Antikörperinjektion begonnen und bis zum siebten Tag fortgeführt. Im Protokoll 3 (Progressionsphase, 16 Wochen) wurde die Behandlung mit Bay 41-2272 eine Woche nach der Erkrankungsinduktion begonnen und in 15 Wochen beendet. In diesem Protokoll wurde als interne Kontrolle eine Gruppe von nierenkranken Tieren mit dem reinen Vasodilator Hydralazin behandelt.

In der Schädigungsphase war die glomeruläre Expression und Aktivität der löslichen Guanylatzyklase hoch signifikant vermindert, während die NO-cGMP-Signaltransduktion in der nachfolgenden Matrixexpansionsphase deutlich hochreguliert gefunden wurde. Während der Progressionsphase veränderten sich die glomeruläre und tubulointerstitielle sGC-Signalvermittlung diskontinuierlich und zeigte eine merklich hochregulierte sGC-Expression und -Aktivität in Gegenwart von tubulointerstitieller Fibrose und eine verminderte NO-cGMP-Signalaktivität bei persistierender Glomerulosklerose. Diese Befunde dokumentieren, dass die Aktivität der löslichen Guanylatzyklase im Verlauf von akuter und chronischer Nierenfibrose erheblich und eigenständig auf der transkriptionellen Ebene reguliert wird und dass die transkriptionell-vermittelten Veränderungen der sGC-Aktivität eng mit den pathologischen Veränderungen der Schädigungs-, Matrixexpansions- und

Progressionsphase korrelieren. Die Ergebnisse weisen darauf hin, dass das sGC-Enzym eine aktive und unabhängige Rolle im NO-Signalweg spielt und dass der pathophysiologische Phänotyp „NO-Mangel“ nicht nur als Folge verminderter NO-Synthese, sondern auch aus unzureichender Produktion seines Signalmoleküls cGMP resultieren kann.

Der sGC-Stimulator Bay 41-2272 verstärkte signifikant die renale NO-stimulierte cGMP-Produktion. In der Matrixexpansionsphase der akuten Anti-Thy1-Glomerulonephritis ging die gesteigerte NO-cGMP-Produktion mit signifikant verminderter glomerulärer TGF-beta-Überexpression und Matrixakkumulation einher. Infolge des fast vollständigen Verlustes der sGC-Expression in der Schädigungsphase war Bay 41-2272 nicht in der Lage die NO-cGMP-Signaltransduktion zu verbessern, so dass die Anti-Thy1-Antikörper-induzierte Mesangialzellschädigung auch nicht beeinflusst wurde. In der Progressionsphase des chronischen Anti-Thy1-Nierenfibrosemodells verlangsamte die Behandlung mit Bay 41-2272 den eigenständig fortschreitenden Verlauf der Erkrankung zur Glomerulosklerose, tubulointerstitiellen Fibrose und eingeschränkten Nierenfunktion. Im Gegensatz zu Bay 41-2272 hatte der Vasodilator Hydralazin keinen Einfluss auf die NO-cGMP-Signaltransduktion und die Progression von renaler Fibrose und Insuffizienz. Dieses spricht dafür, dass die nephroprotektiven Effekte von Bay 41-2272 zumindest teilweise über blutdruckunabhängige Mechanismen vermittelt werden. In weitere Analysen konnte gezeigt werden, dass diese blutdruckunabhängigen Wirkungen von Bay 41-2272 zum Teil über eine direkte Reduktion der Expression des zentralen Fibrosemediators TGF-beta1 und eine Verminderung der renalen Thrombozytendeposition und Makrophageninfiltration vermittelt werden. Zusammengefasst zeigen die Ergebnisse in der Matrixexpansions- und Progressionsphase, dass die pharmakologische Stimulation der sGC-Aktivität einen neuen blutdruckunabhängigen Ansatz darstellt, um die pathologische renale Matrixakkumulation zu vermindern und den progressiven Funktionsverlust von chronischen Nierenerkrankung zu verlangsamen.

Über die Modelle Anti-Thy1-induzierten Nierenerkrankungen hinaus, zeigen die Ergebnisse dieser Arbeit neue Perspektive im Verständnis und der Behandlung von Nierenerkrankung im Allgemeinen auf. Es ist zuvor gezeigt worden, dass die Gabe von

L-Arginin zur Steigerung der renalen NO-Synthese sowohl mit günstigen als auch mit ungünstigen Effekten auf experimentelle Nierenerkrankung einhergehen kann. Die Resultate dieser Arbeit weisen darauf hin, dass die protektiven L-Arginineffekte wahrscheinlich über eine gesteigerte NO-cGMP-Signaltransduktion vermittelt werden und dass mittels der spezifische Stimulation der sGC-Aktivität ein praktisch anwendbarer Modus gefunden ist, um die günstigen und ungünstigen Wirkungen des L-Argininstoffwechsels bei Nierenerkrankung zu trennen. Da die meisten chronischen experimentellen und humanen Nierenerkrankungen gleichermaßen durch fortlaufende TGF-beta-Überproduktion und progressive Nierenmatrixakkumulation gekennzeichnet sind, sollten zukünftige Studien analysieren, ob auch in anderen chronischen Nierenerkrankungen, wie z. B. der hypertensiven und diabetischen Nephropathie, die lösliche Guanylatzyklase eine unabhängige Rolle spielt und ob sich auch hier über eine Verbesserung der NO-cGMP-Signaltransduktion das Fortschreiten zur progressiven Nierenfibrose und Insuffizienz verzögert werden kann.

Reference list

- [1] Stengel, B.; Billon, S.; Van Dijk, P. C.; Jager, K. J.; Dekker, F. W.; Simpson, K. und Briggs, J. D. (2003): Trends in the incidence of renal replacement therapy for end-stage renal disease in Europe, 1990-1999, *Nephrol.Dial.Transplant.* (volume 18), issue 9, pp. 1824-1833. URL: PM:12937231
- [2] Border, W. A. und Noble, N. A. (1994): Transforming growth factor beta in tissue fibrosis, *N.Engl.J.Med.* (volume 331), issue 19, pp. 1286-1292. URL: PM:7935686
- [3] Kone, B. C. (1997): Nitric oxide in renal health and disease, *Am.J.Kidney Dis.* (volume 30), issue 3, pp. 311-333. URL: PM:9292559
- [4] Noris, M. und Remuzzi, G. (1999): Physiology and pathophysiology of nitric oxide in chronic renal disease, *Proc.Assoc.Am.Physicians* (volume 111), issue 6, pp. 602-610. URL: PM:10591090
- [5] Peters, H.; Border, W. A. und Noble, N. A. (1999): From rats to man: a perspective on dietary L-arginine supplementation in human renal disease, *Nephrol.Dial.Transplant.* (volume 14), issue 7, pp. 1640-1650. URL: PM:10435871
- [6] Reyes, A. A.; Karl, I. E. und Klahr, S. (1994): Role of arginine in health and in renal disease, *Am.J.Physiol* (volume 267), issue 3 Pt 2, pp. F331-F346. URL: PM:8092248
- [7] Schmidt, R. J. und Baylis, C. (2000): Total nitric oxide production is low in patients with chronic renal disease, *Kidney Int.* (volume 58), issue 3, pp. 1261-1266. URL: PM:10972689
- [8] Bohle, A.; Muller, G. A.; Wehrmann, M.; Mackensen-Haen, S. und Xiao, J. C. (1996): Pathogenesis of chronic renal failure in the primary glomerulopathies, renal vasculopathies, and chronic interstitial nephritides, *Kidney Int.Suppl* (volume 54), pp. S2-S9. URL: PM:8731185
- [9] Klahr, S.; Schreiner, G. und Ichikawa, I. (1988): The progression of renal disease, *N.Engl.J.Med.* (volume 318), issue 25, pp. 1657-1666. URL: PM:3287163
- [10] Peters, H. und Noble, N. A. (1997): Angiotensin II and L-arginine in tissue fibrosis: more than blood pressure, *Kidney Int.* (volume 51), issue 5, pp. 1481-1486. URL: PM:9150462

- [11] Noble, N. A. und Border, W. A. (1997): Angiotensin II in renal fibrosis: should TGF-beta rather than blood pressure be the therapeutic target?, *Semin.Nephrol.* (volume 17), issue 5, pp. 455-466. URL: PM:9316214
- [12] Border, W. A.; Okuda, S.; Languino, L. R.; Sporn, M. B. und Ruoslahti, E. (1990): Suppression of experimental glomerulonephritis by antiserum against transforming growth factor beta 1, *Nature* (volume 346), issue 6282, pp. 371-374. URL: PM:2374609
- [13] Border, W. A.; Noble, N. A.; Yamamoto, T.; Harper, J. R.; Yamaguchi, Y.; Pierschbacher, M. D. und Ruoslahti, E. (1992): Natural inhibitor of transforming growth factor-beta protects against scarring in experimental kidney disease, *Nature* (volume 360), issue 6402, pp. 361-364. URL: PM:1280332
- [14] Jefferson, J. A. und Johnson, R. J. (1999): Experimental mesangial proliferative glomerulonephritis (the anti-Thy-1.1 model), *J Nephrol.* (volume 12), issue 5, pp. 297-307. URL: PM:10630692
- [15] Narita, I.; Border, W. A.; Ketteler, M. und Noble, N. A. (1995): Nitric oxide mediates immunologic injury to kidney mesangium in experimental glomerulonephritis, *Lab Invest* (volume 72), issue 1, pp. 17-24. URL: PM:7837786
- [16] Peters, H.; Daig, U.; Martini, S.; Ruckert, M.; Schaper, F.; Liefeldt, L.; Kramer, S. und Neumayer, H. H. (2003): NO mediates antifibrotic actions of L-arginine supplementation following induction of anti-thy1 glomerulonephritis, *Kidney Int.* (volume 64), issue 2, pp. 509-518. URL: PM:12846746
- [17] Moncada, S. (1997): Nitric oxide in the vasculature: physiology and pathophysiology, *Ann.N.Y.Acad.Sci.* (volume 811), pp. 60-67. URL: PM:9186585
- [18] Peters, H. und Noble, N. A. (1996): Dietary L-arginine in renal disease, *Semin.Nephrol.* (volume 16), issue 6, pp. 567-575. URL: PM:9125801
- [19] Levillain, O.; Hus-Citharel, A.; Morel, F. und Bankir, L. (1990): Localization of arginine synthesis along rat nephron, *Am.J.Physiol* (volume 259), issue 6 Pt 2, pp. F916-F923. URL: PM:2260685
- [20] Denninger, J. W. und Marletta, M. A. (1999): Guanylate cyclase and the .NO/cGMP signaling pathway, *Biochim.Biophys.Acta* (volume 1411), issue 2-3, pp. 334-350. URL:

PM:10320667

[21] Kone, B. C. und Baylis, C. (1997): Biosynthesis and homeostatic roles of nitric oxide in the normal kidney, *Am.J.Physiol* (volume 272), issue 5 Pt 2, pp. F561-F578. URL: PM:9176366

[22] Groves, J. T. (1999): Peroxynitrite: reactive, invasive and enigmatic, *Curr.Opin.Chem.Biol.* (volume 3), issue 2, pp. 226-235. URL: PM:10226050

[23] Ford, P. C.; Wink, D. A. und Stanbury, D. M. (1993): Autoxidation kinetics of aqueous nitric oxide, *FEBS Lett.* (volume 326), issue 1-3, pp. 1-3. URL: PM:8325356

[24] Cattell, V. (2002): Nitric oxide and glomerulonephritis, *Kidney Int.* (volume 61), issue 3, pp. 816-821. URL: PM:11849431

[25] Bachmann, S. und Mundel, P. (1994): Nitric oxide in the kidney: synthesis, localization, and function, *Am.J.Kidney Dis.* (volume 24), issue 1, pp. 112-129. URL: PM:7517625

[26] Martin, E.; Davis, K.; Bian, K.; Lee, Y. C. und Murad, F. (2000): Cellular signaling with nitric oxide and cyclic guanosine monophosphate, *Semin.Perinatol.* (volume 24), issue 1, pp. 2-6. URL: PM:10709849

[27] Forstermann, U.; Nakane, M.; Tracey, W. R. und Pollock, J. S. (1993): Isoforms of nitric oxide synthase: functions in the cardiovascular system, *Eur.Heart J.* (volume 14 Suppl I), pp. 10-15. URL: PM:7507435

[28] Keil, A.; Blom, I. E.; Goldschmeding, R. und Rupperecht, H. D. (2002): Nitric oxide down-regulates connective tissue growth factor in rat mesangial cells, *Kidney Int.* (volume 62), issue 2, pp. 401-411. URL: PM:12110001

[29] Narita, I.; Border, W. A.; Ketteler, M.; Ruoslahti, E. und Noble, N. A. (1995): L-arginine may mediate the therapeutic effects of low protein diets, *Proc.Natl.Acad.Sci.U.S.A* (volume 92), issue 10, pp. 4552-4556. URL: PM:7753841

[30] Murad, F. (1999): Discovery of some of the biological effects of nitric oxide and its role in cell signaling, *Biosci.Rep.* (volume 19), issue 3, pp. 133-154. URL: PM:10513891

[31] Theilig, F.; Bostanjoglo, M.; Pavenstadt, H.; Grupp, C.; Holland, G.; Slosarek, I.; Gressner, A. M.; Russwurm, M.; Koesling, D. und Bachmann, S. (2001): Cellular distribution and function of soluble guanylyl cyclase in rat kidney and liver,

- J.Am.Soc.Nephrol. (volume 12), issue 11, pp. 2209-2220. URL: PM:11675397
- [32] Pfeilschifter, J. (2000): Signalling pathways of nitric oxide, *Kidney Blood Press Res.* (volume 23), issue 3-5, pp. 159-161. URL: PM:11031709
- [33] Schultz, G.; Bohme, E. und Munske, K. (1969): Guanyl cyclase. Determination of enzyme activity, *Life Sci.* (volume 8), issue 24, pp. 1323-1332. URL: PM:5363364
- [34] Wedel, B. J. und Garbers, D. L. (1997): New insights on the functions of the guanylyl cyclase receptors, *FEBS Lett.* (volume 410), issue 1, pp. 29-33. URL: PM:9247117
- [35] Koesling, D. und Friebe, A. (1999): Soluble guanylyl cyclase: structure and regulation, *Rev.Physiol Biochem.Pharmacol.* (volume 135), pp. 41-65. URL: PM:9932480
- [36] Stone, J. R. und Marletta, M. A. (1995): The ferrous heme of soluble guanylate cyclase: formation of hexacoordinate complexes with carbon monoxide and nitrosomethane, *Biochemistry* (volume 34), issue 50, pp. 16397-16403. URL: PM:8845366
- [37] Condorelli, P. und George, S. C. (2001): In vivo control of soluble guanylate cyclase activation by nitric oxide: a kinetic analysis, *Biophys.J.* (volume 80), issue 5, pp. 2110-2119. URL: PM:11325714
- [38] Koesling, D.; Bohme, E. und Schultz, G. (1991): Guanylyl cyclases, a growing family of signal-transducing enzymes, *FASEB J.* (volume 5), issue 13, pp. 2785-2791.
- [39] Raeymaekers, L.; Eggermont, J. A.; Wuytack, F. und Casteels, R. (1990): Effects of cyclic nucleotide dependent protein kinases on the endoplasmic reticulum Ca²⁺ pump of bovine pulmonary artery, *Cell Calcium* (volume 11), issue 4, pp. 261-268. URL: PM:2163283
- [40] Wang, G. R.; Zhu, Y.; Halushka, P. V.; Lincoln, T. M. und Mendelsohn, M. E. (1998): Mechanism of platelet inhibition by nitric oxide: in vivo phosphorylation of thromboxane receptor by cyclic GMP-dependent protein kinase, *Proc.Natl.Acad.Sci.U.S.A* (volume 95), issue 9, pp. 4888-4893. URL: PM:9560198
- [41] Pryzwansky, K. B.; Wyatt, T. A. und Lincoln, T. M. (1995): Cyclic guanosine monophosphate-dependent protein kinase is targeted to intermediate filaments and phosphorylates vimentin in A23187-stimulated human neutrophils, *Blood* (volume 85), issue 1, pp. 222-230. URL: PM:7803796

- [42] Gambaryan, S.; Hausler, C.; Markert, T.; Pohler, D.; Jarchau, T.; Walter, U.; Haase, W.; Kurtz, A. und Lohmann, S. M. (1996): Expression of type II cGMP-dependent protein kinase in rat kidney is regulated by dehydration and correlated with renin gene expression, *J.Clin.Invest* (volume 98), issue 3, pp. 662-670. URL: PM:8698857
- [43] Dousa, T. P. (1999): Cyclic-3',5'-nucleotide phosphodiesterase isozymes in cell biology and pathophysiology of the kidney, *Kidney Int.* (volume 55), issue 1, pp. 29-62. URL: PM:9893113
- [44] Haneda, M.; Kikkawa, R.; Maeda, S.; Togawa, M.; Koya, D.; Horide, N.; Kajiwara, N. und Shigeta, Y. (1991): Dual mechanism of angiotensin II inhibits ANP-induced mesangial cGMP accumulation, *Kidney Int.* (volume 40), issue 2, pp. 188-194. URL: PM:1719265
- [45] Levitzki, A. (1996): Targeting signal transduction for disease therapy, *Curr.Opin.Cell Biol.* (volume 8), issue 2, pp. 239-244. URL: PM:8791424
- [46] Uhlenius, N.; Miettinen, A.; Vuolteenaho, O. und Tikkanen, I. (2002): Renoprotective Mechanisms of Angiotensin II Antagonism in Experimental Chronic Renal Failure, *Kidney Blood Press Res.* (volume 25), issue 2, pp. 71-79. URL: PM:12077487
- [47] Vetter, M.; Chen, Z. J.; Chang, G. D.; Che, D.; Liu, S. und Chang, C. H. (2003): Cyclosporin A disrupts bradykinin signaling through superoxide, *Hypertension* (volume 41), issue 5, pp. 1136-1142. URL: PM:12695417
- [48] Kelly, L. K.; Wedgwood, S.; Steinhorn, R. H. und Black, S. M. (2004): Nitric oxide decreases endothelin-1 secretion through the activation of soluble guanylate cyclase, *Am.J.Physiol Lung Cell Mol.Physiol* (volume 286), issue 5, pp. L984-L991. URL: PM:14695117
- [49] Lewko, B.; Wendt, U.; Szczepanska-Konkel, M.; Stepinski, J.; Drewnowska, K. und Angielski, S. (1997): Inhibition of endogenous nitric oxide synthesis activates particulate guanylyl cyclase in the rat renal glomeruli, *Kidney Int.* (volume 52), issue 3, pp. 654-659. URL: PM:9291184
- [50] Lewko, B. und Stepinski, J. (2002): Cyclic GMP signaling in podocytes, *Microsc.Res Tech.* (volume 57), issue 4, pp. 232-235. URL: PM:12012390
- [51] Friebe, A. und Koesling, D. (1998): Mechanism of YC-1-induced activation of soluble

- guanylyl cyclase, *Mol.Pharmacol.* (volume 53), issue 1, pp. 123-127. URL: PM:9443939
- [52] Stasch, J. P.; Becker, E. M.; Alonso-Alija, C.; Apeler, H.; Dembowski, K.; Feurer, A.; Gerzer, R.; Minuth, T.; Perzborn, E.; Pleiss, U.; Schroder, H.; Schroeder, W.; Stahl, E.; Steinke, W.; Straub, A. und Schramm, M. (2001): NO-independent regulatory site on soluble guanylate cyclase, *Nature* (volume 410), issue 6825, pp. 212-215. URL: PM:11242081
- [53] Kagota, S.; Tamashiro, A.; Yamaguchi, Y.; Sugiura, R.; Kuno, T.; Nakamura, K. und Kunitomo, M. (2001): Downregulation of vascular soluble guanylate cyclase induced by high salt intake in spontaneously hypertensive rats, *Br.J.Pharmacol.* (volume 134), issue 4, pp. 737-744. URL: PM:11606313
- [54] Machado, J. D.; Gomez, J. F.; Betancor, G.; Camacho, M.; Brioso, M. A. und Borges, R. (2002): Hydralazine reduces the quantal size of secretory events by displacement of catecholamines from adrenomedullary chromaffin secretory vesicles, *Circ.Res.* (volume 91), issue 9, pp. 830-836. URL: PM:12411398
- [55] Peters, H.; Border, W. A. und Noble, N. A. (1999): L-Arginine supplementation increases mesangial cell injury and subsequent tissue fibrosis in experimental glomerulonephritis, *Kidney Int.* (volume 55), issue 6, pp. 2264-2273. URL: PM:10354274
- [56] Peters, H.; Border, W. A. und Noble, N. A. (1998): Targeting TGF-beta overexpression in renal disease: maximizing the antifibrotic action of angiotensin II blockade, *Kidney Int.* (volume 54), issue 5, pp. 1570-1580. URL: PM:9844133
- [57] Okuda, S.; Nakamura, T.; Yamamoto, T.; Ruoslahti, E. und Border, W. A. (1991): Dietary protein restriction rapidly reduces transforming growth factor beta 1 expression in experimental glomerulonephritis, *Proc.Natl.Acad.Sci.U.S.A* (volume 88), issue 21, pp. 9765-9769. URL: PM:1946401
- [58] Peters, H.; Eisenberg, R.; Daig, U.; Liefeldt, L.; Westenfeld, R.; Gaedeke, J.; Kramer, S. und Neumayer, H. H. (2004): Platelet inhibition limits TGF-beta overexpression and matrix expansion after induction of anti-thy1 glomerulonephritis, *Kidney Int.* (volume 65), issue 6, pp. 2238-2248. URL: PM:15149337
- [59] Lynch, K. M.; Sellers, T. S. und Gossett, K. A. (1996): Evaluation of an automated

- pyrogallol red-molybdate method for the measurement of urinary protein in rats, *Eur.J Clin.Chem.Clin.Biochem.* (volume 34), issue 7, pp. 569-571. URL: PM:8864407
- [60] Watanabe, N.; Kamei, S.; Ohkubo, A.; Yamanaka, M.; Ohsawa, S.; Makino, K. und Tokuda, K. (1986): Urinary protein as measured with a pyrogallol red-molybdate complex, manually and in a Hitachi 726 automated analyzer, *Clin.Chem.* (volume 32), issue 8, pp. 1551-1554. URL: PM:3731450
- [61] Green, L. C.; Wagner, D. A.; Glogowski, J.; Skipper, P. L.; Wishnok, J. S. und Tannenbaum, S. R. (1982): Analysis of nitrate, nitrite, and [¹⁵N]nitrate in biological fluids, *Anal.Biochem.* (volume 126), issue 1, pp. 131-138. URL: PM:7181105
- [62] Heid, C. A.; Stevens, J.; Livak, K. J. und Williams, P. M. (1996): Real time quantitative PCR, *Genome Res.* (volume 6), issue 10, pp. 986-994. URL: PM:8908518
- [63] Lie, Y. S. und Petropoulos, C. J. (1998): Advances in quantitative PCR technology: 5' nuclease assays, *Curr.Opin.Biotechnol.* (volume 9), issue 1, pp. 43-48. URL: PM:9503586
- [64] Pfaffl, M. W. (2001): A new mathematical model for relative quantification in real-time RT-PCR, *Nucleic Acids Res.* (volume 29), issue 9, pp. e45. URL: PM:11328886
- [65] Peters, H.; Border, W. A.; Ruckert, M.; Kramer, S.; Neumayer, H. H. und Noble, N. A. (2003): L-Arginine supplementation accelerates renal fibrosis and shortens life span in experimental lupus nephritis, *Kidney Int.* (volume 63), issue 4, pp. 1382-1392. URL: PM:12631354
- [66] Perez-Sala, D.; Cernuda-Morollon, E.; Diaz-Cazorla, M.; Rodriguez-Pascual, F. und Lamas, S. (2001): Posttranscriptional regulation of human iNOS by the NO/cGMP pathway, *Am.J.Physiol Renal Physiol* (volume 280), issue 3, pp. F466-F473. URL: PM:11181408
- [67] Nath, K. A. (1998): The tubulointerstitium in progressive renal disease, *Kidney Int.* (volume 54), issue 3, pp. 992-994. URL: PM:9734628
- [68] Strutz, F. und Muller, G. A. (1999): Interstitial pathomechanisms underlying progressive tubulointerstitial damage, *Kidney Blood Press Res.* (volume 22), issue 1-2, pp. 71-80. URL: PM:10352410
- [69] Peters, H.; Border, W. A. und Noble, N. A. (2000): Tandem antifibrotic actions of L-arginine supplementation and low protein diet during the repair phase of experimental

- glomerulonephritis, *Kidney Int.* (volume 57), issue 3, pp. 992-1001. URL: PM:10720952
- [70] Peters, H.; Border, W. A. und Noble, N. A. (2000): Angiotensin II blockade and low-protein diet produce additive therapeutic effects in experimental glomerulonephritis, *Kidney Int.* (volume 57), issue 4, pp. 1493-1501. URL: PM:10760085
- [71] Feelisch, M. (1998): The use of nitric oxide donors in pharmacological studies, *Naunyn Schmiedebergs Arch.Pharmacol.* (volume 358), issue 1, pp. 113-122. URL: PM:9721012
- [72] Pedraza, C. E.; Baltrons, M. A.; Heneka, M. T. und Garcia, A. (2003): Interleukin-1beta and lipopolysaccharide decrease soluble guanylyl cyclase in brain cells: NO-independent destabilization of protein and NO-dependent decrease of mRNA, *J.Neuroimmunol.* (volume 144), issue 1-2, pp. 80-90. URL: PM:14597101
- [73] Filippov, G.; Bloch, D. B. und Bloch, K. D. (1997): Nitric oxide decreases stability of mRNAs encoding soluble guanylate cyclase subunits in rat pulmonary artery smooth muscle cells, *J.Clin.Invest* (volume 100), issue 4, pp. 942-948. URL: PM:9259594
- [74] Bremer, V.; Tojo, A.; Kimura, K.; Hirata, Y.; Goto, A.; Nagamatsu, T.; Suzuki, Y. und Omata, M. (1997): Role of nitric oxide in rat nephrotoxic nephritis: comparison between inducible and constitutive nitric oxide synthase, *J.Am.Soc.Nephrol.* (volume 8), issue 11, pp. 1712-1721. URL: PM:9355074
- [75] Ruetten, H.; Zabel, U.; Linz, W. und Schmidt, H. H. (1999): Downregulation of soluble guanylyl cyclase in young and aging spontaneously hypertensive rats, *Circ.Res.* (volume 85), issue 6, pp. 534-541. URL: PM:10488056
- [76] Taylor, T. A.; Pollock, J. S. und Pollock, D. M. (2003): Down-regulation of soluble guanylyl cyclase in the inner medulla of DOCA-salt hypertensive rats, *Vascul.Pharmacol.* (volume 40), issue 3, pp. 155-160. URL: PM:13678647
- [77] Yamamoto, T. und Wilson, C. B. (1987): Quantitative and qualitative studies of antibody-induced mesangial cell damage in the rat, *Kidney Int.* (volume 32), issue 4, pp. 514-525. URL: PM:2892961
- [78] Landmesser, U.; Dikalov, S.; Price, S. R.; McCann, L.; Fukai, T.; Holland, S. M.; Mitch, W. E. und Harrison, D. G. (2003): Oxidation of tetrahydrobiopterin leads to uncoupling of endothelial cell nitric oxide synthase in hypertension, *J.Clin.Invest* (volume 111), issue 8,

pp. 1201-1209. URL: PM:12697739

[79] Mayer, B. und Koesling, D. (2001): cGMP signalling beyond nitric oxide, Trends Pharmacol.Sci. (volume 22), issue 11, pp. 546-548. URL: PM:11698077

[80] Bauersachs, J.; Bouloumie, A.; Fraccarollo, D.; Hu, K.; Busse, R. und Ertl, G. (1999): Endothelial dysfunction in chronic myocardial infarction despite increased vascular endothelial nitric oxide synthase and soluble guanylate cyclase expression: role of enhanced vascular superoxide production, Circulation (volume 100), issue 3, pp. 292-298. URL: PM:10411855

[81] Marques, M.; Millas, I.; Jimenez, A.; Garcia-Colis, E.; Rodriguez-Feo, J. A.; Velasco, S.; Barrientos, A.; Casado, S. und Lopez-Farre, A. (2001): Alteration of the soluble guanylate cyclase system in the vascular wall of lead-induced hypertension in rats, J.Am.Soc.Nephrol. (volume 12), issue 12, pp. 2594-2600. URL: PM:11729227

[82] Mollnau, H.; Wendt, M.; Szocs, K.; Lassegue, B.; Schulz, E.; Oelze, M.; Li, H.; Bodenschatz, M.; August, M.; Kleschyov, A. L.; Tsilimingas, N.; Walter, U.; Forstermann, U.; Meinertz, T.; Griendling, K. und Munzel, T. (2002): Effects of angiotensin II infusion on the expression and function of NAD(P)H oxidase and components of nitric oxide/cGMP signaling, Circ.Res. (volume 90), issue 4, pp. E58-E65. URL: PM:11884382

[83] Witte, K.; Jacke, K.; Stahrenberg, R.; Arlt, G.; Reitenbach, I.; Schilling, L. und Lemmer, B. (2002): Dysfunction of soluble guanylyl cyclase in aorta and kidney of Goto- Kakizaki rats: influence of age and diabetic state, Nitric.Oxide. (volume 6), issue 1, pp. 85-95. URL: PM:11829539

[84] Wedel, B.; Humbert, P.; Harteneck, C.; Foerster, J.; Malkewitz, J.; Bohme, E.; Schultz, G. und Koesling, D. (1994): Mutation of His-105 in the beta 1 subunit yields a nitric oxide-insensitive form of soluble guanylyl cyclase, Proc.Natl.Acad.Sci.U.S.A (volume 91), issue 7, pp. 2592-2596. URL: PM:7908439

[85] Laber, U.; Kober, T.; Schmitz, V.; Schrammel, A.; Meyer, W.; Mayer, B.; Weber, M. und Kojda, G. (2002): Effect of hypercholesterolemia on expression and function of vascular soluble guanylyl cyclase, Circulation (volume 105), issue 7, pp. 855-860. URL: PM:11854127

- [86] Kloss, S.; Bouloumie, A. und Mulsch, A. (2000): Aging and chronic hypertension decrease expression of rat aortic soluble guanylyl cyclase, *Hypertension* (volume 35), issue 1 Pt 1, pp. 43-47. URL: PM:10642273
- [87] Raij, L.; Azar, S. und Keane, W. (1984): Mesangial immune injury, hypertension, and progressive glomerular damage in Dahl rats, *Kidney Int.* (volume 26), issue 2, pp. 137-143. URL: PM:6239058
- [88] Gabbai, F. B.; De Nicola, L.; Peterson, O. W.; Obagi, S.; Thomson, S. C.; Tucker, B. J.; Keiser, J. A.; Wilson, C. B. und Blantz, R. C. (1996): Renal response to blood pressure elevation in normal and glomerulonephritic rats, *J.Am.Soc.Nephrol.* (volume 7), issue 12, pp. 2590-2599. URL: PM:8989737
- [89] Yoshida, Y.; Fogo, A. und Ichikawa, I. (1989): Glomerular hemodynamic changes vs. hypertrophy in experimental glomerular sclerosis, *Kidney Int.* (volume 35), issue 2, pp. 654-660. URL: PM:2709670
- [90] Brenner, B. M. (1985): Nephron adaptation to renal injury or ablation, *Am.J.Physiol* (volume 249), issue 3 Pt 2, pp. F324-F337. URL: PM:3898871
- [91] Greco, B. A. und Breyer, J. A. (1997): Atherosclerotic ischemic renal disease, *Am.J.Kidney Dis.* (volume 29), issue 2, pp. 167-187. URL: PM:9016887
- [92] Peters, H.; Ruckert, M.; Gaedeke, J.; Liefeldt, L.; Ketteler, M.; Sharma, A. M. und Neumayer, H. H. (2003): Angiotensin-converting enzyme inhibition but not beta-adrenergic blockade limits transforming growth factor-beta overexpression in acute normotensive anti-thy1 glomerulonephritis, *J.Hypertens.* (volume 21), issue 4, pp. 771-780. URL: PM:12658024
- [93] Wenzel, U. O.; Wolf, G.; Thaiss, F.; Helmchen, U. und Stahl, R. A. (2000): Renovascular hypertension does not influence repair of glomerular lesions induced by anti-thymocyte glomerulonephritis, *Kidney Int.* (volume 58), issue 3, pp. 1135-1147. URL: PM:10972677
- [94] van Goor, H.; Albrecht, E. W.; Heeringa, P.; Klok, P. A.; van der Horst, M. L.; Jager-Krikken, A.; Bakker, W. W. und Moshage, H. (2001): Nitric oxide inhibition enhances platelet aggregation in experimental anti-Thy-1 nephritis, *Nitric.Oxide.* (volume 5), issue 6,

pp. 525-533. URL: PM:11730359

[95] Moro, M. A.; Russel, R. J.; Cellek, S.; Lizasoain, I.; Su, Y.; Darley-USmar, V. M.; Radomski, M. W. und Moncada, S. (1996): cGMP mediates the vascular and platelet actions of nitric oxide: confirmation using an inhibitor of the soluble guanylyl cyclase, Proc.Natl.Acad.Sci.U.S.A (volume 93), issue 4, pp. 1480-1485. URL: PM:8643658

[96] Segerer, S.; Nelson, P. J. und Schlondorff, D. (2000): Chemokines, chemokine receptors, and renal disease: from basic science to pathophysiologic and therapeutic studies, J.Am.Soc.Nephrol. (volume 11), issue 1, pp. 152-176. URL: PM:10616852

[97] Ahluwalia, A.; Foster, P.; Scotland, R. S.; McLean, P. G.; Mathur, A.; Perretti, M.; Moncada, S. und Hobbs, A. J. (2004): Antiinflammatory activity of soluble guanylate cyclase: cGMP-dependent down-regulation of P-selectin expression and leukocyte recruitment, Proc.Natl.Acad.Sci.U.S.A (volume 101), issue 5, pp. 1386-1391. URL: PM:14742866

Abbreviations

°C	Degrees Celsius
aGN	Acute glomerulonephritis
APAAP	Alkaline Phosphatase and Anti-Alkaline Phosphatase
ATP	Adenosine triphosphate
cDNA	Complementary DNA
CO ₂	Carbon dioxide
cGMP	cyclic guanosine monophosphate
cGS	Chronic glomerulosclerosis
dATP	Deoxyadenosine 5'-triphosphate
dCTP	Deoxycytidine 5'-triphosphate
dGTP	Deoxyguanosine 5'-triphosphate
dTTP	Deoxythymidine 5'-triphosphate
DEA/NO	Diethylamine-NONOate
DEPC	Diethyl Pyrocarbonate
DNA	Deoxyribonucleic acid
DMEM	Dulbecco's Modified Eagle's Medium
dsDNA	Double-stranded DNA
ECM	Extracellular matrix
EDTA	Ethylenediaminetetraacetic acid
ELISA	Enzyme-Linked Immunosorbent Assay

Abbreviations

GAPDH	Glyceraldehyde-3-phosphate dehydrogenase
GTP	Guanosine 5`-triphosphate
HRP	Horseradish peroxidase
H ₂ SO ₄	Sulphuric acid
HCl	Hydrochloric acid
IBMX	3-Isobutyl-1-methylxanthine
Ig	Immunoglobulin
LPS	Lipopolysaccharide
Min	Minutes
mRNA	Messenger ribonucleic acid
NADPH	Nicotinamide Adenine Dinucleotide Phosphate Reduced
NO	Nitric oxide
NOS	NO synthase
eNOS	Endothelial NOS
iNOS	Inducible NOS
nNOS	Neuronal NOS
OPD	O-Phenylenediamine dihydrochloride
PAI-1	Plasminogen-activator-inhibitor-type 1
PAS	Periodic acid Schiff
PBS	Phosphate-buffered saline
PCR	Polymerase chain reaction

Abbreviations

PDE	Phosphodiesterase
PKG	cGMP-dependent protein kinase
rpm	Revolutions per minute
RPMI	Roswell Park Memorial Institute medium
sec	Seconds
sGC	Soluble guanylate cyclase
TBS	Tris-buffered saline
TGF-beta	Transforming growth factor-beta
TNF-alpha	Tumor necrosis factor-alpha

Acknowledgements

Although I have met a lot of difficulties during my studies in Germany, due to the support and help from my teachers, colleagues, family and friends, I have finished the project of my doctoral thesis.

First of all, I thank my supervisor, Dr. Harm Peters, who offered me the chance and guided me in this interesting project at the research laboratory of work group Peters, Center of Cardiovascular Research and Department of Nephrology, Charité Mitte Hospital of Medical University at Berlin. He has given me much help and support and introduced me to many scientific concepts and ideas, which will be helpful for my future career.

There are many laboratory methods used in my project. I thank all my colleagues in the lab, Stephanie Krämer, Tanja Loof, Sebastian Martini, Matthias Rückert, Susanne Kron and Lysann Hinz, who gave me wonderful technical support. Three years of a great working experience in the happy fibrosis research family will stay in my mind forever.

Of course, I thank my family in China. Their support and encouragement have stood by me in solving all difficulties.

Lastly, I am grateful for the support from a DAAD (Deutscher Akademischer Austauschdienst) scholarship in finishing the project.

Erklärung an Eides Statt

I hereby assure on oath that I, Yingrui Wang, born on June 8th, 1974, in Guangdong of the People's Republic of China, independently have written the present work myself, without the illegal help of any third party. The dissertation does not represent, even in parts, a copy of the works of others. Any sources, literary or otherwise, that I have used are stated in full.

Hiermit versichere ich, Yingrui Wang, geboren am 08.06.1974 in Guangdong in der Volksrepublik China, an Eides statt, dass ich die vorliegende Arbeit selbst und ohne die Hilfe Dritter verfasst habe. Sie stellt auch in Teilen keine Kopie anderer Arbeiten dar und die benutzten Hilfsmittel sowie die Literatur sind vollständig angegeben.

Yingrui Wang

Berlin, den 22.09.2004